メカノケミカルを利用した無焼成セラミックスの作製

FABRICATION OF NON-FIRING CERAMICS BY MECHANOCHEMICALLY ASSISTED CHEMICAL SOLIDIFICATION

2011

APILUCK EIAD-UA

名古屋工業大学博士論文
甲第804号(課程修了による)
平成２３年３月３１日授与

FABRICATION OF NON-FIRING CERAMICS BY MECHANOCHEMICALLY ASSISTED CHEMICAL SOLIDIFICATION

BY

APILUCK EIAD-UA

DOCTOR OF ENGINEERING

in

FRONTIER MATERIAL

NAGOYA INSTITUTE OF TECHNOLOGY,

NAGOYA, JAPAN

MARCH, 2011

論文題目

メカノケミカルを利用した無焼成セラミックスの作製

未来材料創成工学専攻博士後期課程

アピラック　イエアド　ウア

APILUCK EIAD-UA

指導教員　藤　正督　教授

名古屋工業大学

セラミックス基盤工学研究センター

2011年3月

ABSTRACT

A novel method for fabrication non-firing ceramics have been proposed using mechanochemically assisted chemical solidification. This method allows the activate surface of powder and control of the properties of powder not only by varying mechano-chemical conditions but also by managing the chemical solidification process with alkaline activation (binding). After drying at 25°C for 3 days, the ceramic green body was obtained. The mechano-chemical treatment of solid is one of the common and widely used operations. At the present, mechano-chemical treatment has a wide range of application potential. Mechano-chemical treatments are used to modify the properties of materials, activate surface of particles, enhance the reactivity of materials and produce advanced materials. When materials are subjected to intensive milling, the surface and microstructure characters of material change widely. Then, ceramic green body (non-firing ceramic) was obtained from chemical reaction of alkaline binding in chemical solidification process. This study is particularly taking advantage of mechanochemically assisted chemical solidification for the solidification time and strength of ceramic green body. The use of X-ray diffraction line broadening measurements, BET, PSD, FTIR, Raman, ICP, TG-DTA, SEM, TEM, mechanical strength and etc., have been proved to be useful in the characterization of microstructure and structural characteristics.

The objective of this study is to investigate the influence of mechano-chemical treatment by the milling operation variables on the microstructure and interface surface changes of particles. The influence of the three variables, rotation speed, milling time and diameter of balls, through an experimental design was investigated using different characterization. The study is mainly organized as the followings.

Chapter 1 presents the applications mechano-chemical process assisted chemical solidification on fabrication of non-firing ceramics. Accordingly, the firing ceramics has been disadvantageous in term of high cost and harmful to the environment. Low Temperature Co-firing Ceramic, Cement and Geopolymer have been proposed. The negative influence of these methods on the hydration reaction based binders requires further study in order to optimize the characteristics of these binders. The possible of mechano-chemical process assisted chemical solidification to reduce cost and friendly to environment were suggested. Based on such disadvantageous, the goal of this study was conceptualized.

Chapter 2 investigates the influence of mechano-chemical treatment, rotation speed, milling time and diameter of balls on the interfaced surface of alumina particles for fabrication green ceramic bodies. The results revealed that mechano-chemical treatment of alumina brings about great changes in interfaced surface between particles and microstructural characteristics with increased the mechano-chemical intensity, whatever milling methods are applied.

Chapter 3 investigates the composition ratio of alumina-silica system assisted by mechano-chemical treatment on fabricated ceramic green body. Because of alumina-silica system is probably the most important binary oxide system both in technology and science. It was found visually that the mechano-chemical treatment has a great effect on alumina surface better than silica surface. All the compositions can be solidified at ambient temperature and pressure, the higher alumina contents resulted in lower solidification time and mechanical strength. The alumina-silica system is of great importance and utility.

Chapter 4 describes the fabrication of non-firing ceramics from paper sludge ash by mechano-chemical treatment using planetary ball mill. It was indicate that the mechano-chemical treatment of planetary ball mill affects the fabrication of non-firing ceramics when the rotational speed and milling time were varied. The chemical reaction depends on several

factors such as the particle size distribution, mineral composition of paper sludge ash, kinds and concentration of the activator, reaction time, reaction temperature, etc.

Chapter 5 illustrates the fabrication porous ceramics using waste materials by non-firing process. It was confirmed that the addition tire ash influenced the gas generating in slurry. The mechano-chemical treatment with alkaline activation was used as a chemical synthesis of ceramic particles to form porous structure and porosity of solidified specimen by gas generating. The porous structure and mechanical strength, developed from mechano-chemical conditions, concentration of KOH, amount of tire ash and etc.

Chapter 6 describes the overall conclusions of present work and the future directions for research. The novel technique presented in this study easy for operation, low cost and friendly to environment. This technique has an attractive route for shaping materials into ceramics without firing process.

PREFACE

This thesis presents the scientific work done during my PhD studies in Intelligent Processing Group, Ceramic Research Laboratory Divisions, Department of Frontier Material at Nagoya Institute of Technology, from April 2008 until March 2011. The work has been aimed at achieving control surface of particles, in particular crystalline phase and amorphous phase formation and stability. This goal was approached by combination of experimental studies of mechano-chemical process to obtain activated particles and chemical solidification process to obtain non-firing ceramics (ceramic green body). The thesis consists of three published papers and three papers on processing preceded by an introduction part. The work was financed through the Ministry of Education, Culture, Sports, Science and Technology (MEXT), Project "Cooperation for Innovative Technology and Advanced Research in Evolution Area".

March 2011

RESEARCH ACTIVITIES

Here the six publications and presentations, which are included in the thesis, are listed together with the author's contribution to each of them.

List of publications

1. **Apiluck Eiad-ua,** Takashi Shirai, Hideo Watanabe, Masayoshi Fuji, Koji Orito and Minoru Takahashi, **Fabrication of non-firing ceramics by surface particle activation using a planetary ball mill,** Ceramic Transactions, 219 (2010) 129-135.

2. **Apiluck Eiad-ua,** Takashi Shirai, Tomoaki Kato, Koji Orito, Hideo Watanabe, Masayoshi Fuji and Minoru Takahashi, **Novel fabrication route for porous ceramics using waste materials by non-firing process,** Journal of Ceramic Society of Japan, 118 (2010) 745-748.

3. **Apiluck Eiad-ua,** Takashi Shirai, Hideo Watanabe, Masayoshi Fuji, Koji Orito and Minoru Takahashi, **Application of mechano-chemical process for fabrication of porous ceramics from waste materials,** Journal of the Japan Society of Powder and powder Metallurgy, (2011) In press.

4. **Apiluck Eiad-ua,** Takashi Shirai, Masayoshi Fuji, Koji Orito and Minoru Takahashi, **Microstructural characterization of mechanochemically activated alumina for non-firing ceramics process,** Ceramics International, Submitted.

5. **Apiluck Eiad-ua,** Takashi Shirai, Masayoshi Fuji, Koji Orito and Minoru Takahashi, **A novel fabrication route for non-firing ceramic,** Journal of Physics and Chemistry of Solids, Submitted.

6. **Apiluck Eiad-ua,** Takashi Shirai, Masayoshi Fuji, Koji Orito and Minoru Takahashi, **Fabrication and characterization of Al_2O_3-SiO_2 composites via mechano-chemical treatment,** Journal of Material Science, Submitted.

List of presentations

2010

1. Apiluck Eiad-ua, Takashi Shirai, Hideo Watanabe, Masayoshi Fuji, Koji Orito and Minoru Takahashi, **Microstructural characterization of mechanochemically activated alumina.** International Conference on Ceramic Processing Science (ICCPS11), August, 29-September, 1, 2010, Zurich, Switzerland (Presenter-Oral).

2. Eiad-ua Apiluck、白井　孝　、渡辺　秀夫　、藤　正督　、折戸　浩二、高橋 実、**Mechano-chemical synthesis of alumina-silica composites.** 「ナノテクノロジー材料分野」1回シンポジウム、November, 5, 2010, Tajimi, Japan (Presenter-Poster).

3. **Apiluck Eiad-ua,** Takashi Shirai, Hideo Watanabe, Masayoshi Fuji, Koji Orito and Minoru Takahashi, **Application of mechano-chemical process for fabrication of porous ceramics from waste materials.** 3rd International Congress on Ceramic (ICC3), November, 14-18, 2010, Osaka, Japan (Presenter-Oral).

4. Takashi Shirai, **Apiluck Eiad-ua,** Hideo Watanabe, Masayoshi Fuji, and Minoru Takahashi. **Effects of powder surfaces condition on the fabrication of non-firing ceramics.** 3rd International Congress on Ceramic (ICC3), November, 14-18, 2010, Osaka, Japan.

2009

1. **Apiluck Eiad-ua,** Takashi Shirai, Hideo Watanabe, Masayoshi Fuji, Koji Orito and Minoru Takahashi, **Surface activation of solidified paper sludge ash (PSA) by mechanochemical treatment**, 38th Summer Seminar of the Association Tokai Young Ceramists, July, 9-10, 2009, Mie, Japan (Presenter-Poster).

2. **Apiluck Eiad-ua,** Takashi Shirai, Hideo Watanabe, Masayoshi Fuji, Koji Orito and Minoru Takahashi, **Fabrication of non-firing ceramics assisted by particle surface activation using a planetary ball-mill**, The Third International Conference on the Characterization and Control of Interfaces for High Quality Advanced Materials, and Joining Technology for New Metallic Glasses and Inorganic Materials (ICCCI 2009), September, 6-9, 2009, Kurashiki, Japan (Presenter-Poster).

3. 白井　孝、**Eiad-ua Apiluck,** 渡辺　秀夫, 藤　正督、高橋　実。**無焼成セラミックス作製における粉体表面状態の影響。**第 22 回秋季シンポジウム, September, 16-18, 2009, Ehime, Japan.

4. **Apiluck Eiad-ua,** Takashi Shirai, Hideo Watanabe, Masayoshi Fuji, Koji Orito and Minoru Takahashi, **Pore structure of porous ceramics fabricated from solid waste by non-firing process**. The 2nd Thailand-Japan International Academic (TJIA) Conference 2009, November, 20, Kyoto Japan (Presenter-poster).

2008

1. **Apiluck Eiad-ua,** Tomohiro Yamakawa, Hideo Watanabe, Masayoshi Fuji, Koji Orito and Minoru Takahashi, **Fabrication of Non-firing Ceramic from Paper Sludge Ash Pre-Treated by Planetary Ball-milling,** 36th Summer Seminar of the Association Tokai Young Ceramists, July, 10-11, 2008, Gifu, Japan (Presenter-Poster).

2. **Apiluck Eiad-ua,** Takashi Shirai, Hideo Watanabe, Masayoshi Fuji, Koji Orito and Minoru Takahashi, **Mechanochemically-assisted chemical solidification of Al_2O_3/SiO_2,** The 8th young man study meeting, September, 10-11, 2008, Inuyama, Japan (Presenter-Oral).

3. **Apiluck Eiad-ua,** Takashi Shirai, Hideo Watanabe, Masayoshi Fuji, Koji Orito and Minoru Takahashi, **The Effect of composition range of SiO_2/Al_2O_3 on mechanochemically-assisted chemical solidification,** 21st Fall Meeting of the Ceramic Society of Japan, 2008, September, 17-19, Kitakyushu, Japan (Presenter-Oral).

4. **Apiluck Eiad-ua,** Takashi Shirai, Hideo Watanabe, Masayoshi Fuji, Koji Orito and Minoru Takahashi, **Production of non-firing ceramic from paper sludge ash,** The 1st Thailand-Japan International Academic (TJIA) Conference 2008, November, 21, Tokyo Japan (Presenter-poster).

5. **Apiluck Eiad-ua,** Takashi Shirai, Hideo Watanabe, Masayoshi Fuji, Koji Orito and Minoru Takahashi, **Effect of mechanochemical treatment on the crystallization behavior of alumina for chemical solidification,** Annual Ceramic Convention in Tajimi, 2009, March, 4, Tajimi, Japan (Presenter-Poster).

6. **Apiluck Eiad-ua,** Takashi Shirai, Hideo Watanabe, Masayoshi Fuji, Koji Orito and Minoru Takahashi, **Influence of calcinations treatment in chemical solidification using mechanochemical approach,** Annual Meeting of the Ceramic Society of Japan, 2009, March, 16-18, Chiba, Japan (Presenter-Oral).

ACKNOWLEDGEMENTS

The research work presented in this thesis has been carried out at Intelligent Processing Group, Division of Ceramics Research Laboratory, Department of Frontier Material, Graduate School of Engineering at Nagoya Institute of Technology under the supervision of Professor Masayoshi Fuji.

First of all, I would like to express my sincere gratitude to my supervisor, Professor Masayoshi Fuji, for providing me an opportunity to do this research with circumstances, his contribution, guidance, and fruitful discussions with valuable suggestions for the present thesis. I was never able to dream.

I am also wish to express my thanks to my advisor Assoc. Prof. Takashi Shirai who provided valuable insights, guidance, constructive comments on my work to make it more scientifically relevant and his kindness and moral support concerning all my life.

I would like to thanks to Assoc. Prof. Hideo Watanabe, for guidance and comments on my work.

I would like to express my deepest gratitude and sincere thank to Prof. Minoru Takahashi, President of Nagoya Institute of technology, for his professional advices and his kindness for suggestion and help me on the NGK scholarship during doctoral course.

Special thanks are to express to my long lasting junior friend, Mr. Pramote Puengjinda, for financial support during doctoral course and sincere support me every things, to all my friends, who have been helpful attitude and spirit.

I am very grateful to Mr. Virtudazo Raymond for revising the English language of the manuscript.

I greatly appreciate Mr. Hiroki Kawade who is my tutor, Dr.Chika Takai, Mr. Seiji Yamashi and Mr. Tomoaki Kato for them kind help. Furthermore, I also thank other students, post

doctoral researchers and all staffs of Ceramics research Laboratory for their kind help during the course of my experiment.

I would like to thank Monbukagakusho scholarship, NGK scholarship and Research Assistantship offered in the Processing Group of CRL for providing me enough financial support until my completion of research work.

I am very much grateful to my parents for their love, support and patience during the PhD period. I also thank my young sister for her spirit.

The last but not the least, I would also like to thank all

I thank you all!

Apiluck Eiad-ua

March 2011

CONTENTS

LIST OF FIGURES

CHAPTER 1

CHAPTER 2

CHAPTER 3

CHAPTER 4

CHAPTER 5

LIST OF TABLES

CHAPTER 1

CHAPTER 2

CHAPTER 3

CHAPTER 5

I. INTRODUCTION

I often get asked, "I want to start doing ceramics, what do I need?" This thesis I will talk about the fabrication of non-firing ceramics by mechanochemically assisted chemical solidification and how an understanding of the mechano-chemical treatment produces the activated particle using planetary ball mill leading to a better understanding of reaction form new bonding during milling, understanding the mechanism on surface activation of particles by surface characterization and chemical bonding from alkaline activation (binding) during chemical solidification to obtain ceramic green body. Research on non-firing ceramic is involved with mechano-chemical process which's a subfield of mechanochemistry. Therefore, it is appropriate to review the history of mechanochemistrty.

1.1 Non-firing ceramics: history and development

The history of ceramic processing technology is very interesting in that both simple processes developed in ancient times for natural materials, and recently developed, relatively sophisticated processes dependent on synthetic materials are used extensively near the end of the 20^{th} century. Handing mixing, handing building, and scratch and slip decorating of earthenware date back to before 5000 BC. The first forming machine was probably the potter's wheel, which was used earlier than 3500 BC for throwing plastic earthenware body and later for turning somewhat dried, leather, hard body. Shaping by pressing material in fired molds and firing in a closed kiln were subsequent developments.

Ceramics processing commonly begins with one or more ceramic materials, one or more liquids, and one or more special additives called processing aids. The starting materials or batch system may be beneficiated chemically and physically using operations such as crushing, milling, washing, chemical dissolving, settling, flotation, magnetic separation, dispersion, mixing, classification, de-airing, filtration, and spray-drying.

View as a science, ceramics processing is the sequence of operations that purpose fully and systematically changes the chemical and physical aspects of structure, which we call the characteristics of the system. The properties at each stage are a function of the characteristics of the system at each stage and the ambient pressure and temperature, as is shown in Fig. 1.1.

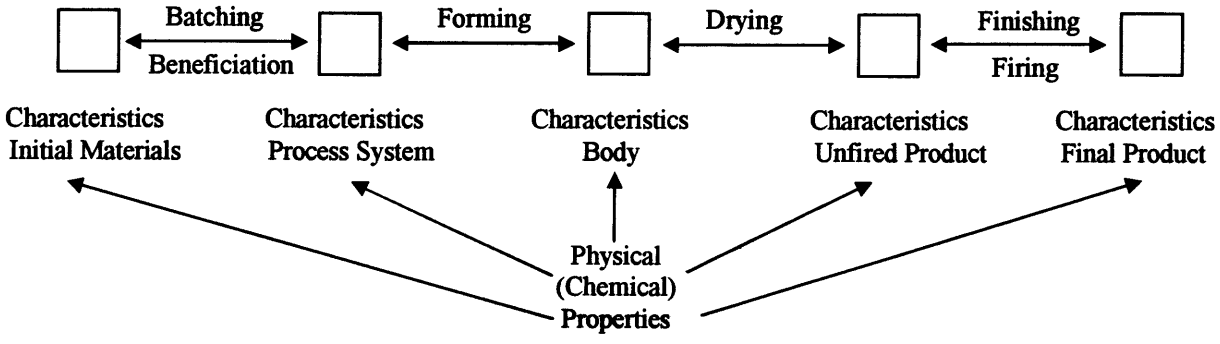

Figure 1.1 Processing develops the characteristics of the system.

Principles of processing science can provide insights into fundamental causes of behavior, procedures for modifying and controlling materials and processes, and avenues for improving manufacturing productivity. The role of ceramics processing science in ceramic manufacturing will surely increase.

Ceramic products are used in applications where the performance and reliability of the product must be predictable and assured and the product must be fabricated successfully in a productive manner. The manufacture of these products from a complex batch containing ceramic materials and processing additives into a finished product involves many operations. All of the materials and operations must be carefully controlled. Principles of science should be used in addition to empirical tests for understanding, improving, and controlling ceramics processing.

Products that have been dried and surface finished, traditionally called "green products," are heat treated in a kiln or furnace to develop the desired microstructure and properties. This process, called firing, proceeds in three stages: (1) reactions preliminary to sintering, which

include organic burn out and the elimination of gaseous products of decomposition and oxidation; (2) sintering; and (3) cooling, which may include thermal and chemical annealing.

Nowadays, with background of lively activity there is large demand in ceramic industry. Firing ceramics is one of the most common techniques in fabrication porous or dense materials [1]. However, this method has been disadvantageous in term of high cost and can be harmful to the environment because the coal which is burnt as fuel emits, CO_2, SO_x and NO_x, ash dust during the burning process.

CO_2 is inevitably created by burning fuels like e.g. oil, natural gas, and diesel during burning process. Carbon dioxide emissions therefore are the most important cause of global warming. The emissions of CO_2 have been dramatically increased within the last 50 years and are still increasing each year [2].

Ceramic industry today requires low cost ceramic fabrication, while at the same time demanding excellent performance. Recently, Low Temperature Co-fired Ceramics (LTCCs) [3], cement [4] and geopolymer [5] have been intensively studied for these applications.

Low temperature co-fired ceramic (LTCC) is a well-established multi-layer technology which has been in use for many years in the microelectronics packaging industry. Each of the layers are processed in parallel and only brought together in an accurately aligned stack immediately prior to firing. This is the key differentiator to serially produced multi-layer structures such as thick film hybrid interconnect and components such as ceramic capacitors. LTCC technology is especially beneficial for RF and high-frequency applications. In RF and wireless applications, LTCC technology is also used to produce multilayer hybrid integrated circuits, which can include resistors, inductors, capacitors, and active components in the same package. LTCC hybrids have a smaller initial ("non recurring") cost as compared with ICs, making them an attractive alternative to ASICs for small scale integration devices. This technology presents advantages compared to other packaging technologies such as HTCC: the ceramic is

generally fired below 1000°C due to a special composition of the material. This permits the co-firing with highly conductive materials (silver, copper and gold). LTCC also features the ability to embed passive elements, such as resistors, capacitors and inductors into the ceramic package minimizing the size of the completed module.

In the most general sense of the word, cement is a binder, a substance that sets and hardens independently, and can bind other materials together. Cement used in construction is characterized as hydraulic or non-hydraulic. Hydraulic cements (e.g. Portland cement) harden because of hydration chemical reactions that occur independently of the mixture's water content; they can harden even underwater or when constantly exposed to wet weather. The chemical reaction that results when the anhydrous cement powder is mixed with water produces hydrates that are not water-soluble. Non-hydraulic cements (e.g. lime and gypsum plaster) must be kept dry in order to retain their strength. The most important use of cement is the production of mortar and concrete - the bonding of natural or artificial aggregates to form a strong building material that is durable in the face of normal environmental effects. Concrete should not be confused with cement because the term cement refers to the material used to bind the aggregate materials of concrete. Concrete is a combination of a cement and aggregate.

Geopolymer is a term covering a class of synthetic aluminosilicate materials with potential use in number of areas, essentially as a replacement for Portland cement and for advanced high-tech composites, ceramic applications or as form of cast stone. The name Geopolymer was first applied to these materials by Joseph Davidovits in the 1970s, although similar materials had been developed in the former Soviet Union since the 1950s, originally under the name "soil cement". However, this name never found widespread usage in the English language, as it is more often applied to the description of soils which are consolidated with a small amount of Portland cement to enhance strength and stability. Geopolymer cements are

an example of the broader class of alkali-activated binders, which also includes alkali-activated metallurgical slags and other related materials. Much of the drive behind research carried out in academic institutions is to investigate the development of geopolymer cements as a potential large-scale replacement for concrete produced from Portland cement. This is due to geopolymer's lower alleged carbon dioxide production emissions, greater chemical and thermal resistance and better mechanical properties at both ambient and extreme conditions. On the other side, industry has implemented geopolymer binders in advanced high-tech composites and ceramics for heat and fire-resistant applications, up to 1200 degrees C. There is some debate as to whether geopolymer cement has lower CO_2 emissions compared to Portland cement. Calcination of limestone in production of Portland cements is responsible for CO_2 emission (one ton of cement produced releases one ton CO_2), while some processes of formation of lye also release CO_2. Mainly it's the ratio of CO_2 reduction that is under debate, and its process depends.

However, at present, there cost is high and remain in the release of CO_2. Non-firing ceramics by mechanochemically assisted chemical solidification has been proposed. Mechano-chemical treatment as a novel method involving the mechanical activation [6], a process for introduction of additional energy to the system applies worldwide. During the treatment, various structural changes of the material are taking place. These structural changes of the material cause its properties changes (chemical, electrical, thermal, mechanical, etc) as well as its reactivity improvement. The most popular devices, in which mechano-chemical processes can be conducted are vibratory, planetary and attritor ball mills. They differ in their capacities, efficiencies of milling and additional arrangements such as cooling. In all these devices, the ground material is periodically thrown into zones of ball collisions. Energy transfer to the powdered particles takes place by shearing and/or impact action of the balls [6, 7]. Mechano-chemical treatment by planetary ball mill is now recognized as a powerful tool for the

synthesis of materials, such as amorphous alloys [7], nanocrystalline metals and alloys [8] and ceramic materials [9]. This method is very simple and economic for the production of powders of very small size. The use of fine starting materials and mechano-chemical treatment by efficient activation are the key steps in this process. Therefore, this study examined whether mechano-chemical treatment of starting materials using ball milling activation can reduce the sintering temperature of solid state reacted [10-11].

1.2 Mechano-chemical treatment

A. Mechano-chemical process

A variety of methods exist for the synthesis of ceramic powders. Mechanical methods are generally used to prepare powders of traditional ceramics from naturally occurring raw materials. Powder preparation by mechanical methods is fairly mature area of ceramic processing in which the scope for new developments is rather small. However, in recent years, the preparation of fine powders of some advanced ceramics by mechanical methods involving milling at high speeds has received a fair amount of interest.

In comminution, our interest lines mainly in achieving certain physical characteristics, such as particle size and particle size distribution. However, the exploitation of chemical changes during milling for the preparation of powders has received some interest in recent years. Grinding enhances the chemical reactivity of powders. Rupture of the bonds during particle fracture results in surfaces with unsatisfied valences. This combined with the high surface area favors reaction between mixed particles or between the particles and their surroundings.

Powder preparation by high-energy ball milling of elemental mixtures is referred to by various terms, including mechano-chemical synthesis, mechano-synthesis, mechanical driven synthesis, and high energy milling. We will use the term mechano-chemical process in this thesis.

Mechano-chemical process can be carried out inside batch reactors, the grinding of powder by ball milling consists in a series of impacts during which powder particles become trapped between the external surfaces of two colliding bodies. Considerable efforts are currently devoted to a deeper understanding of fundamentals of mechanically driven processes and to the optimization of ball milling devices, which are intimately connected. Indeed, the nature and the rate of structural and chemical transformations depend on both the powder properties and the ultimate limit of structural and thermodynamic stability reached during the mechanical processing. The latter one, in turn, should be related to the severity of the force acting on, or to the energy transferred to, the powder trapped during a collision [6-11].

An advantage of mechano-chemical process is that the easy method for preparation of ceramic powders, solid state reaction is activated due to mechanical energy instead of the temperature that the chemical reactivity of starting materials could be improved significantly after mechano-chemical activation and subsequently, the calcinations temperature was reduced [12]. The mechanism of mechano-chemical process is not clear. One possibility is the occurrence of the reaction by a solid state diffusion mechanism.

The model and fabrication route of non-firing ceramics via mechanochemcally assisted chemical solidification were shown in Figure 1.2 and Figure 1.3, respectively. Key concept of non-firing ceramic, providing ceramic green body with an improved mechanical strength, wherein the ceramic green body is fabricated by activating ceramic powder through mechano-chemical treatment and solidifying the activated powder through alkali treatment. Activated ceramic powder having mechanochemically activated surfaces is obtained by milling ceramic powder using planetary ball mill (mechano-chemical process), and ceramic green body is obtained by adding alkali water solution containing alkaline metal hydroxide to the powder (alkali treatment process).

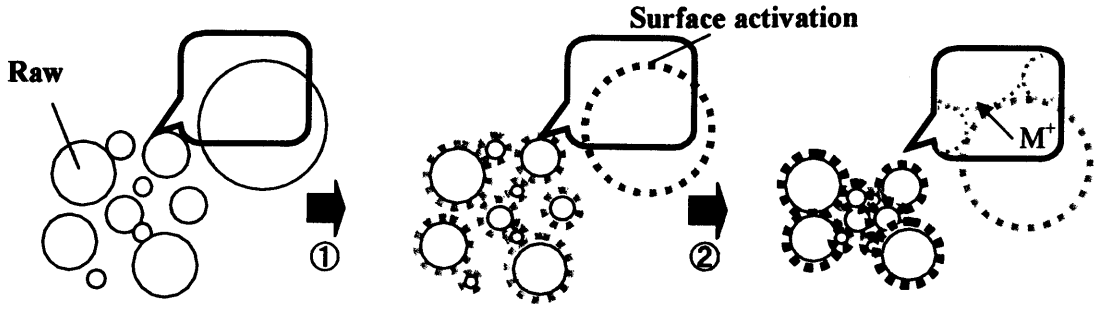

Figure 1.2 Non-firing ceramics fabricated from mechanochemically assisted chemical solidification

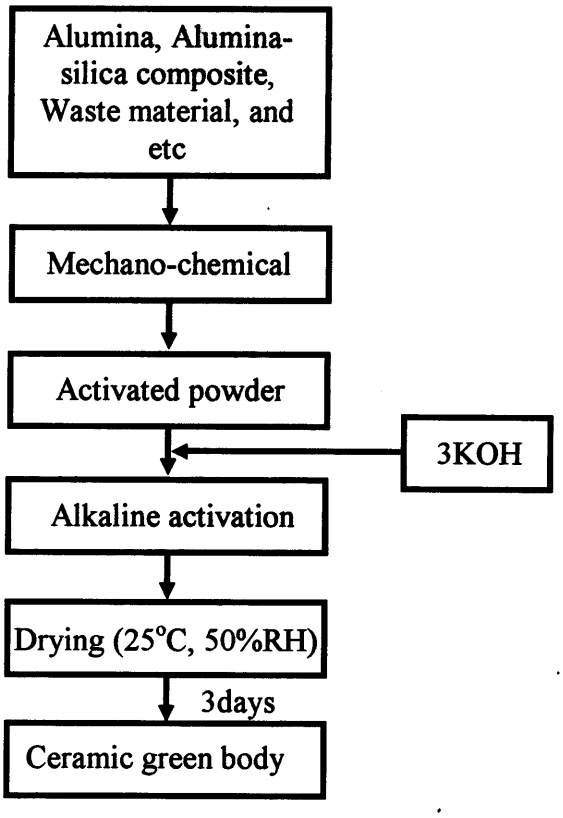

Figure 1.3 Fabrication routes of non firing ceramics

B. Planetary ball mills

The material is crushed and torn apart in two or four grinding bowls by grinding balls. The grinding balls and the material in the grinding bowl are acted upon by the centrifugal forces due to the rotation of the grinding bowl about its own axis and due to the rotating supporting disc.

The grinding bowl and the supporting disc rotate in opposite directions, so that the centrifugal forces alternately act in the same and opposite directions, This results in, as a frictional effect, the grinding balls running along the manner wall of the bowl, and as an impact effect, the balls impacting against the opposite wall of the grinding bowl. The impact effect is enhanced by the grinding balls impacting against one another.

Loss-free grinding, even in the case of grinding of suspensions, is guaranteed by a hermetic seal between the grinding bowl and the cover.

All samples in this thesis were milled using a Fritsch Pulverisette 5 Planetary Ball Mill. Movements of working part and ball in planetary ball mill were shown in Figure 1.4.

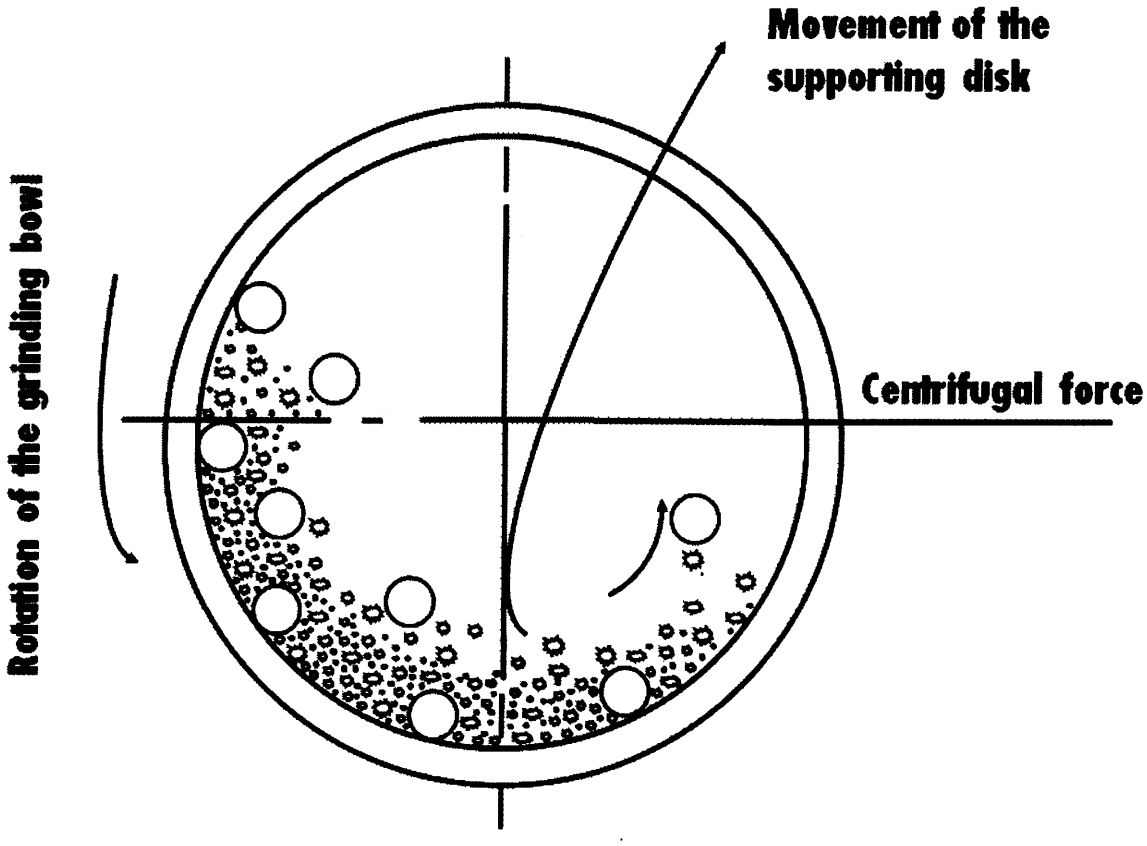

Figure 1.4 Movements of working part and ball in planetary ball mill [6]

1.3 Chemical solidification

Alkaline activation of ceramics powder using alkaline hydroxide and/or silicate solutions can be used to synthesis inorganic geopolymeric binders, or alkali-activated cements, displaying excellent physical and chemical properties [13]. Experimental evidence suggests that the principal binding phase within geopolymers, where activated powder obtain from mechano-chemical treatment are used, is ceramic green body consisting of framework of activated powder linked by K^+ alkali metal cations and shared Al, Si, O atom during chemical solidification.

1.4 Ceramic materials

Powder production is an important step in the synthesis of ceramics for structural as well as functional materials. The alumina-silica system, including the end members of the pure oxides, is probably the most important binary oxide system both in technology and science. Alumina, silica, and aluminosilicate compounds are widely used high-temperature materials, are important in mineralogy and geology, are basic material in glasses, and have many specialty applications. Then the compound mullite ($3Al_2O_3.2SiO_2$), which is the only stable unhydrated compound in the alumina-silica system, is considered.

The science of alumina (Al_2O_3) [14] is old and tremendous amounts of research work have been done over the years. Alumina was known long before that. The properties of alumina are described in this section.

A. Alumina

Aluminum, oxygen, and hydrogen form three crystalline compounds: A_2O_3, AlOOH, and $Al(OH)_3$. Pure, stoichiometrically defined aluminum oxide occurs in the crystalline modification corundum, α-A_2O_3. Two crystalline forms of AlOOH exist: diaspore, α-AlOOH, and boehmite, γ-AlOOH. Bayerite, α-$Al(OH)_3$; gibbsite, γ-$Al(OH)_3$; and nordstrandite are the three trihydroxides.

A comparison of nomenclatures from Ref. 14 is given in Table 1.1

Table 1.1. Comparison of Nomenclatures

Mineral Name	Chemical Composition	Accepted Crystallographic Designation	Alcoa (1930)
Gibbsite Hydrargillite	Aluminum trihydroxide	γ-$Al(OH)_3$	Alpha alumina trihydrate
Bayerite	Aluminum trihydroxide	α-$Al(OH)_3$	Beta alumina trihydrate
Nordstrandite	Aluminum trihydroxide	$Al(OH)_3$	
Boehmite	Aluminum oxide hydroxide	γ-AlOOH	Alpha alumina monohydrate
Diaspore	Aluminum oxide hydroxide	α-AlOOH	Beta alumina monohydrate
Corundum	Aluminum oxide	α-Al_2O_3	Alpha alumina

Alumina has many properties which makes the material interesting for applications in many different areas. For example, it is hard, stable, insulating, transparent, beautiful, etc. Alumina exist in a number of crystal phase, three of the most important being γ, θ, and α.

The α structure is thermodynamically stable at all temperature up to its melting point at 2051°C, but the meta stable phase (e.g., γ and θ) still appear frequently in alumina growth studies for reasons that are discussed in the following sections. All alumina phase are involved in transformation sequences, which all have in common that they end in the α phase

at high temperature. The transformations to the α phase are irreversible and typically take place at above 1000°C.

The α form of aluminum oxide is also known as *corundum* (the name comes from the naturally occurring mineral corundum, which consists of pure α-Al_2O_3). It is transparent and uncolored and is known in its single crystal form as *sapphire.*

Corundum, α-Al_2O_3, is the only thermodynamically stable form of aluminum oxide. It is a common mineral in igneous and metamorphic rocks; large, clear specimens have been used as gemstones for many centuries.

Corundum is one of the most important ceramic raw materials. Up to the 1960s, metallurgical alumina used in the Hall-Heroult process contained high amounts of α-Al_2O_3. In today's practice, lower calcinations temperatures are used to obtain a product which is only partially transformed to the stable oxide.

Corundum is very hard, its hardness exceeded only by that of diamond and a few synthetic compounds having the diamond structure. Alpha Al_2O_3 crystallizes in the hexagonal-rhombohedral system. Its structure was first investigated by Bragg and Bragg and by Pualing and Hendricks. The lattice represents a hexagonal closest packing of oxygen ions. Each Al ion is octahedrally coordinated by six oxygens. A model of structure is shown in Figure 1.5.

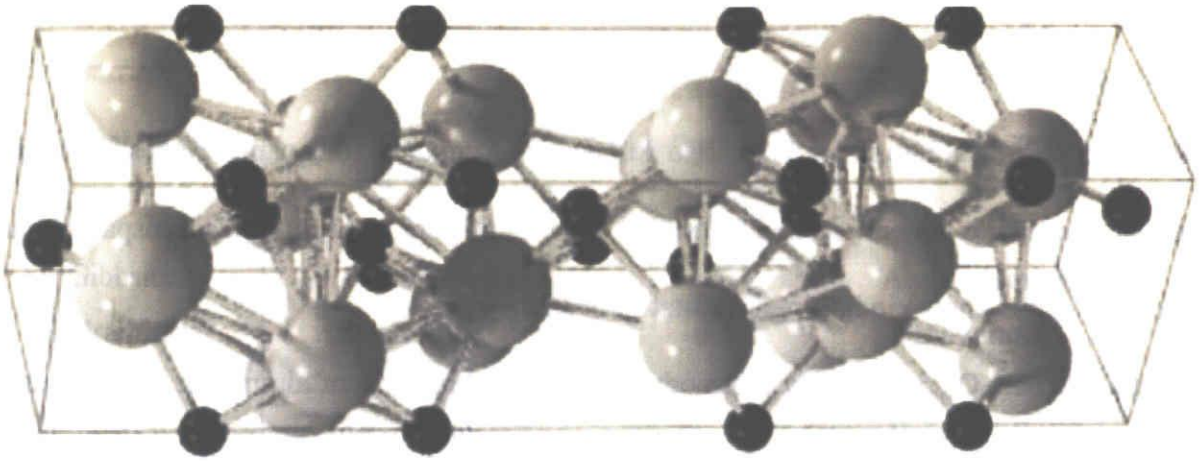

Figure 1.5 Unit cell of α-aluminum oxide (corundum). Black spheres represent aluminum and gray spheres correspond to oxygen atoms. Reprinted from [Al-Abadleh and Grassian (2003)], Copyright 2003, with permission from Elsevier.

B. Silica

Silicon dioxide (SiO_2) has a variety of structural forms. The building block of silica structures is the silicon-oxygen tetrahedron. Each silicon atom is surrounded by four oxygen atoms; each oxygen atom is bonded by two silicons. This tetrahedral configuration is remarkably stable and forms the elemental unit of structure in all silicates. In the pure silicas, these tetrahedral are bonded in a three-dimensional network, which has great chemical and mechanical durability. When the crystalline silica melts, the three-dimensional network is retained, so that the molten silica has a structure close to the crystalline. The result is a low heat of fusion and low-energy differences between different structures, leading to many structures. Above about 1350°C silica begins to vaporize by the reaction to silicon monoxide:

$$SiO_2 = SiO + \frac{1}{2}O_2$$

The SiO exists only in the vapor; it forms a mixture of SiO_2 and silicon on a solid surface as shown in Figure 1.6.

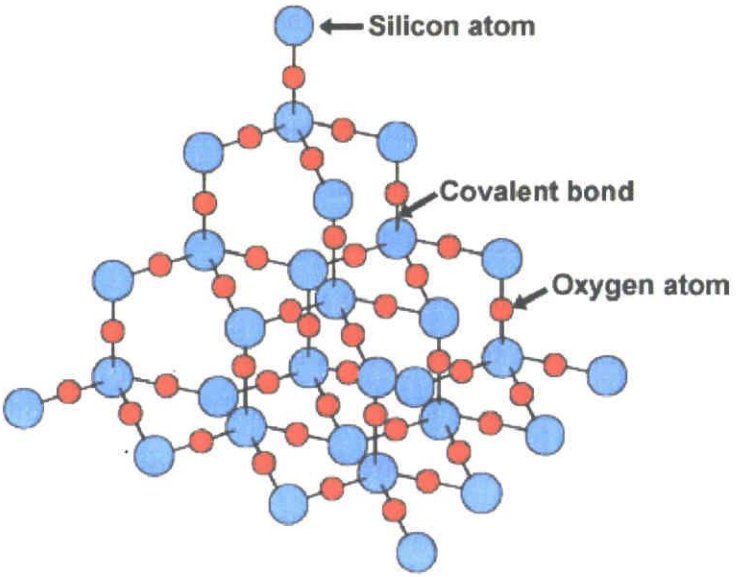

Figure 1.6 Unit cell of Silica. Blue spheres represent silicon atom and red spheres correspond to oxygen atoms.

C. Alumina-Silica System

The only stable unhydrated compound in the alumina-silica system is mullite ($3Al_2O_3.2SiO_2$) as shown in Figure 1.7. Mullite has been widely used in refractory brick and other high-temperature applications. It is often made by heating natural clays such as kaolinite, which is a hydrated aluminosilicate:

$$\underset{\text{kaolinite}}{3Al_2O_3.2SiO_2.2H_2O} = \underset{\text{mullite}}{3Al_2O_3.2SiO_2} + 4SiO_2 + 6H_2O$$

As mined, the kaolin includes impurities, especially oxides of alkali and alkaline earths and ion. Thus mullite made in this way is impure; because of the excess silica, a glassy silicate phase usually forms. This glassy phase flows at temperatures above 1200°C, limiting the usefulness of mullite made from the usual raw materials.

Mullite cannot be easily sintered to high density from mixed powders of silica and alumina; usually high porosity and a glassy silicate phase result. A dense, pure mullite can be made by sol-gel methods, for example, from mixtures of colloidal, hydrated alumina, and tetraethyl silicate or aluminum and silicon alkoxides. This mullite has superior high-temperature

properties; it shows much better creep resistance than polycrystalline alumina at temperatures from 1400 to 1650°C.

Mullite has a complex orthorhombic crystal structure containing chains of aluminum ions six- and four- coordinated to oxygen, and tetrahedral of silica. Both silicon and aluminum ions can move into normally unoccupied tetradedral sites, which is one reason for the solid-solution and nonstoichiometric phase boundaries. The unit cell can be represented by the formula $Al_{(4+2x)}Si_{(2-2x)}O_{(10-x)}$, in which x is the number of oxygen vacancies per unit cell. Values of x from 0.25 to 0.4 give mullite-alumina solid solutions from Al_2O_3 to SiO_2 ratios from 3:2 to 2:1. Mullite is chemically durable in acid metal slags and most gases at high temperatures as shown in Figure 1.8. It has a low thermal expansion coefficient, giving it good thermal shock resistance. The value of mullite as a quality high-temperature material appears to have been underestimated in the past; it has excellent intrinsic properties, and the above and new methods of synthesis should make mullite to be one of the most important "advanced" high-temperature oxides.

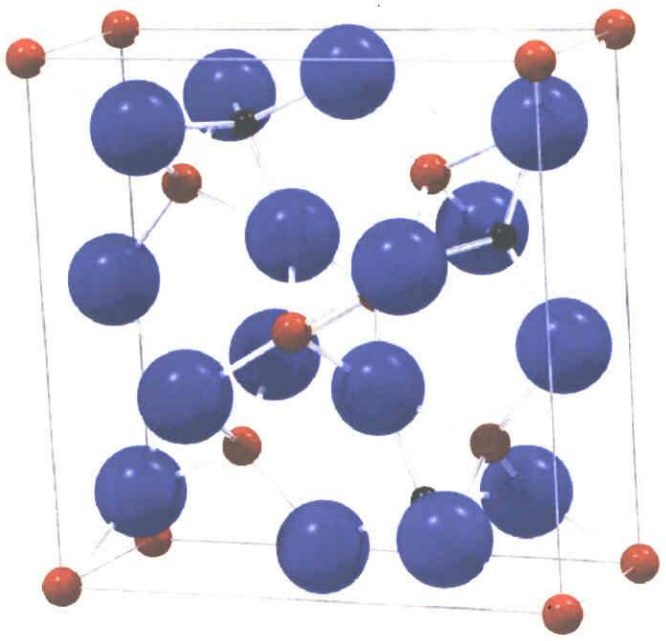

Figure 1.7 Unit cell of Mullite. Blue spheres represent alumina atom, red sphere represent silica atom, and black spheres correspond to oxygen atoms.

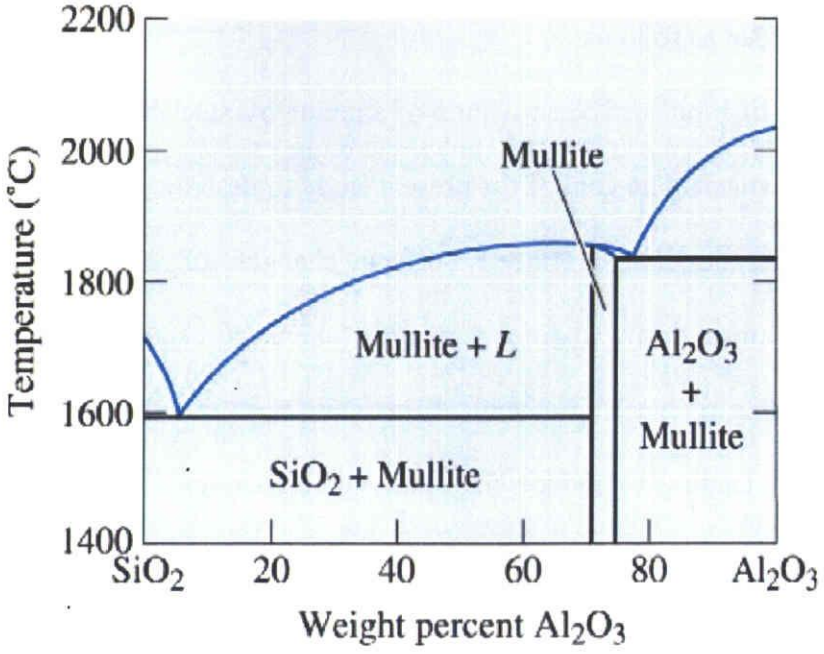

Figure 1.8 Alumina-silica phase diagrams [15]

4. Objective of this work

The goal of this thesis is to studies the influence of the operational conditional conditions (rotation speed, milling time, size of ball, and etc) using planetary ball mill on the introduction of microstructure characteristics and chemical bonding between interface surface of particles during mechano-chemical treatment on alumina, alumina-silica composite and/or waste materials. Another goal of this thesis was also to establish appropriate conditions for fabricating non-firing ceramics by mechanochemically assisted chemical solidification. As part of this study, the chemical bonding between interface surfaces of particles are confirmed on the mechanochemically activated particles with solidification mechanism by surface characterization. Accordingly, the determined conditions are used for fabricating non-firing ceramics by mechano-chemical treatment. This thesis is expected to contribute new method to fabricating non-firing ceramics, which a low cost, simple method and reduce sintering temperatures to environment-friendly.

The thesis is organized as follows:

In Chapter 2, Investigation surface activation of alumina by mechano-chemical treatment and solidification mechanism. The goal of the present study to describe the influence of mechano-chemical treatment on the interfaced surface changes of alumina (corundum) and solidification mechanism during alkaline activation (chemical reaction), as well as to visualize how an understanding of mechano-chemical treatment produces the activated powder using planetary ball mill leading to reduce the sintering temperature, improved the mechanical strength of ceramic green body and produce the non-firing ceramics.

In Chapter 3, Preparation alumina-silica composite assisted by mechano-chemical treatment. In this present study to investigation the effect of composition ratio between alumina-silica by mechano-chemical treatment which should lead to new applications of ceramics.

In Chapter 4, Fabrication of non-firing ceramics from paper sludge ash by mechano-chemical treatment using planetary ball mill. In this study, the effects of the operational conditions in the MC treatment process such as rotational speed, milling time and size of ball on the mechanical properties of the solidified body were investigated to fabricate non-firing ceramic products.

In Chapter 5, Fabrication porous ceramics using waste materials by non-firing process. This present study is focusing on the development of pore structure of BPSA by presence of the tire composite, mechano-chemical effect and addition of alkaline solution at various reaction temperatures to fabricate porous ceramics material.

Finally, in Chapter 6, the concluding remarks of the present work were stated and the future directions of this research work were recommended.

References

[1] H. N. Rahanan, Ceramic Processing and sintering, 2nd ed, Marcel Dekker, Inc, USA, 2003.

[2] T. J. Wallington, J. Srinivasan, O. J. Nielsen, E. J. Highwood, Greenhouse gases and global warming, Encyclopedia of Life Support Systems (EOLSS)

[3] H. Jantunen, R. Rautioaho, S Leppavuori &Uusimaki A, Preparing low loss LTCC material without glass addition. J. Eur. Ceram. Soc., 83 (2000) 2855-2857.

[4] H. Eroglu, O. Ucuncu, H. H. Acar, The effect of dry sludge addition supplied from pulp mill on the compressive strength cement. J. Uni. Chem. Tech. Met., 42, 2 (2007) 169-174.

[5] J. L. Provis, Modelling the formation of geopolymers; Doctoral Thesis, The University of Melbourne, 2006.

[6] F. Delogu, R. Orru, G. Cao, A novel macrokinetic approach for mechanochemical reactions. Chem. Eng. Sci., 58 (2003) 815-821.

[7] F. Delogu, G. Cocco, Compositional effects on the mechanochemical synthesis of Fe-Ti and Cu-Ti amorphous alloys by mechanical alloying. J. Allo. Com., 352 (2003) 92-98.

[8] T. Tsuzuki, P. G. McCormick, Synthesis of Cr_2O_3 Nanoparticles by mechanochemical processing. Acta. Mater., 48 (2000) 2795-2801.

[9] G. Tzvetkov, N. Minkova, Sol. Sta. Ion., 116 (1999) 241-248.

[10] H-I. Hsing, F-S. Yen, Effects of mechanical treatment on phase transformation and sintering of nano-sized γ-Fe_2O_3 powder. Cer. Int., 29 (2003) 1-6.

[11] V. P. Balema, V. K. Pecharsky, K. W. dennis, Solid state phase transformation in LiAlH4 during high-energy ball-milling. J. Allo. Com., 313 (2000) 69-74.

[12] B. D. Stojanovic, Mechanochemical synthesis of ceramic powders with perovskite structure. J. Mat. Pro. Tech., 143-144 (2003) 78-81.

[13] W. K. W. Lee, J. S. H. van Deventer, Chemical interactions between siliceous aggregates and low-Ca alkali-activated cements. Cem. Con. Res., 37 (2007) 844-855.

[14] L. D. Hart, Alumina chemicals. Science and Technology Handbook, Amer. Cer. Soc, Inc, USA, 1990.

[15] J. Temuujin, K. Okada, K. J. D. MacKenzie, Formation of mullite from mechanochemically activated oxides and hydroxides. J. Eur. Cer. Soc., 18 (1998) 831-835.

II. INVESTIGATION SURFACE ACTIVATION OF ALUMINA BY MECHANO-CHEMICAL TREATMENT AND SOLIDIFICATION MECHANISM

2.1 Introduction

Recently, Mechano-chemical treatment as a novel method involving the mechanical activation [1, 2], a process for introduction of additional energy to the system applies worldwide. During the treatment, various structural changes of the material are taking place. These structural changes of the material cause its properties changes (chemical, electrical, thermal, mechanical, etc) as well as its reactivity improvement. The most popular devices, in which mechano-chemical processes can be conducted are vibratory, planetary and attritor ball mills. They differ in their capacities, efficiencies of milling and additional arrangements such as cooling. In all these devices, the ground material is periodically thrown into zones of ball collisions. Energy transfer to the powdered particles takes place by shearing and/or impact action of the balls [3, 4]. Mechano-chemical treatment by planetary ball mill is now recognized as a powerful tool for the synthesis of materials, such as amorphous alloys [5], nanocrystalline metals and alloys [6] and ceramic materials [7]. This method is very simple and economic for the production of powders of very small size. The use of fine starting materials and mechano-chemical treatment by efficient activation are the key steps in this process. Therefore, this study examined whether mechano-chemical treatment of starting materials using ball milling activation can reduce the sintering temperature of solid state reacted [8].

Powder production is an important step in the synthesis of ceramics for structural as well as functional materials. Alumina (Aluminum oxide; α-Al_2O_3) has advantages such as its thermal, chemical, and physical properties when compared with several ceramic materials. It's a wide variety of application. Alumina ceramics are also well known for their low electrical and thermal conductivity, refractory bricks, electrical insulating components abrasives and integrated circuit (IC) packages [9]. Thereby lending themselves to many practical applications. Because of their technological importance, their non-firing ceramic processing by chemical bonding from mechano-chemical treatment deserves investigation.

The goal of the present study to describe the influence of mechano-chemical treatment on the microstructure and interfaced surface changes of α-alumina, as well as to visualize how an understanding of the mechano-chemical treatment produces the activated powder using planetary ball mill lead to a better understanding of reaction form new bonding during milling and solidification.

2.2 Experimental Procedure

2.2.1 Activated powder from mechano-chemical treatment

The experimental flowchart of non-firing ceramic was presented in Figure 3.1. The α-alumina, Al_2O_3 or corundum (Al-160SG-4, Showa-denko Co., Japan) of 0.6 μm mean particle size (D_{50}), was used as starting material. Planetary ball mill (pulverisettle 5, Fritsch, Germany) was used for mechano-chemical treatment under air at room temperature. To investigate the effect of milling conditions, controlled milling was performed in shearing mode, where the powders experience mostly shear forces, and in the higher impact mode, where significant impact forces are produced via ball-ball and ball-mill collisions. The mechano-chemical conditions were

varied as follow.

2.2.1.1 Rotation speed

Each milling was carried out with a 100 g sample in a 500 ml capacity ceramic zirconia pot with 400 g zirconia balls of 10 mm in diameter. The mill was rotated at different periods of rotate speed interval up to 300 rpm at 60 min.

2.2.1.2 Milling time

Each milling was carried out with a 100 g sample in a 500 ml capacity ceramic zirconia pot with 400 g zirconia balls of 10 mm in diameter. The mill was rotated at different time speed interval up to 60 min at 300 rpm.

2.2.1.3 Diameter of ball

Each milling was carried out with a 100 g sample in a 500 ml capacity ceramic zirconia pot with 400 g zirconia balls. The mill was rotated at rotation speed 300 rpm and milling time 60 min. The diameter of ball was varied from 1-15 mm, respectively.

2.2.1.4 Ball to Powder weight ratio

Each milling was carried out sample in a 500 ml capacity ceramic zirconia pot with 400 g zirconia balls. The mill was rotated at rotation speed 300 rpm, milling time 60 min and diameter of ball 10 mm. The ball to powder weight ratio was varied from 2:1 to 40:1, respectively.

All milling parameter of mechano-chemical conditions using planetary ball mill were shown in Table.1.

2.2.2 Ceramic green body

Then, activated alumina powder was mixed with 3 mol dm^{-3} of KOH at 2,000 rpm for 5 min with an electric mixer. After mixing and reacted, the slurry was pour into the mold at 25°C for 50% relative humidity until it becomes solid, and demolding. Finally, the specimens were dried in the steam oven until 3 days to obtain ceramic green body.

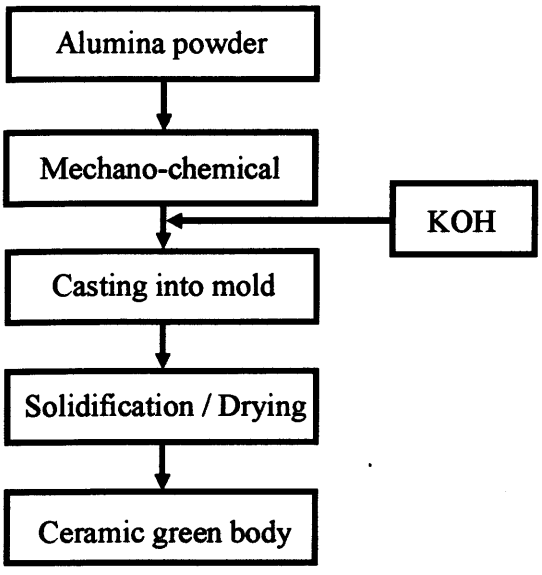

Figure 2.1 Non-firing ceramic flowchart by mechano-chemical treatment

Table 1 Milling parameters of planetary ball mill

Planetary ball mill	Rotation speed	Milling time	Diameter of balls	Ball to Powder weight ratio
Total powder mass (g)	100	100	100	10-200
Ball to powder weight ratio	4:1	4:1	4:1	2:1 – 40:1
Ball material	Zirconia	Zirconia	Zirconia	Zirconia
Vial material	Zirconia	Zirconia	Zirconia	Zirconia
Vial capacity (ml)	500	500	500	500
Rotation speed (rpm)	100-300	300	300	300
Milling time (min)	60	10-60	60	60
Diameter of balls (mm)	10	10	1-15	10

2.2.3 Application mechano-chemical treatment with different alumina

The raw material was α-Al_2O_3 (AA-04) of 0.5 μm mean particle size from Sumitomo Chemical Co., Ltd, and KOH pellets (JIS K 8574). Planetary ball mill was used for mechano-chemical treatment of starting material. The mill was rotated at 300 rpm and different milling time form 0 to 60 min. After being mixed with 3 mol dm^{-3} of KOH (alkali treatment) at 2,000 rpm for 5 min with an electric mixer, the slurry was poured to Teflon mold and kept at room temperature until solidification. After demolding, the specimens were dried at 25°C, 50%RH for 3 days in the steam oven to obtain ceramic green body.

2.3 Results and Discussion

2.3.1 Effect of rotation speed

2.3.1.1 XRD Characterization of activated powder

One of the phenomena of interaction of X-rays with crystalline matter is its diffraction, produced by the reticular planes that form the atoms of the crystal. A crystal diffracts an X-ray beam passing though it to produce beams at specific angles depending on the X-ray wavelength, the crystal orientation and the structure of the crystal.

In the macroscopic version of X-ray diffraction, a certain wavelength of radiation will constructively interface when partially reflected between surface (i.e., the atomic planes) that produce a path difference equal to an integral number of wavelengths. This condition is described by the Bragg law:

$$2d\sin\theta = n\lambda$$

Where n is an integer, λ is the wavelength of the radiation, d is the spacing between surfaces and θ is the angle between the radiation and the surfaces. This relation demonstrates that interference effects are observable only when radiation interacts with physical dimensions that are

approximately the same size as the wavelength of the radiation. Since the distances between atoms or ions are on the order of 10^{-10} m (1A°), diffraction methods require radiation in the X-ray region of the electromagnetic spectrum, or beams of electrons or neutrons with similar wavelength.

So, through X-ray spectra one can identify and analyse any crystalline matter. The degree of crystallinity or order will conditionate the quality of the obtained result. In order to do this, a diffractometer is needed. Basically, an X-ray diffractometer consists in an X-ray generator, a goniometer ans sample holder and an X-ray detector, such as photographic film or a movable proportional counter. The most usually employed instrument to generate X-rays are X-ray tubes, which generate X-rays by bombarding a metal target with high energy (10-100KeV) electrons that knock out core electrons. Thus, an electron in an outer shell fills the hole in the inner shell and emits an X-ray photon. Two common targets are Mo and Cu, which have strong K_α X-ray emissions at 0.71073 and 1.5418 A°, respectively.

The most interesting X-ray diffraction techniques for this work are those related to the analysis of polycrystalline materials and mainly of powders. In this case the powder provides all the possible orientations of the small crystals giving rise to a large number of diffraction cones, each one corresponding to a family of planes satisfying the Bragg' s law. For large grains, rings are discontinuous and formed by small pots. As the size of the grains diminishes, the spots are closer and for an optimum size a continuous ring is obtained, which is transferred into a peak when working with graphic registers or lines in a photographic register. For lower grain sizes the clarity of rings is lost again and wide peaks or band appear. When the crystal is not randomly but preferentially oriented the intensity of the different rings and along each ring is not uniform.

The determination of the size of the crystals in a powder can be carried out thanks to measurements that must be made on the profile of the diffraction peaks. One of the functions that best describes the powder diffraction profiles is the Voigt function. This consists in a convolution product of a Lorentzian and Gaussian function. Model size (Lorentzian component) and strain (Gaussian component) line-broadening contributions simultaneously. Separate instrumental and specimen contributions to the diffracted line profile. Instrumental broadening is due to causes as slit widths, sample size, penetration in the sample, imperfect focusing, etc.

In practice, however, if one can neglect the micro-strain effects, which in addition sometimes give rise to mistakes and incongruencies in the evaluation of grain size, the above formulation reduces to the well-known Scherrer formula. Scherrer showed that the average dimension of the crystals that compose a crystalline powder is related with the profile of the peak by means of the equation:

$$D = \frac{K\lambda}{\beta \cos\theta}$$

Where K is a proportionality constant approximately similar to the unit, β the FWHM of the peak in radians (theoretically corrected from the instrumental broadening), D the size of crystal in the direction perpendicular to the reflecting planes and λ the wavelength of the X-rays used. This is the most usual and simple equation that allows to the evaluate grain size.

The raw and activated alumina powders were characterized by X-ray diffraction (XRD). In order to determine the crystal size change of the treated alumina at different rotational speed using planetary ball mill was picked up at regular intervals for X-ray diffraction analysis in figure 2.2 (a) corresponds to 0, 100, 150, 200, 250 and 300 rpm at 60 min, respectively. The diffraction peaks at different 2θ correspond to the (0 1 2), (1 0 4), (1 1 0), (1 1 3), (0 2 4), (1 1 6), planes, respectively. No changes in XRD patterns were observed. The raw powder presents sharp peaks

indicating the high crystallinity of the sample. The results after treated by mechanochemically indicate that the intensity peaks broaden slightly with increasing rotational speed up to 300 rpm. Since the mechano-chemical treatment creates defects or leads to amorphisation of crystalline size with planetary ball mill. However, there is no measurable shift of these peaks after 300 rpm in rotation speed and 60 min in milling time, even for the peaks with high 2θ values, when compared to the peak positions in XRD pattern for the alumina starting powder.

The effect of KOH addition on ceramic green body synthesis was investigated using activated samples at different mechano-chemical treatment of rotation speed. Figure 2.2(b) shows XRD patterns of solidified alumina at different rotation speed of activated powder. Only the peaks associated with Al_2O_3 and KOH were observed in the patterns of starting materials. After chemical reaction, only typical Potassium alanate ($KAlH_4$) peaks in range $2\theta = 28\text{-}32^\circ$ were detected, indicating that the reaction Al_2O_3 + KOH lead to new bonding and new composition as equation

Al_2O_3 + KOH → $KAlH_4$. It also can be deduced that the mechanical strength depend on total number of bonding from mechano-chemical treatment.

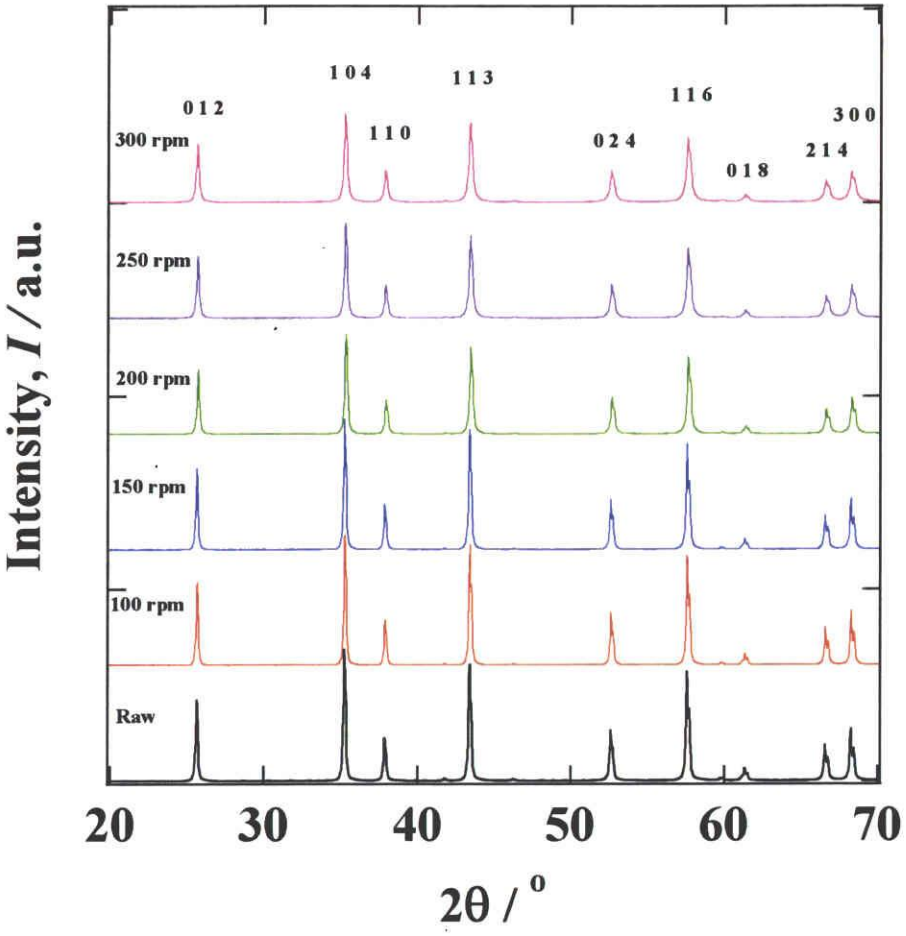
Intensity, I / a.u.
300 rpm
250 rpm
200 rpm
150 rpm
100 rpm
Raw
012
104
110
113
024
116
018
214
300
20
30
40
50
60
70
2θ / °

(a)

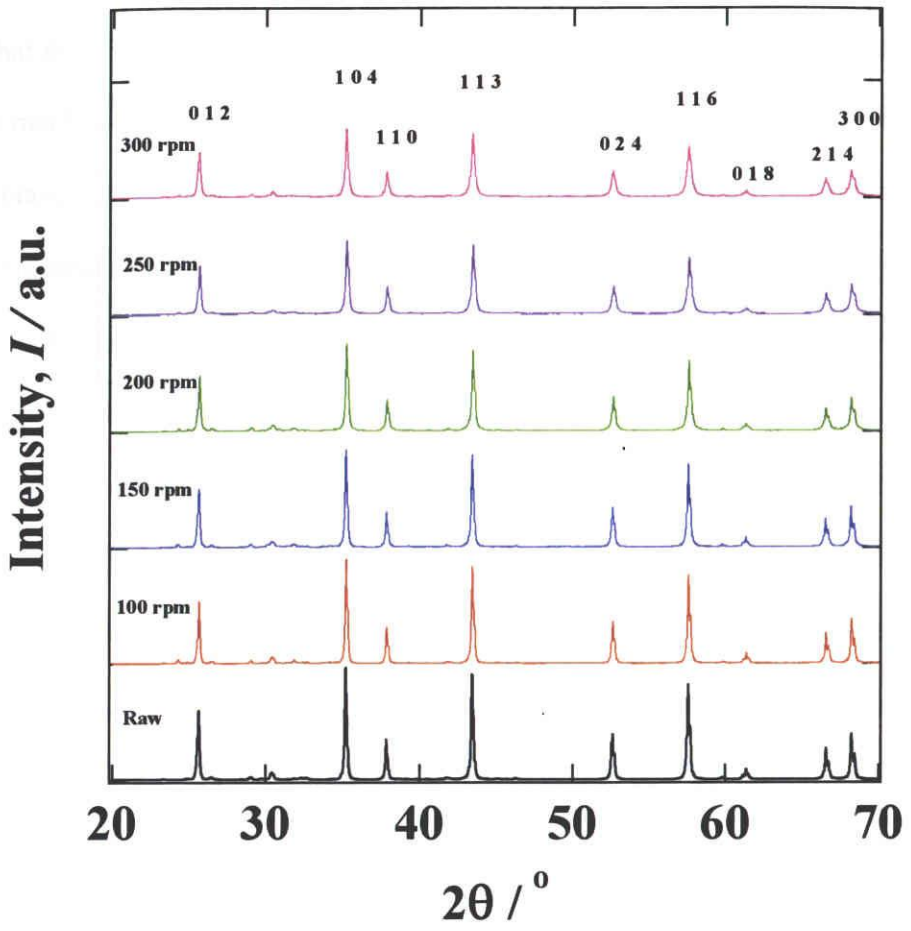

(b)

Figure 2.2 XRD patterns of mechano-chemical treated alumina by planetary ball mill at different rotation speed for 60 min; (a) activated powder, (b) ceramic green body

The XRD measurements of the alumina powders showed that the XRD lines become substantially broadened upon rotation speed (Fig. 2.2). This broadening can be ascribed to crystallite-size reduction and introduction of lattice strain as shown in next sections. From Figure 2.2, it can be further observed that mechano-chemical condition (300 rpm and 60 min) brings about much broader peaks and it is expected to yield smaller crystallite size and higher lattice strain. The quantitative comparison of line breadths (FWHM) is depicted in Figure 2.3 for

samples with different rotation speed of planetary ball mill. It can be observed that the mechano-chemical condition (300 rpm and 60 min) brings about the maximum broadening of reflection peaks. The broadening for the samples milled with planetary ball mill differs primary; the milled product (300 rpm and 60 min) shows slightly larger broadening than the raw material. These indicate the changes in crystallite size and lattice strain in different milling environments.

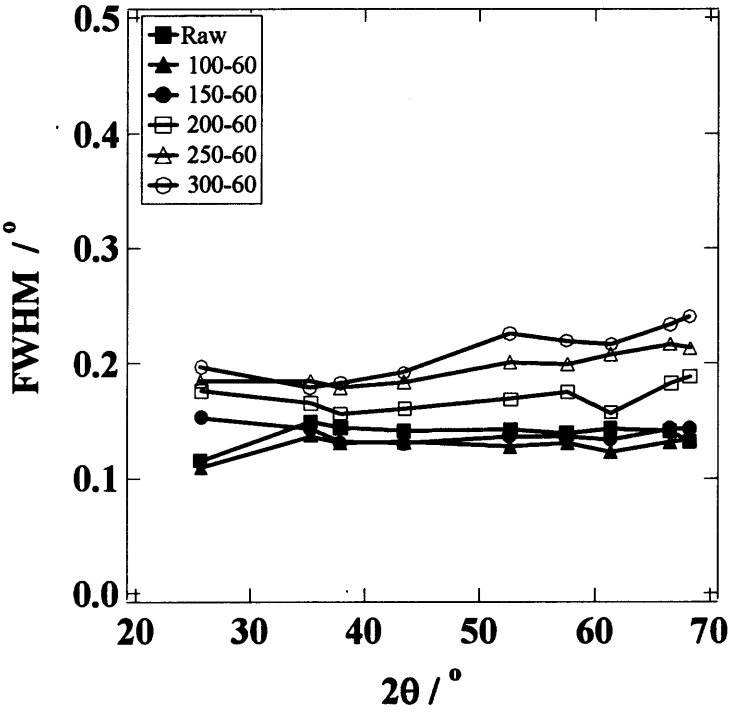

Figure 2.3 The changes of physical FWHM for activated alumina in different mechano-chemical treatment at different rotation speed for 60 min

Upon close examination of a powder diffraction pattern one should notice that as 2θ increases the peaks become broader. There are a number of reason for this, including the focusing of the X-rays onto the sample, the angular aperture of the detector, the nature of the sample itself, and of course the nonlinear relationship between d-spacing and 2θ. The following equation is often used to characterize this broadening for Cauchy profiles

$$FWHM_C = u\tan\theta + \frac{v}{\cos\theta}$$

While for Gaussian profiles the equation is

$$FWHM_G = \sqrt{u\tan^2\theta + v\tan\theta - w}$$

In both case u, v and w are constants determined by fitting the widths of peaks from a line-width standard. Once the instrumental broadening B_{ist} of a diffractometer has been determined one can extract the pure sample broadening $B_{size+strain}$ from the measured sample broadening B_{obs}. In each B refers to the full-width-half-max of the peak, and for the Cauchy profile

$$B_{size+strain} = B_{obs} - B_{ist}$$

While for Gaussian profile

$$B^2_{size+strain} = B^2_{obs} - B^2_{ist}$$

The Scherrer equation

$$B_{size} = \frac{K\lambda}{L_{vol}\cos\theta_B}$$

offers a simple relationship between crystallite size and peak broadening. Here λ is the wavelength of the X-ray, B_{size} is the width (in radians) of the peak due to size effects, K is a constant whose value is approximately 0.9, and θ_B is the Bragg angle. This equation represents broadening that is due to the finite size of the crystal where for very small crystals the intensity of X-rays at close to, but not exactly, the Bragg condition is not zero. And the winner will all be an individual

Lattice strain is due to imperfections within the crystalline lattice, including vacancies, dislocations, stacking faults, and others. The 2θ dependence of lattice strain on peak broadening is

$$B_{strain} = \eta \tan\theta$$

Where η is the strain

The pure sample broadening contains both strain and size broadening

$$B_{size+strain} = B_{size} + B_{strain}$$

$$B_{size+strain} = \frac{K\lambda}{L_{vol}\cos\theta_B} + \eta \tan\theta$$

Afterward, the crystalline size and lattice strain were obtained by fitting to the Williamson-Hall equation

$$B_{size+strain}\cos\theta = \frac{K\lambda}{L} + \eta \sin\theta$$

Which is of the form y = b + mx where η would be the slope of a line on a $\sin\theta$ - $B_{size+strain}\cos\theta$ plot. Once the value of η is known then B_{strain} and can be determined and also L_{vol}.

The crystalline size of the powder was calculated by peaks of XRD patterns using Williamson-Hall and Scherrer formula. From Williamson-Hall plot curves it can be estimated the crystalline size (intercept at $\sin\theta = 0°$), and lattice strain (slope). By Figure 2.4 show the evolution of crystalline size at different rotation speed. The crystalline size slightly decreases with rotation speed, while the behavior of lattice strain increases is the opposite. This suggests that the lattice and size contributions exist simultaneously in activated samples. The increase of physical broadening vs. rotation speed indicates that intensive milling extend great defects and deformations in materials.

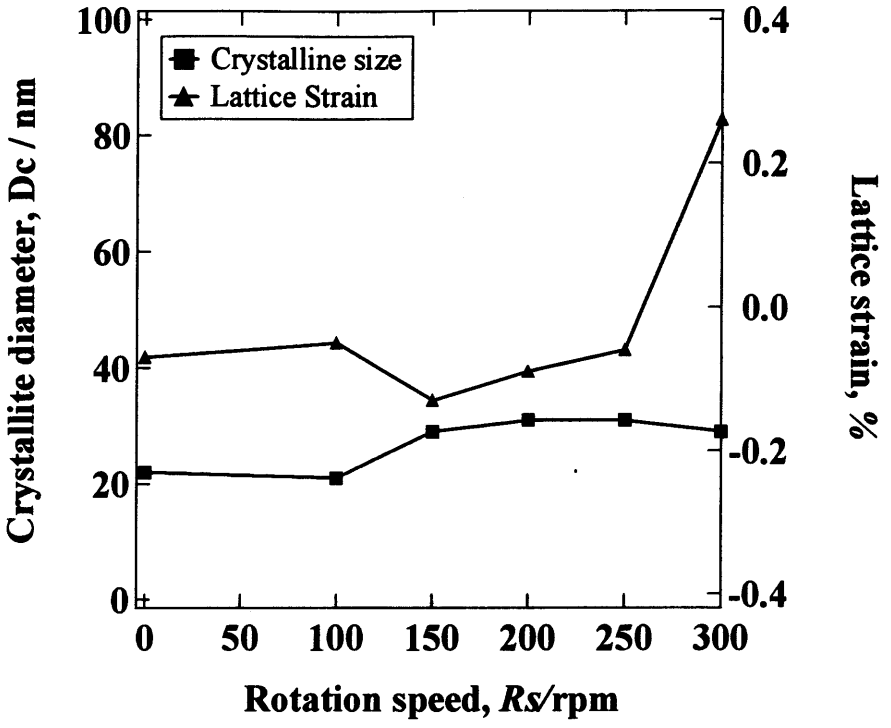

Figure 2.4 X-ray peaks broadening (β) as a function of Bragg angle (θ) for the milled sample and Evolution of crystalline size and lattice strain obtained from Williamson-Hall method at different rotation speed for 60 min

Also, we have determined the crystalline size using the Scherrer formula. Figure 2.5 show average crystalline size at different rotation speed obtained by both the Williamson-Hall and Scherrer methods is compared. By average crystalline size were slightly decrease with mechano-chemical treatment. The crystalline sizes calculated by Scherrer formula are higher than those obtained by Williamson-Hall plot. This difference could be due to the fact of peak broadening associated to lattice stain is not considered in the Scherrer model [15].

$$\text{Crystallite size} = 0.9\lambda / \beta.\cos\theta$$

The width β is usually measured, in radians, at intensity equal to half the maximum intensity (FWHM), λ is the wave length of the x-ray radiation and θ is the Bragg angle.

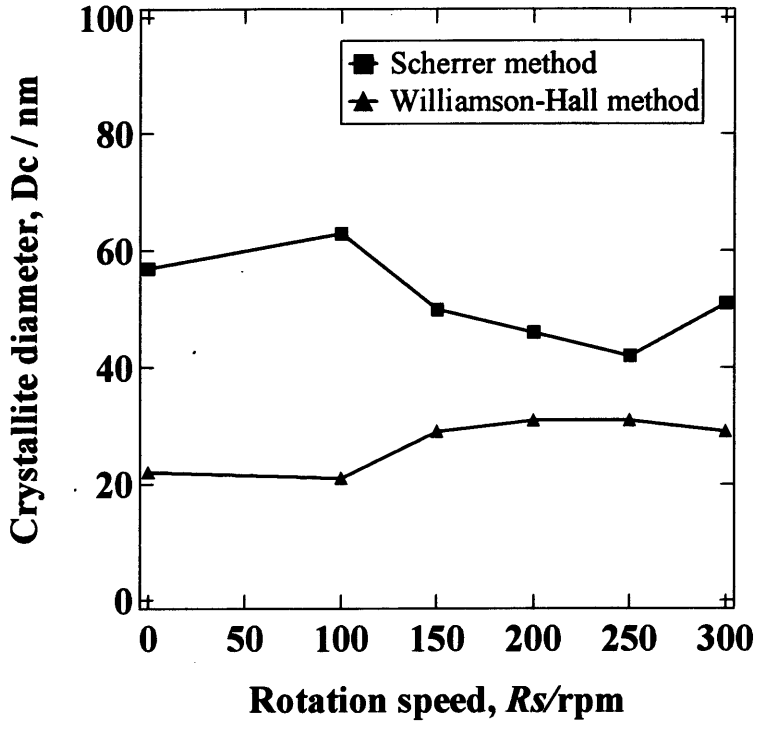

Figure 2.5 Comparison of the evolution of crystalline size between the Scherrer and Williamson-Hall methods at different rotation speed for 60 min

2.3.1.2 BET and Mean particle size characterization of activated powder

The physical adsorption of gas molecules on solid surface and serves as the basis for an important analysis technique for the measurement on the specific surface area of a material were explain by BET theory. The BET equation gives reasonable values in the range of relative pressure (P/P_0) from 0.05 to 0.35. They conclude that in the range of relative pressure, monolayer is formed. The specific surface area of the powders was measured by nitrogen adsorption at 77 K (BET method). Before BET analysis the powders were heated to 200°C in air for 2 h to remove the moisture from the particle surface. On the other hand, the mean particle size of powder after mechano-chemical activated by ball milling was observed by dynamic light scattering particle size analysis (DLS). Dynamic light scattering particle size analyzers are used to measure the size of very small

particles (0.6 nm to 6 um) in solution. This class of particle size analyzer interprets particles' sizes from the fluctuations in scattered laser light created by the particles' Brownian motion. Dynamic light scattering analysis is used in medical, biological research and materials science applications, and is also known as photon correlation spectroscopy or quasi-electron light scattering. By the BET surface area increases but average particle size (d_{50}) decreases during mechano-chemical treatment of rotation speed. Higher levels of specific energy input favor the production of great surface area. The specific surface area slightly increases up to 1.2 times after consuming the energy of 0.0045 $kJ.g^{-1}$ using the planetary ball mill. The generation rate of surface area at lower level of energy input is larger than the higher level of energy input. This can be ascribed to the fact that the breakage rates. The mean particle size of alumina powder decreased from 0.619 μm to 0.467 μm, respectively, after 300 rpm and 60 min of treatment condition.

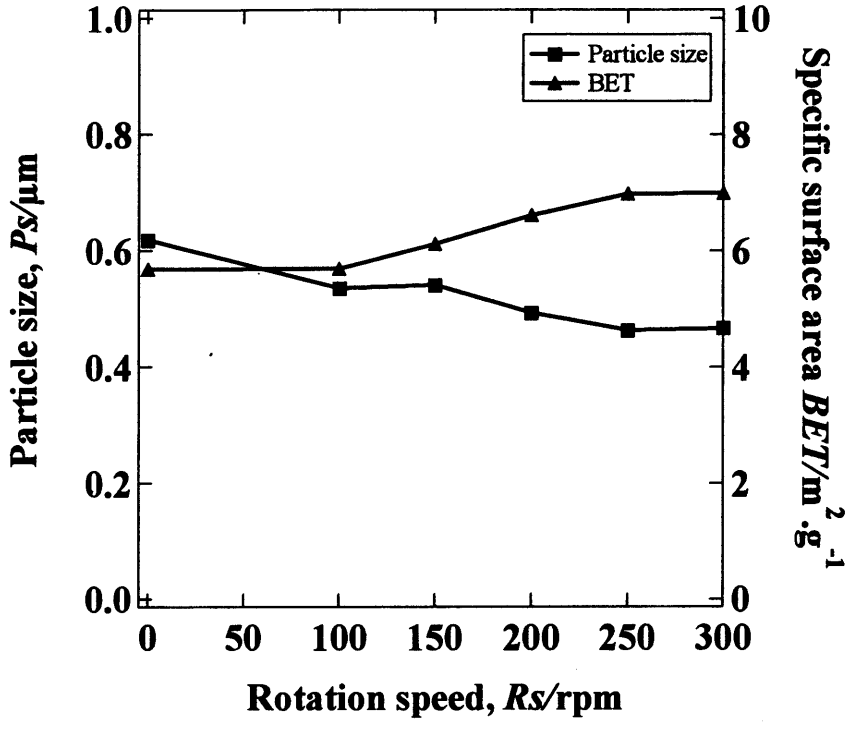

Figure 2.6 BET surface area and Mean particle size of alumina treated by planetary ball mill at different rotation speed for 60 min

2.3.1.3 ICP characterization of activated powder

Flames and electrical discharges have been an important part of chemical analysis for a long time. In these techniques, the sample is decomposed by intense heat into a cloud of hot gases containing free atoms and ions of the element of interest. In optical emission spectrometry (OES) the sample is subjected to temperatures high enough to cause not only dissociation into atoms but to cause significant amounts of collision excitation (and ionization) of the sample atoms to take place. Once the atoms or ions are in their excited states, they can decay to lower states through thermal or radiative (emission) energy transitions. Thus, the intensity of the light emitted at specific wavelengths is measured and used to determine the concentrations of the elements of interest. One of the most important advantages of OES results from the excitation properties of

the high temperature sources used in OES, because they can populate a large number of energy levels that can emit, and this results in the flexibility to choose from several different emission wavelengths for an element and in the ability to measure emission from several different elements concurrently. ICP analysis is one of the most popular elemental analysis techniques, generally a trace analysis technique which utilizes dilute solution of dissolved analyses aspirated into high- energy plasma to generate measurable emission signals for precision analysis. Most samples begin as liquids that are nebulized into an aerosol, a very fine mist of sample droplets, in order to be introduced into the ICP. The aerosol is then carried into the centre of the plasma by an argon flow. The first function of the high temperature plasma is to remove the solvent from the aerosol, usually leaving the sample as microscopic salt particles. The next steps involve decomposing the salt particles into a gas of individual molecules (vaporization) that are then dissociated into atoms (atomization). Afterwards, the sample is excited and noised. The gas temperature in the centre of the ICP is about 8000K, so high as to reduce or eliminate many of the chemical interferences found in flames and furnaces. One way to correct matrix interferences is internal standardization, i.e., the potential for calibration with synthetic standards, which is a major advantage of ICP-OES, as it avoids the need to use chemically analyzed secondary solid standards. Internal standardization is commonly used in a genuine effort to improve performance at high concentration levels. Normally, the internal standard element is introduced at some stage of the dissolution procedure. Although no universal choice of internal standard can be made, an internal standard must satisfy the following conditions: (i) The internal standard element should not be present in the samples; (ii) Chemical compatibility with the sample must be maintained; (iii) Spectral interferences should not be significant on the internal standard line, as the internal standard concentration is usually quite low.

ICP analysis revealed several interesting trends in the chemical composition of material. Results in figure 3.7 showing quantitative evolution of aluminum ion due to mechano-chemical treatment were carried out at different rotation speed which confirms leaching of concentration of aluminium ion increases significantly with mechano-chemical activation. For Al^{3+} in the sample with raw and MC-treated (300rpm and 60 min) of milling, whose concentration was 2.3 and 67 ppm, respectively. The low concentrations of solutions were measured with good reproducibility.

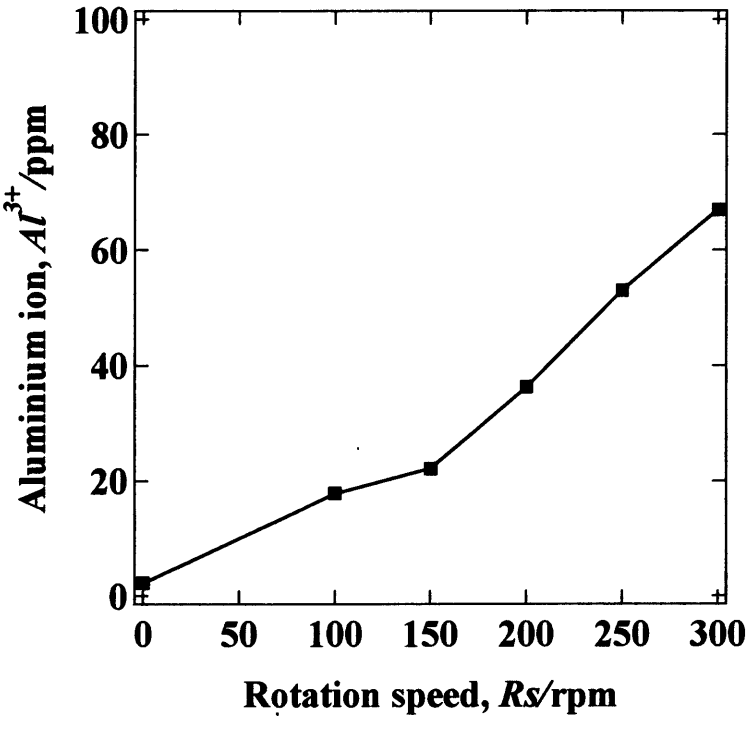

Figure 2.7 Elution behavior of the alumina by planetary ball mill at different rotation speed for 60 min

2.3.1.4 TG-DTA analysis

TG/DTA 8120, Rigaku Thermo Plus, Japan was used exclusively in the present research. The analyses could be carried out in oxygen atmosphere. Ramp rates and gas mixtures were varied depending upon the experiment being performed. Exothermic and endothermic curves from DTA measurements demonstrated the heat expelled by the sample or heat lost from surroundings, respectively, which provided information for temperatures of crystallization and/or temperatures at which structural transitions may be occurring. This information could be compared to known thermal property data to assist with the characterization of samples, as well as to determine a process of heat treatments for the bulk sample. TG measurements provided information on mass loss due to water content in certain hydrated samples produced in this research. The heating rate was at 20°C/min until 1000°C with flow of oxygen.

The thermogravimetric (TG) and differential thermal analysis (DTA) curves for milled alumina powder before and after solidified of mechano-chemical treatment at different rotation speed for 60 min are shown in figure 2.8 and figure 2.9, respectively. It can be observed that DTA peaks of the starting Al_2O_3 are related to the loss weight and are due to the thermal decomposition. The absence of a dehydration effect has about 100°C in green ceramic body. At this temperature the dehydration of alumina takes place. Probably, the water content in alumina system is completely taken. According to the TG analysis the total loss of weight for mechanochemically activated alumina before solidified raw, 100-60, 150-60, 200-60, 250-60 and 300-60 respectively, are 0.30, 0.21, 0.45, 0.34, 0.20 and 0.35%. And alumina after solidified raw, 100-60, 150-60, 200-60, 250-60 and 300-60 respectively, are 3.63, 4.23, 3.98, 3.68, 4.06 and 4.01%. Weight loss of solidified alumina has greater than activated alumina due to relationship of water content in Al_2O_3-KOH system. This weight loss region is mainly attributed to the oxidation of alumina surface with content decreasing with mechano-chemical treatment. Their corresponding oxidation reactions

are exothermic. Apparently, mechano-chemical dehydration occurs predominantly with increasing of rotation speed.

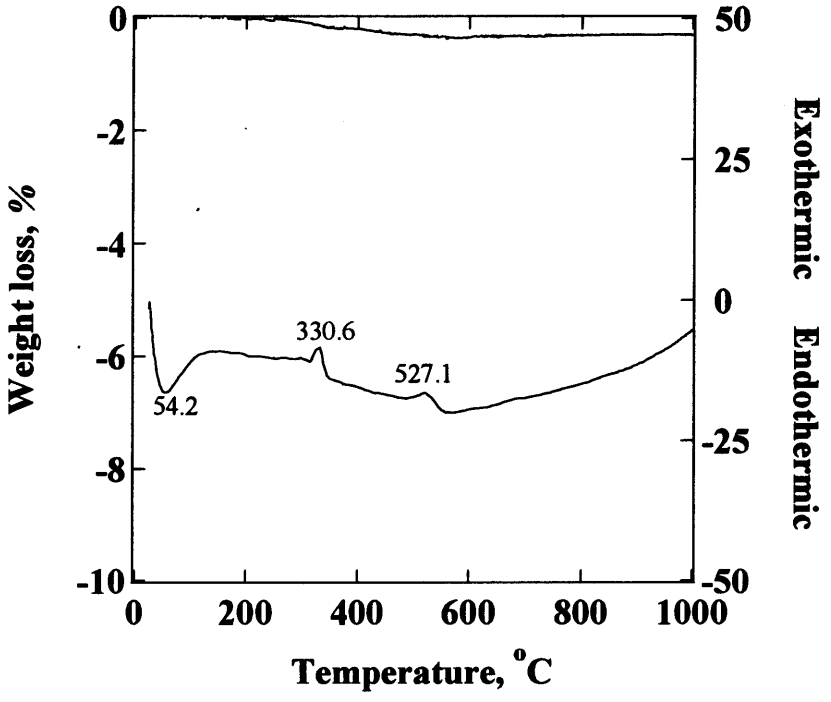

(a)

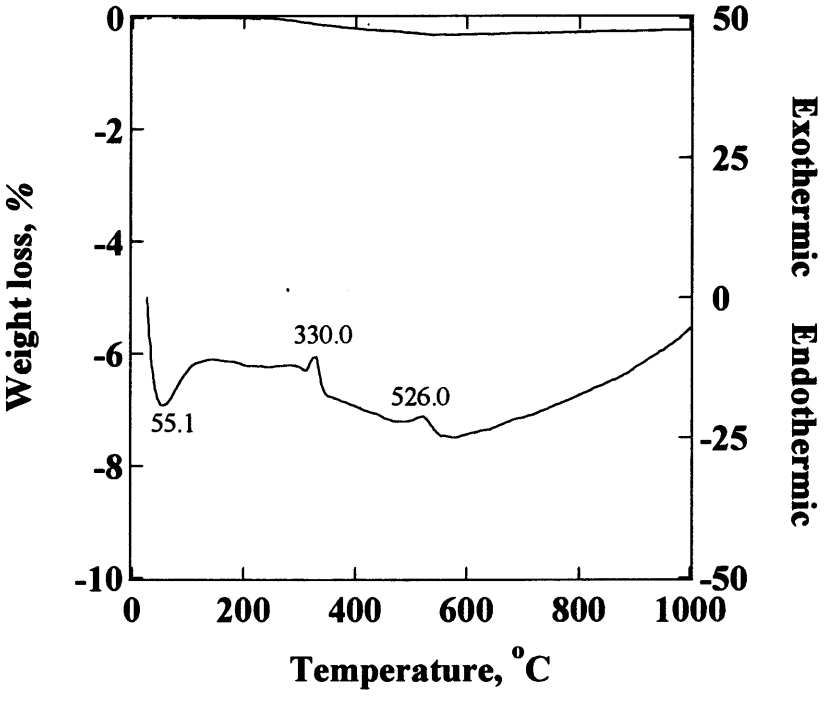

(b)

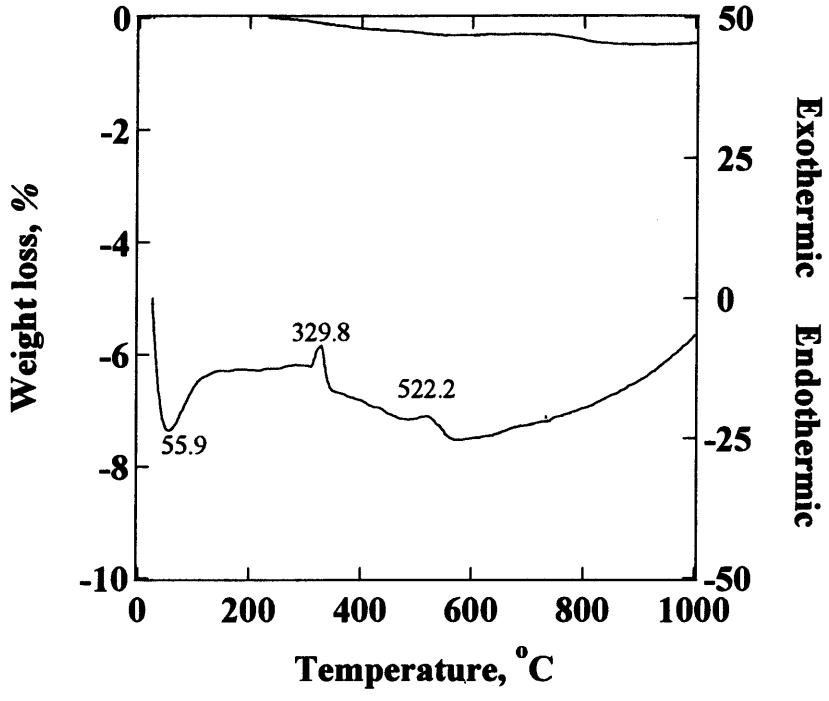
Weight loss, %
Exothermic Endothermic
Temperature, °C
329.8
522.2
55.9
0
-2
-4
-6
-8
-10
50
25
0
-25
-50
0
200
400
600
800
1000

(c)

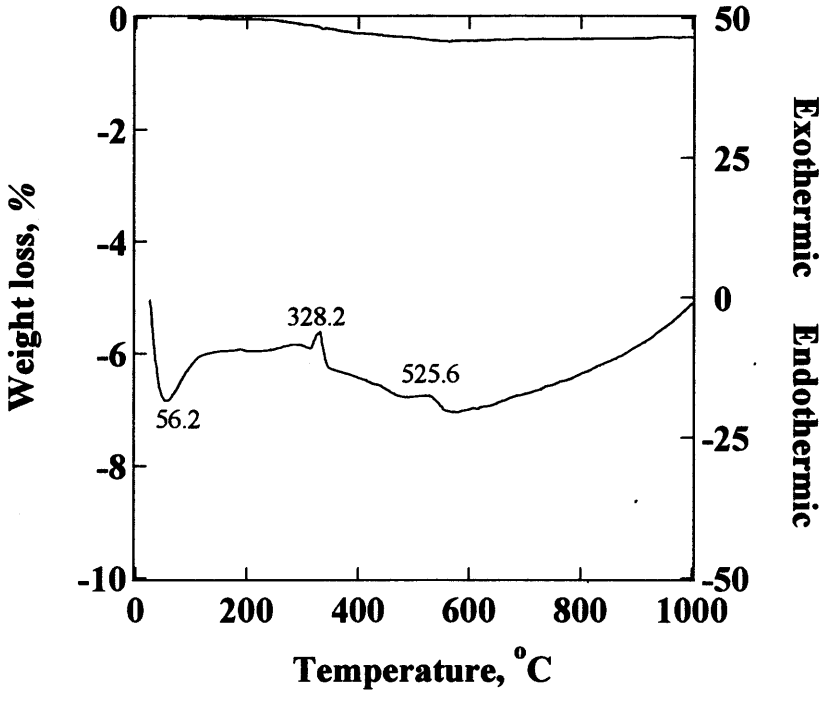
Weight loss, %
Exothermic Endothermic
Temperature, °C
328.2
525.6
56.2
0
-2
-4
-6
-8
-10
50
25
0
-25
-50
0
200
400
600
800
1000

(d)

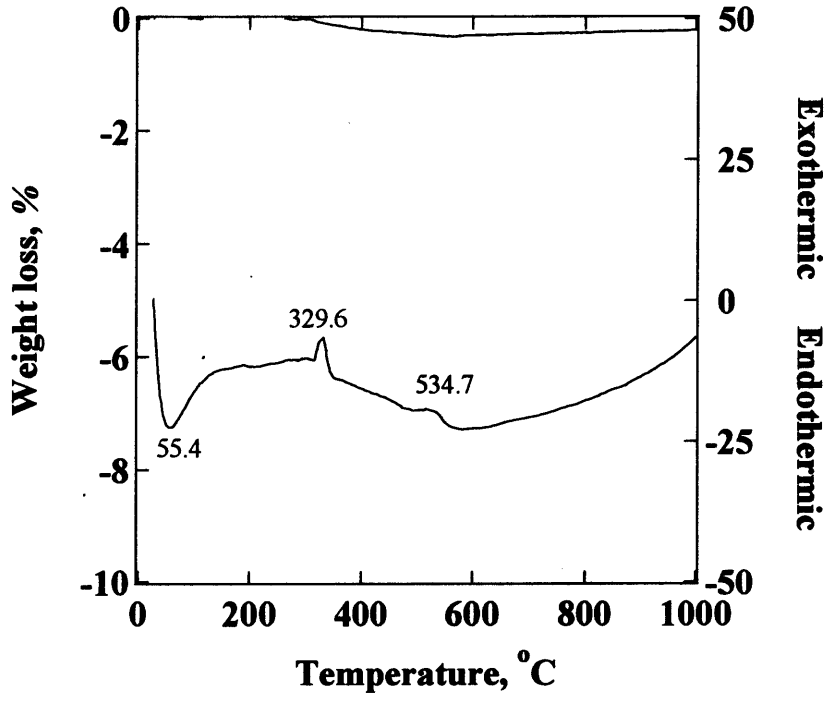

(e)

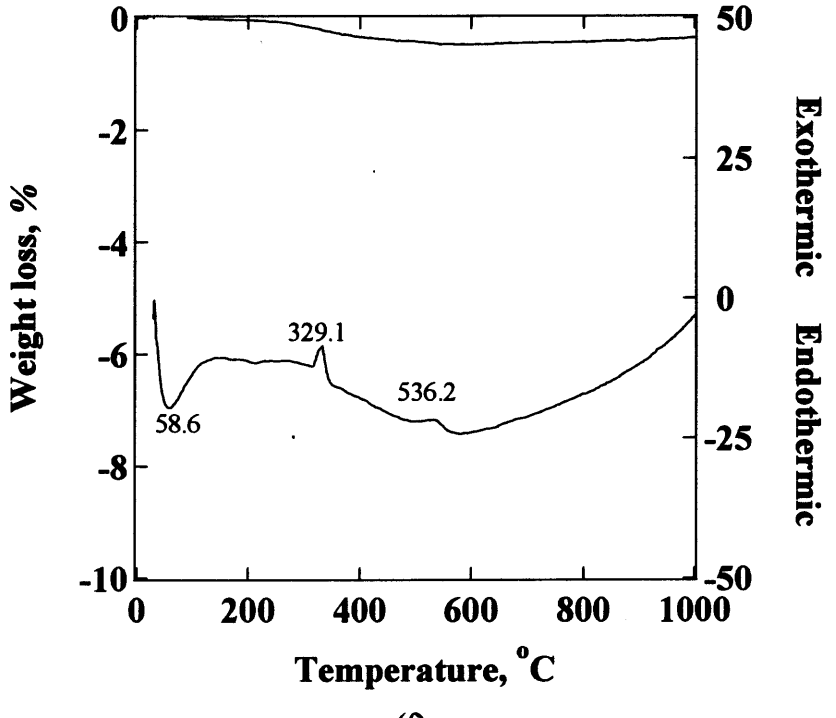

(f)

Figure 2.8 TG-DTA of activated alumina at different mechano-chemical treatment; (a) raw, (b) 100-60, (c) 150-60, (d) 200-60, (e) 250-60, (f) 300-60

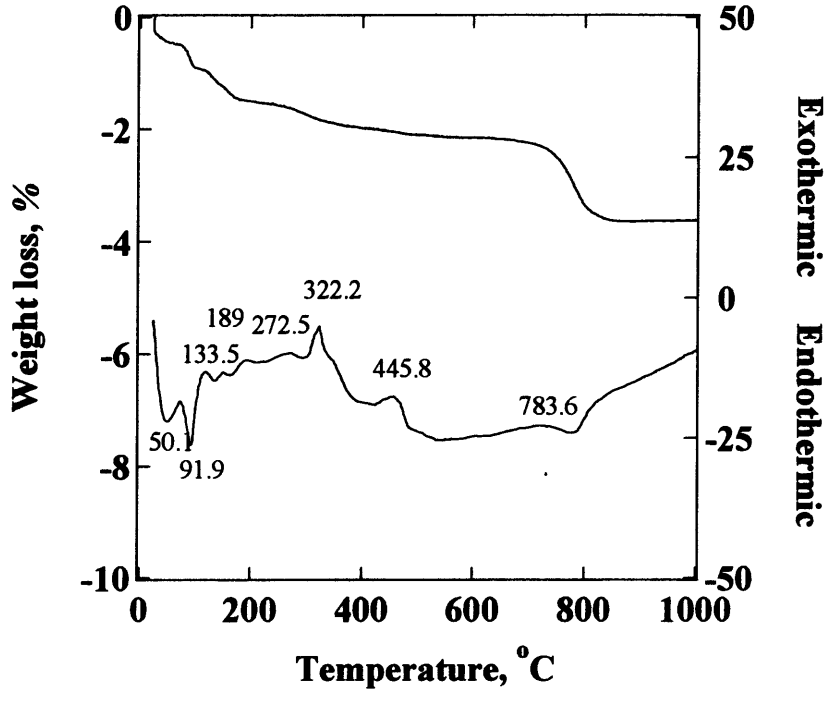
Weight loss, %
Exothermic Endothermic
Temperature, °C
0
-2
-4
-6
-8
-10
50
25
0
-25
-50
0
200
400
600
800
1000
322.2
189
272.5
133.5
445.8
783.6
50.1
91.9

(a)

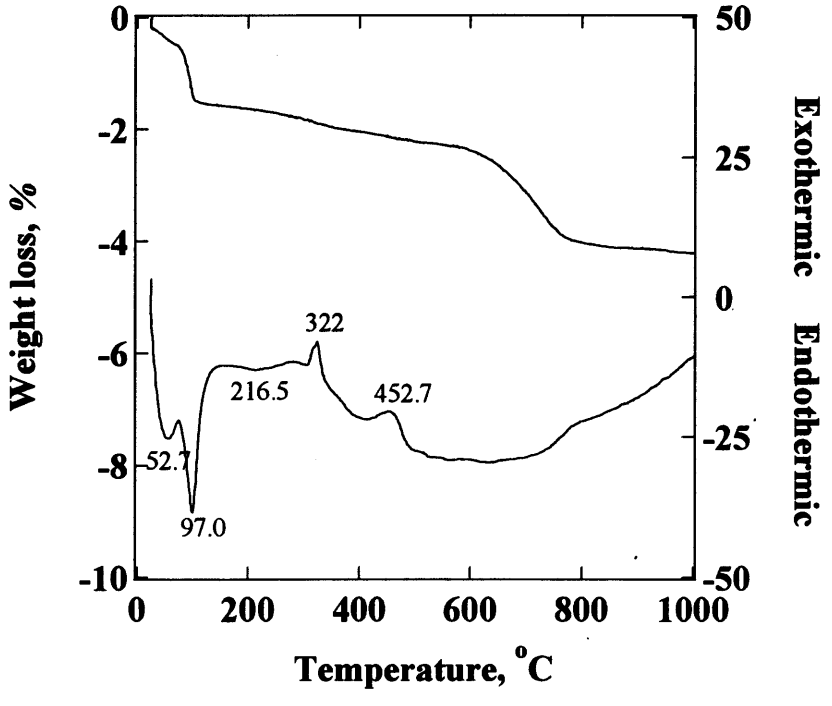
Weight loss, %
Exothermic Endothermic
Temperature, °C
0
-2
-4
-6
-8
-10
50
25
0
-25
-50
0
200
400
600
800
1000
322
216.5
452.7
52.7
97.0

(b)

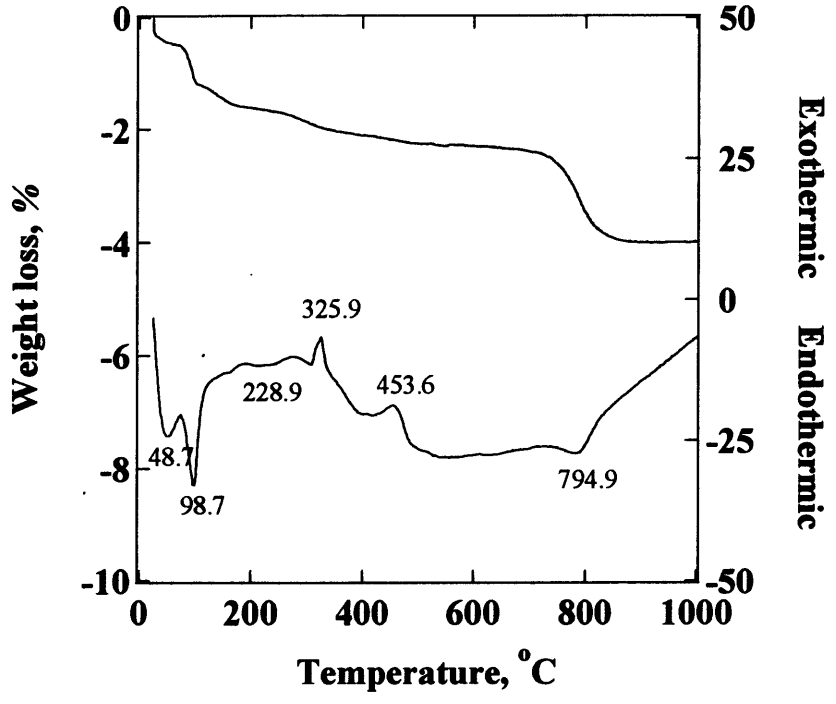
Weight loss, %
Exothermic Endothermic
Temperature, °C
0
-2
-4
-6
-8
-10
50
25
0
-25
-50
0
200
400
600
800
1000
325.9
228.9
453.6
48.7
98.7
794.9

(c)

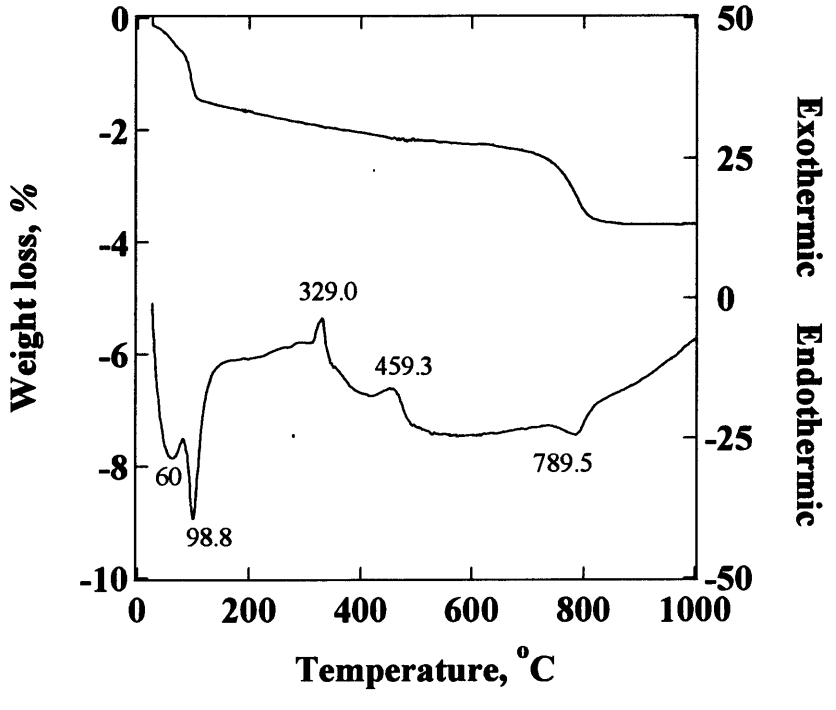
Weight loss, %
Exothermic Endothermic
Temperature, °C
0
-2
-4
-6
-8
-10
50
25
0
-25
-50
0
200
400
600
800
1000
329.0
459.3
60
98.8
789.5

(d)

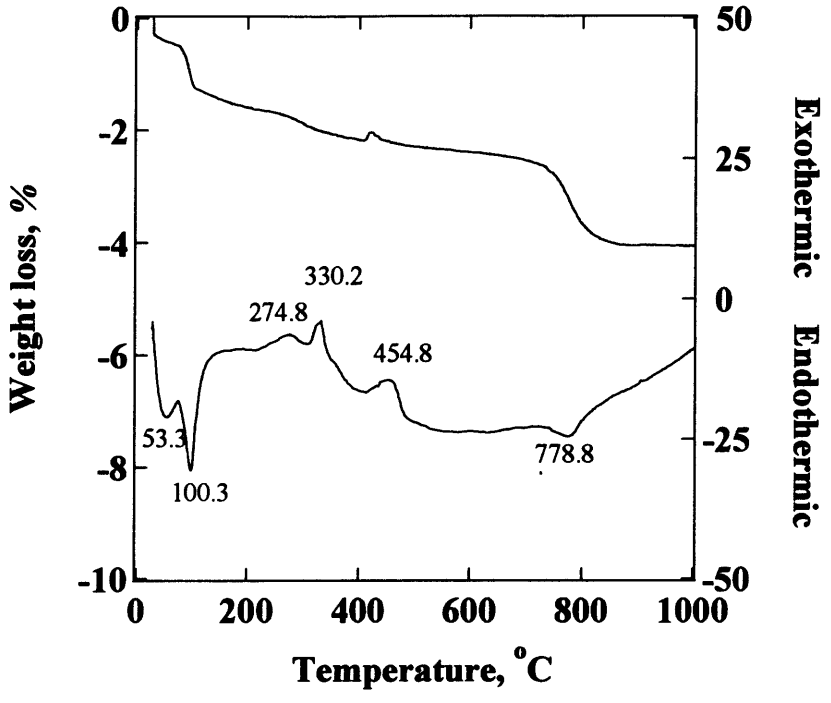

(e)

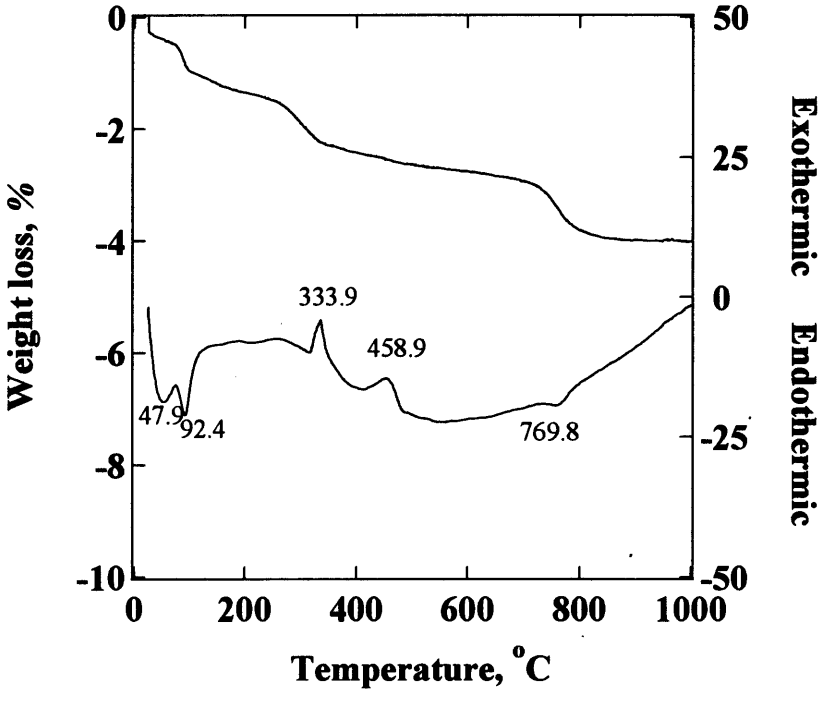

(f)

Figure 2.9 TG-DTA of solidified body at different mechano-chemical treatment;

(a) raw, (b) 100-60, (c) 150-60, (d) 200-60, (e) 250-60, (f) 300-60

2.3.1.5 Microstructure of activated powder

Principle of operation, a field-emission cathode in the electron gun of a scanning electron microscope provides narrower probing beams at low as well as high electron energy, resulting in both improved spatial resolution and minimized sample charging and damage. For applications which demand the highest magnification possible, Secondary Electron Imaging shows the topography of surface features a few nm across. Films and stains as thin as 20 nm produce adequate-contrast images. Materials are viewed at useful magnifications up to 100,000x without the need for extensive sample preparation and without damaging the sample. Even higher magnifications and resolution are routinely obtained by our Field Emission SEM.

In order to study the microstructural and morphological changes of all activated particles by planetary ball mill, the small amount of activated powder was taken and investigated by SEM micrographs. Figure 3.10 shows SEM images of the activated powders for different rotation speed. Since the mean particle size of activated particles slightly decreases with rotation speed, it was somehow different to verify the change of surface area, morphology and powder particle size distribution through planetary ball mill from these SEM images.

(a)

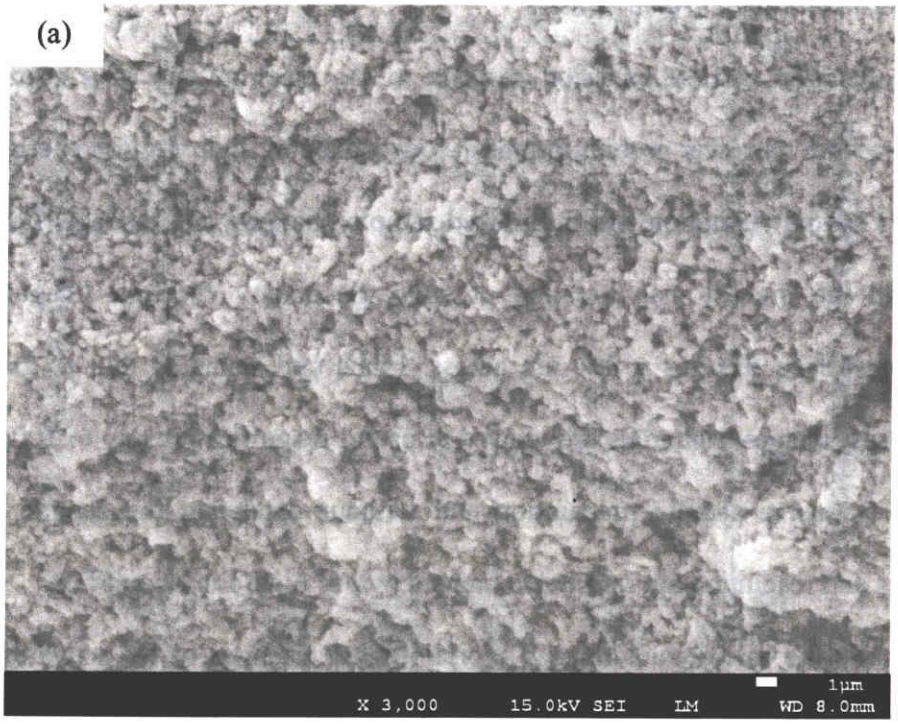

(b)

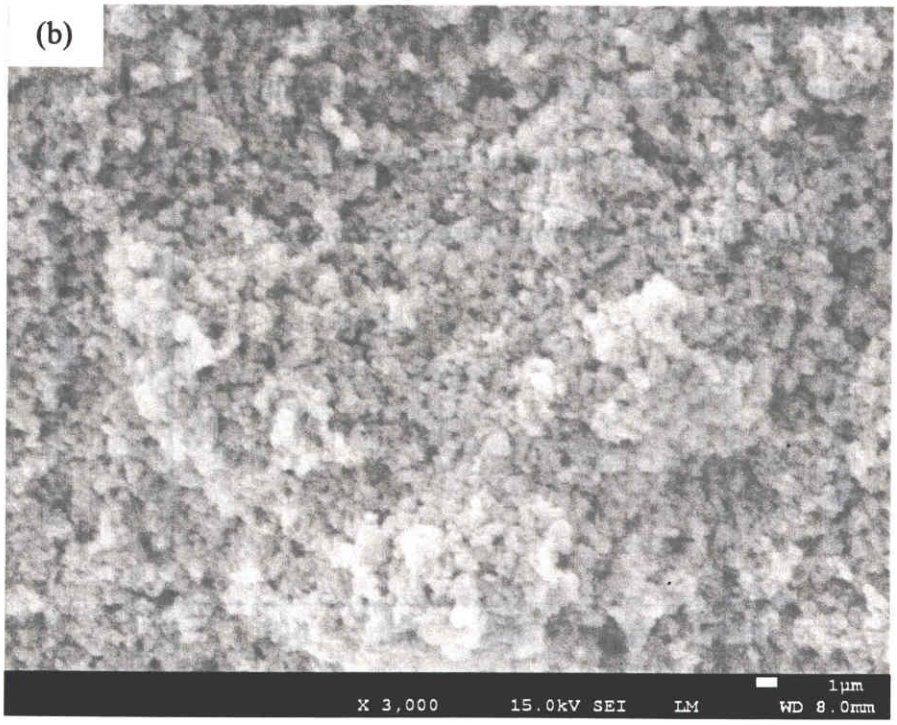

(c)

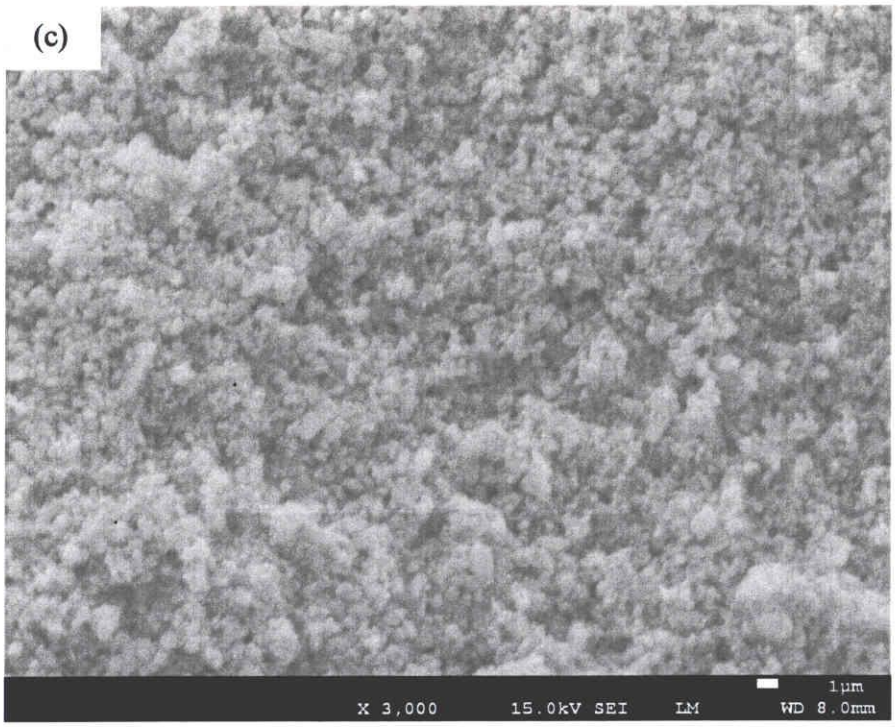

(d)

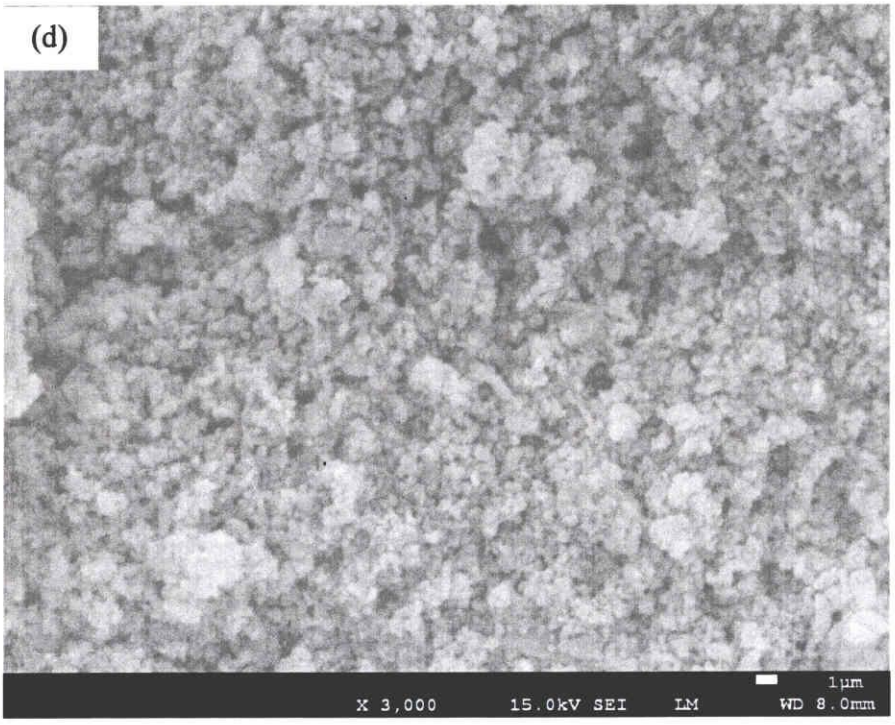

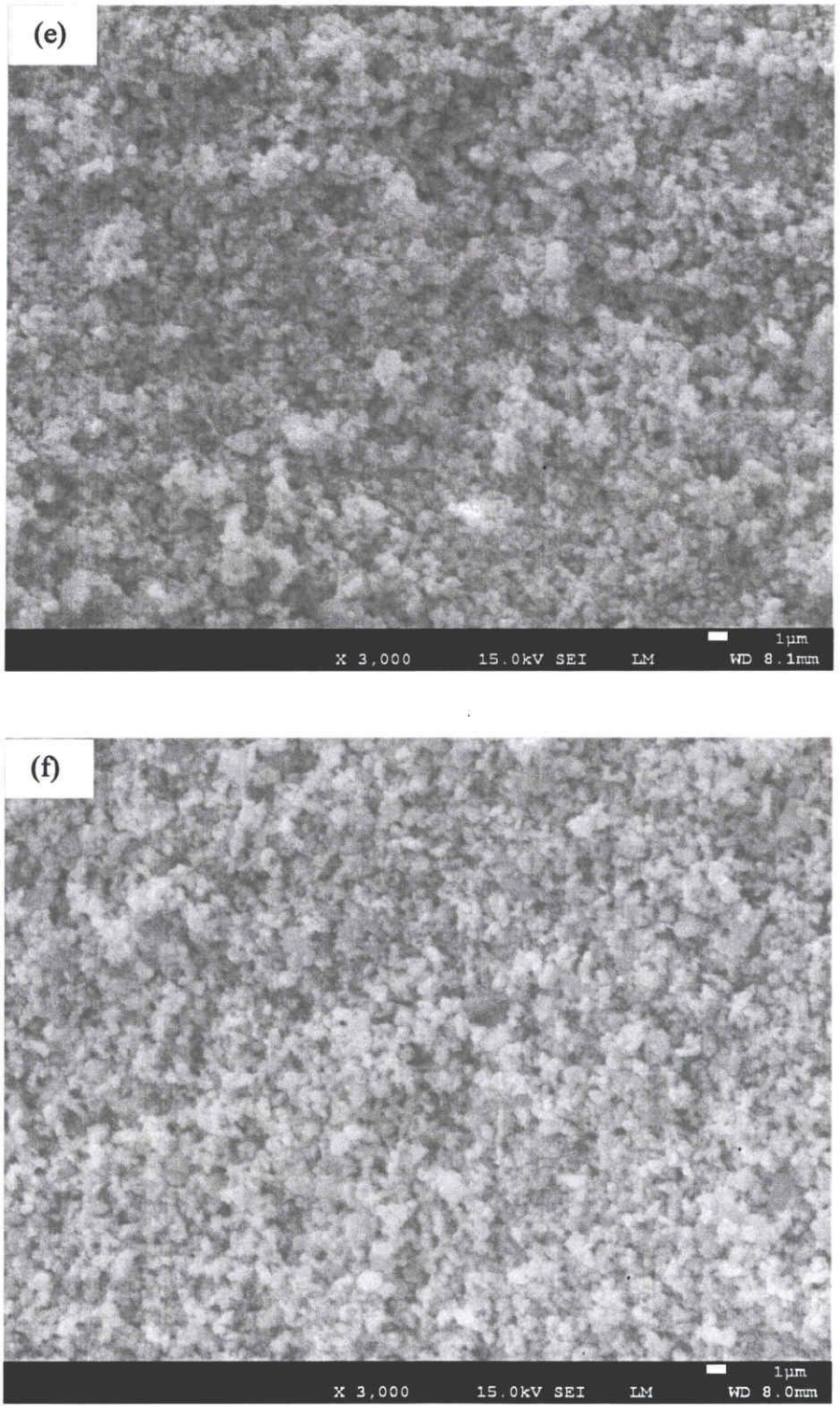

Figure 2.10 Microstructural evolution of activated alumina at different mechano-chemical treatment; (a) raw, (b) 100-60, (c) 150-60, (d) 200-60, (e) 250-60, (f) 300-60

The microstructural and morphological changes of samples during solidification at different rotation speed are shown in figure 2.11. The agglomeration of particles formed after alkaline reaction. This is because of new bonding were formed during solidification. SEM images did not show any noticeable increase from the value of solidified body measured from SEM images.

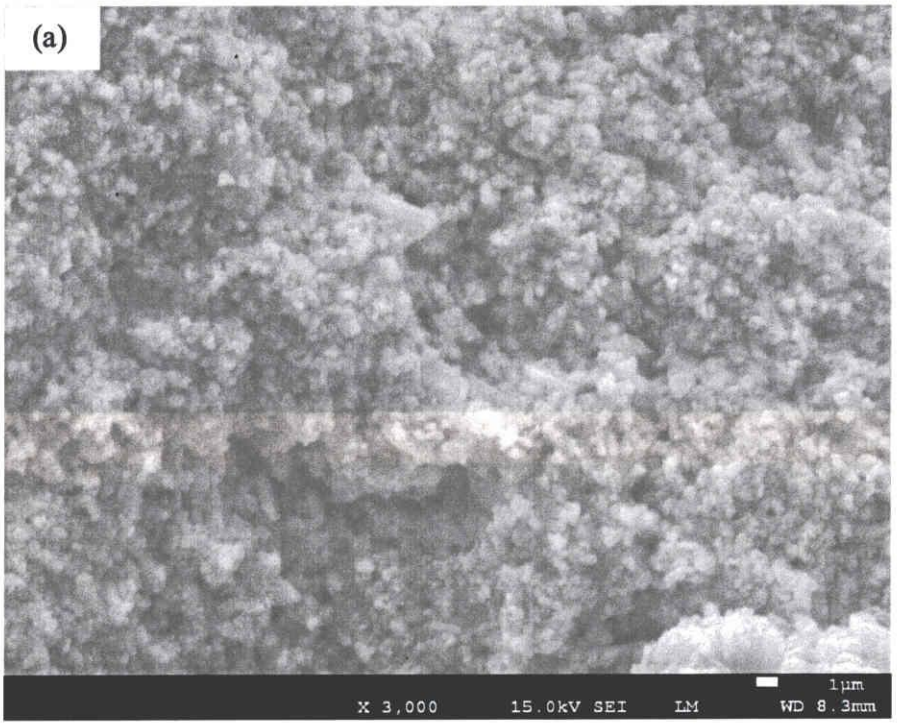

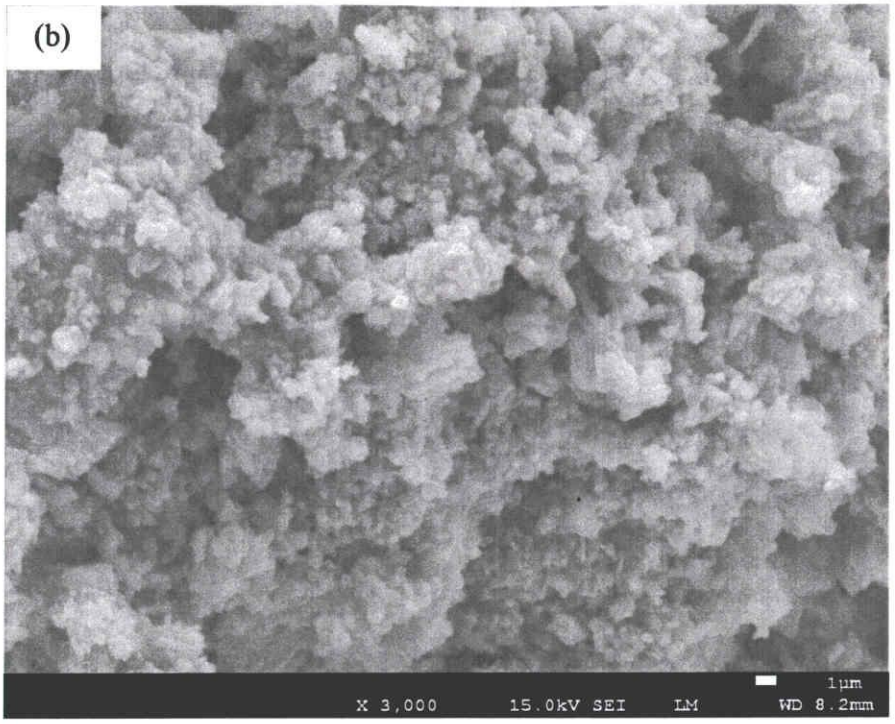
(b)
X 3,000 15.0kV SEI LM WD 8.2mm
1μm

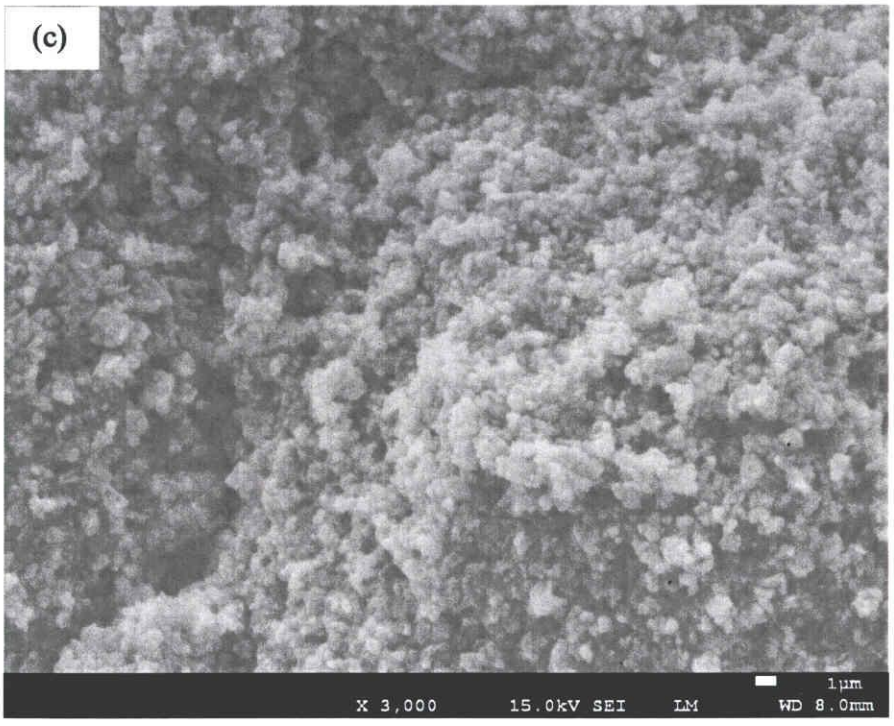
(c)
X 3,000 15.0kV SEI LM WD 8.0mm
1μm

(d)

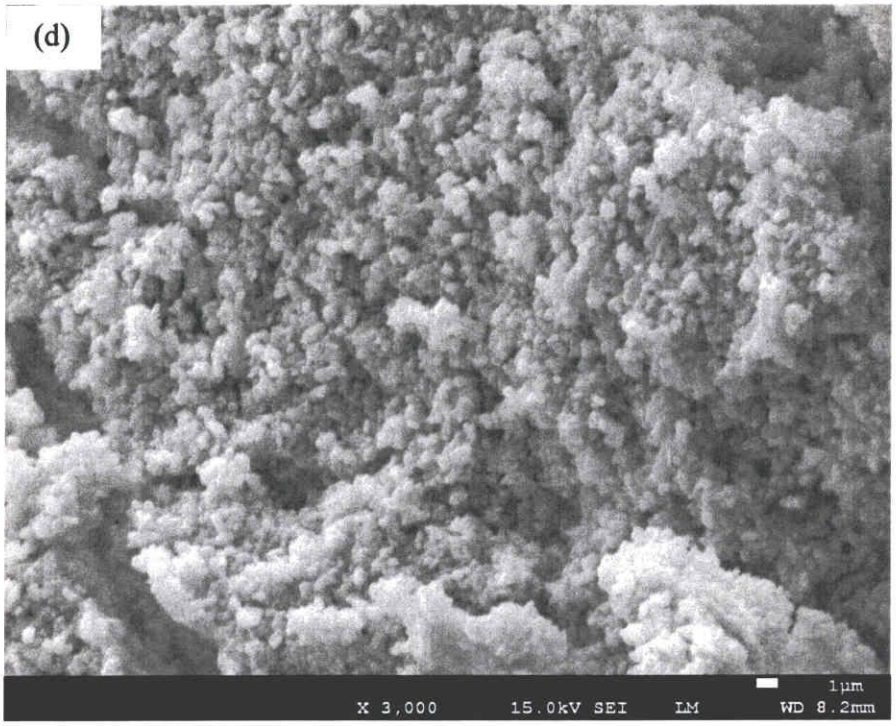

(e)

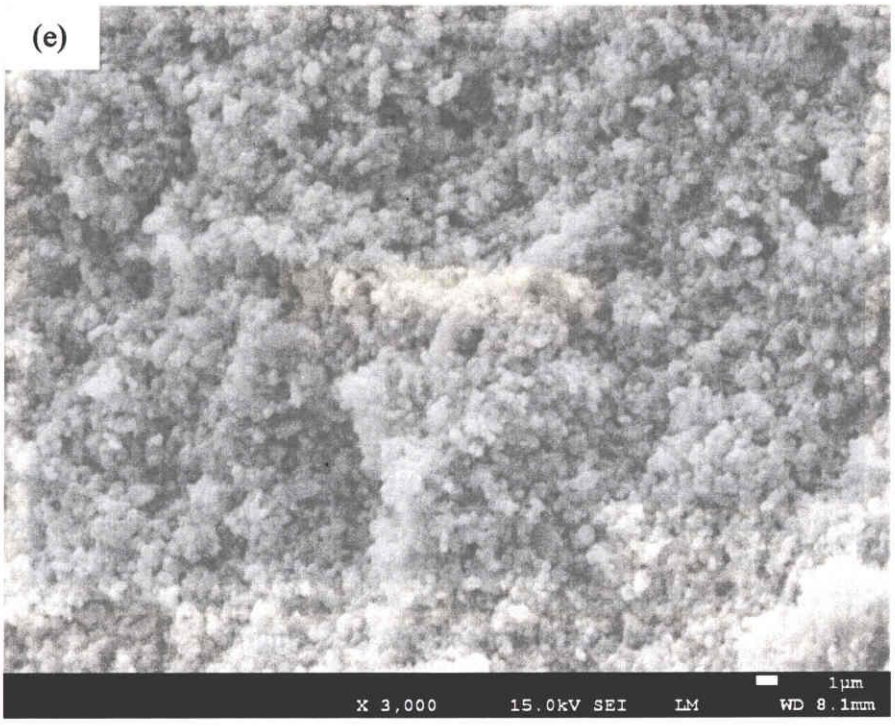

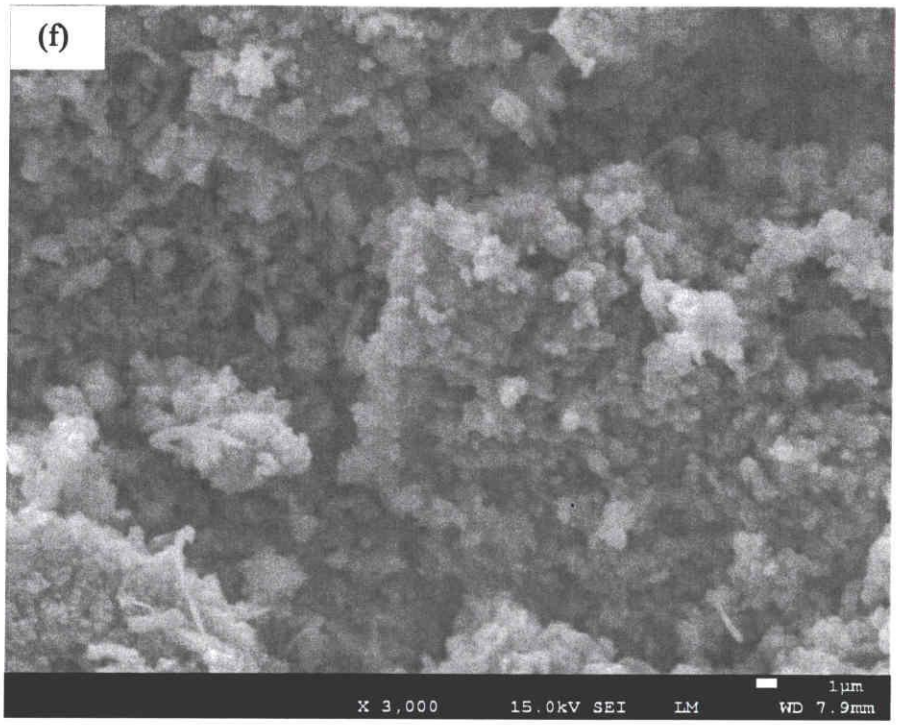

Figure 2.11 Microstructural evolution of solidified body at different mechano-chemical treatment; (a) raw, (b) 100-60, (c) 150-60, (d) 200-60, (e) 250-60, (f) 300-60

2.3.1.6 Solidification time and Bending strength

The Teflon mold with ten rectangular cavities, having all surfaces coated with releasing agent (Vaseline white, Yonehama Chemical Company, Japan) as shown in Figure 2.12, to form mechanical testing bars. The green ceramics body of mechanochemically activated alumina was shown in Figure 2.13.

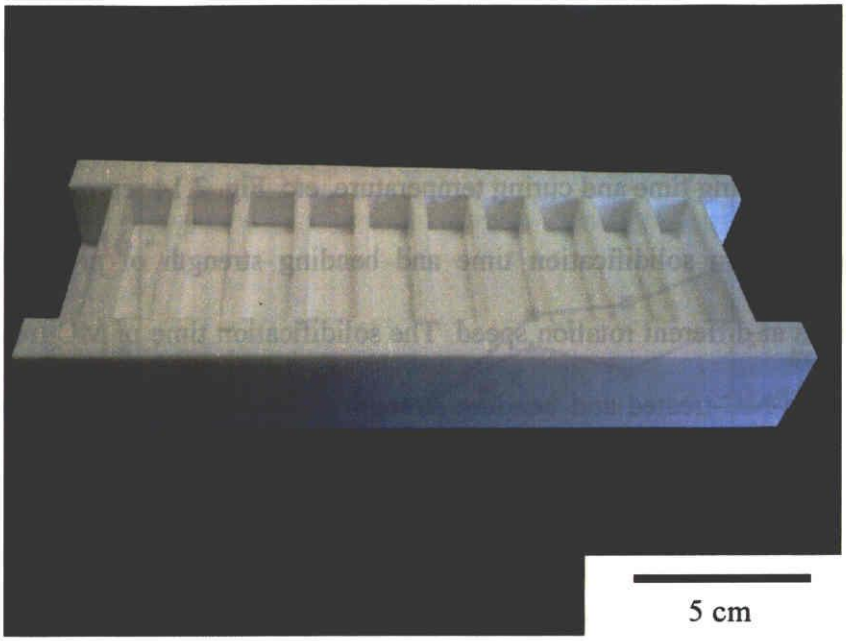

Figure 2.12 Teflon mold with ten rectangular cavities

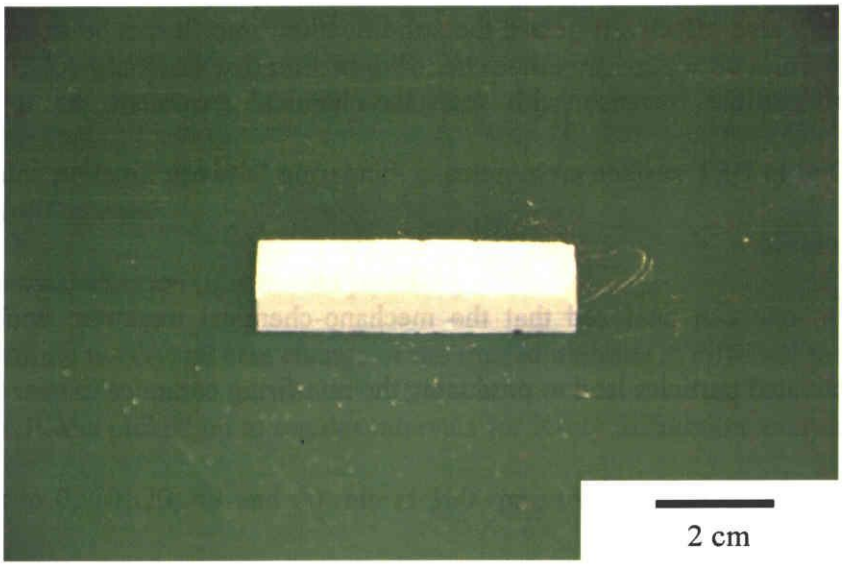

Figure 2.13 Mechanical testing bar

A production of good quality non-firing ceramic with higher mechanical strength and solidification time depends on several parameters like kind and concentration of KOH, mechano-chemical condition, curing time and curing temperature, etc. Fig. 2.14 represents, which illustrate the relationship between solidification time and bending strength of products by mechano-chemical treatment at different rotation speed. The solidification time of MC-treated was clearly prolonged than non-MC-treated and bending strength of MC-treated was clearly stronger non-MC-treated and both significantly increase with increasing of rotation speed and milling time. This is due to the MC treatment enhances surface activation and chemical reaction between interfaced surfaces of products layer bonding between adjoining particles. It can be confirm this reason by ICP analysis as the previous mentioned that Al^{3+} elute can form to new bonding and strong bonding depending on mechano-chemical treatment. On the other hand, mechano-chemical treatment also effectively retard the solidification time. It can be describe the specific surface area of particle increase with mechano-chemical treatment, so it takes time to solidification. Due to BET surface area increase, bindering between alkaline solution and small particles also increase.

From this result, one can analyzed that the mechano-chemical treatment could be powerful technique for activated particles lead to producing the non-firing ceramics in near future.

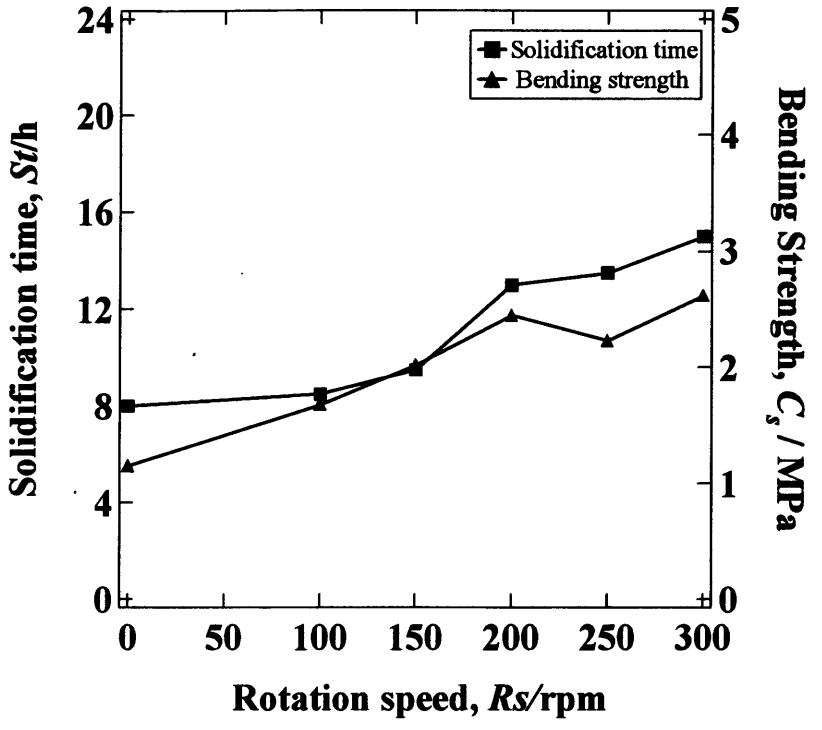

Figure 2.14 Relationship between solidification time and Bending strength by planetary ball mill at different rotation speed for 60 min

2.3.2 Effect of milling time

2.3.2.1 XRD Characterization of activated powder

In order to determine the crystal size change of the treated alumina at different milling time using planetary ball mill was picked up at regular intervals for X-ray diffraction analysis in figure 2.15 (a) corresponds to 0, 10, 20, 40 and 60 min at 300 rpm, respectively. The diffraction peaks at different 2θ correspond to the (0 1 2), (1 0 4), (1 1 0), (1 1 3), (0 2 4), (1 1 6), planes, respectively. No changes in XRD patterns were observed. The raw powder presents sharp peaks indicating the high crystallinity of the sample. On the other hand, the effect of KOH addition on green body synthesis was investigated using activated samples at different mechano-chemical treatment of milling time are shown in Figure 2.15(b). The trend of graphs, XRD patterns, FWHM, crystal

size and lattice strain have similarity with according to rotation speed conditions as previous mentioned.

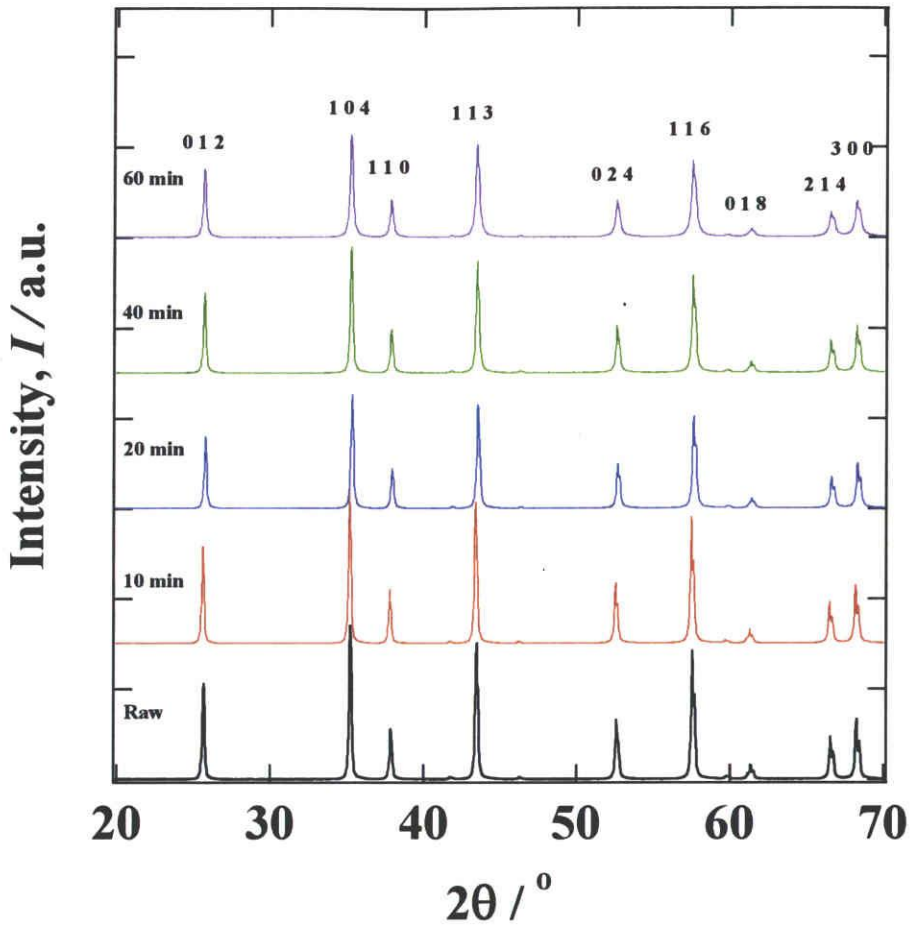

(a)

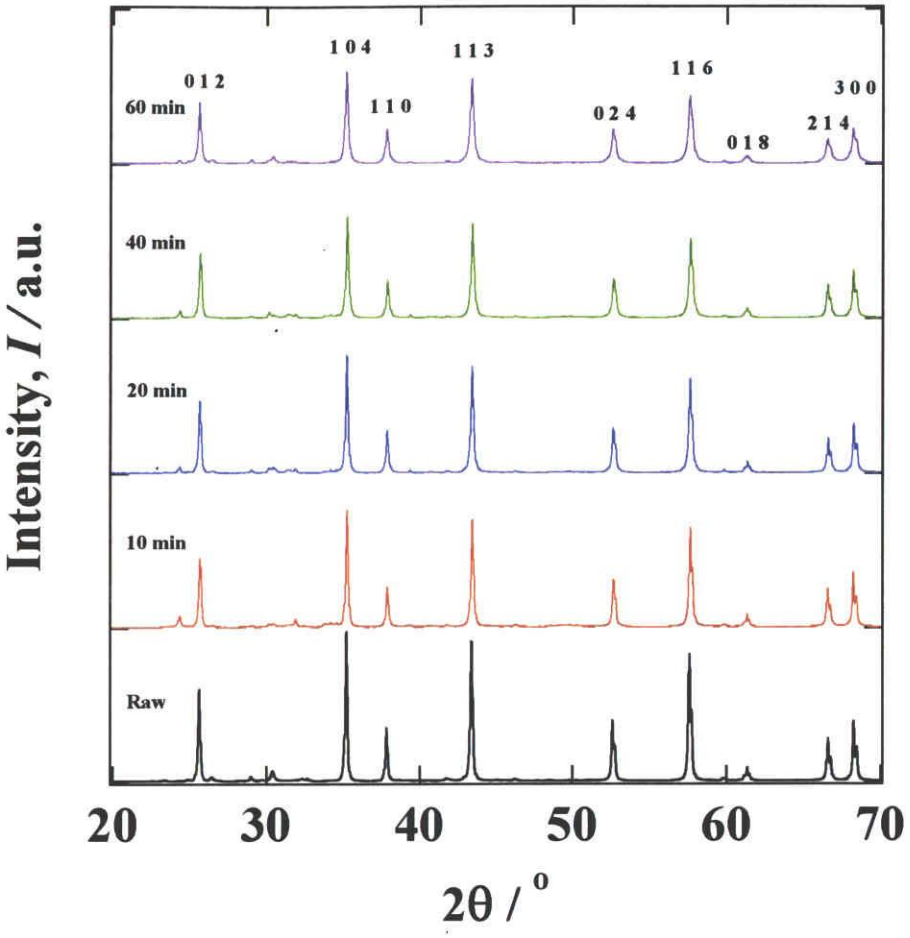

(b)

Figure 2.15 XRD patterns of mechano-chemical treated alumina by planetary ball mill at different milling time at 300 rpm; (a) activated powder, (b) ceramic green body

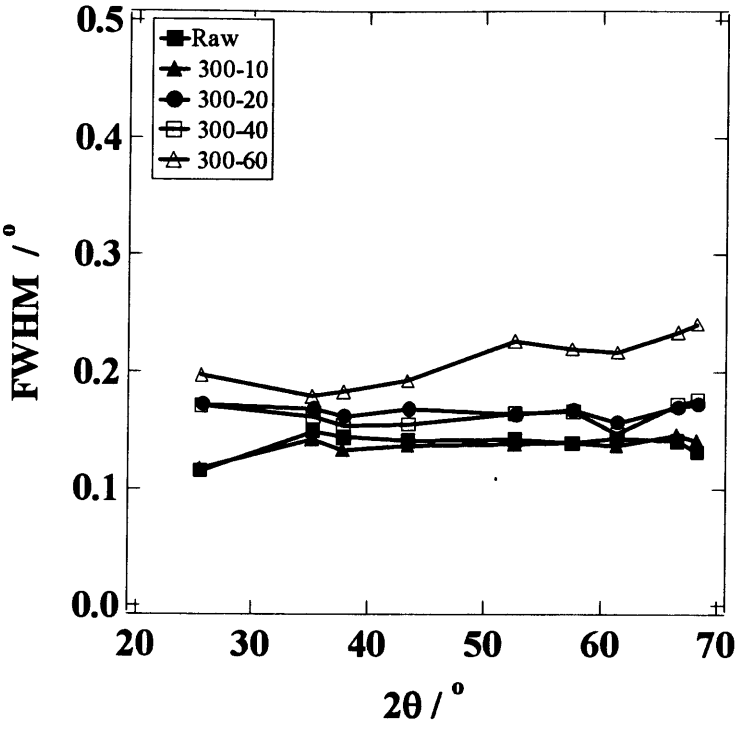

Figure 2.16 The changes of physical FWHM for activated alumina in different mechano-chemical treatment at different milling time for300 rpm

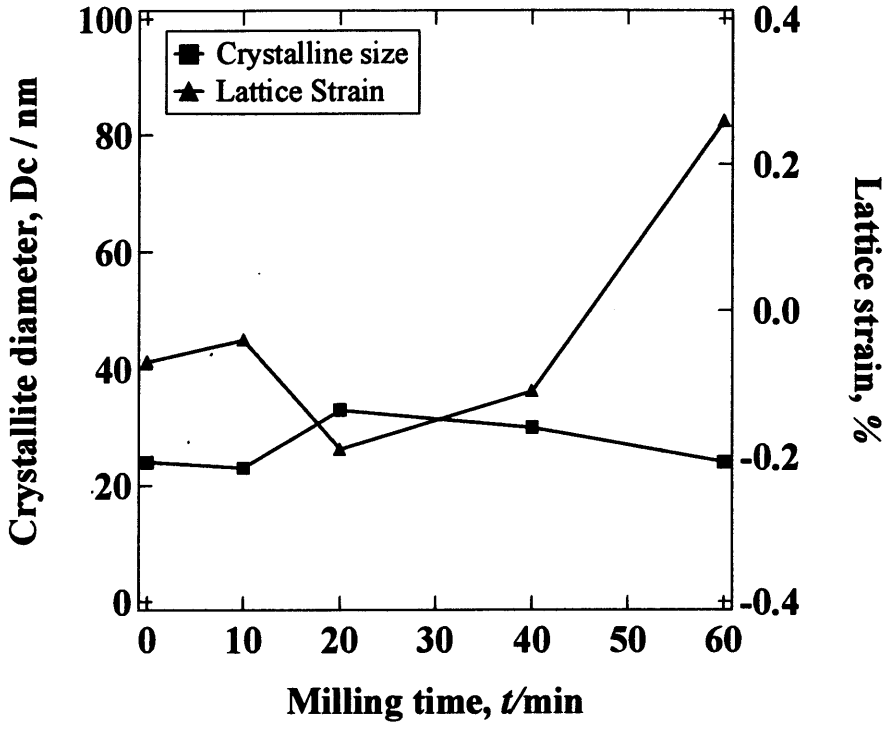

Figure 2.17 X-ray peaks broadening (β) as a function of Bragg angle (θ) for the milled sample and Evolution of crystalline size and lattice strain obtained from Williamson-Hall method at different milling time for300 rpm

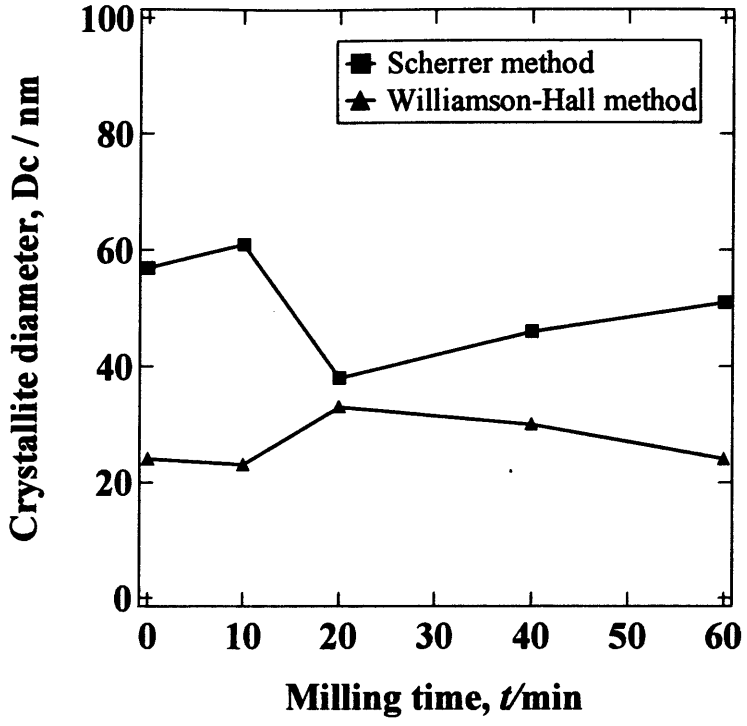

Figure 2.18 Comparison of the evolution of crystalline size between the Scherrer and Williamson-Hall methods at different milling time for 300 rpm

2.3.2.2 BET and Mean particle size characterization of activated powder

This figure show relationship BET and mean particle size at different mechano-chemical treatment of milling time. By the BET surface area increases but average particle size (d_{50}) decreases during mechano-chemical treatment. The trend of graph has similarity with according to rotation speed conditions as previous mentioned.

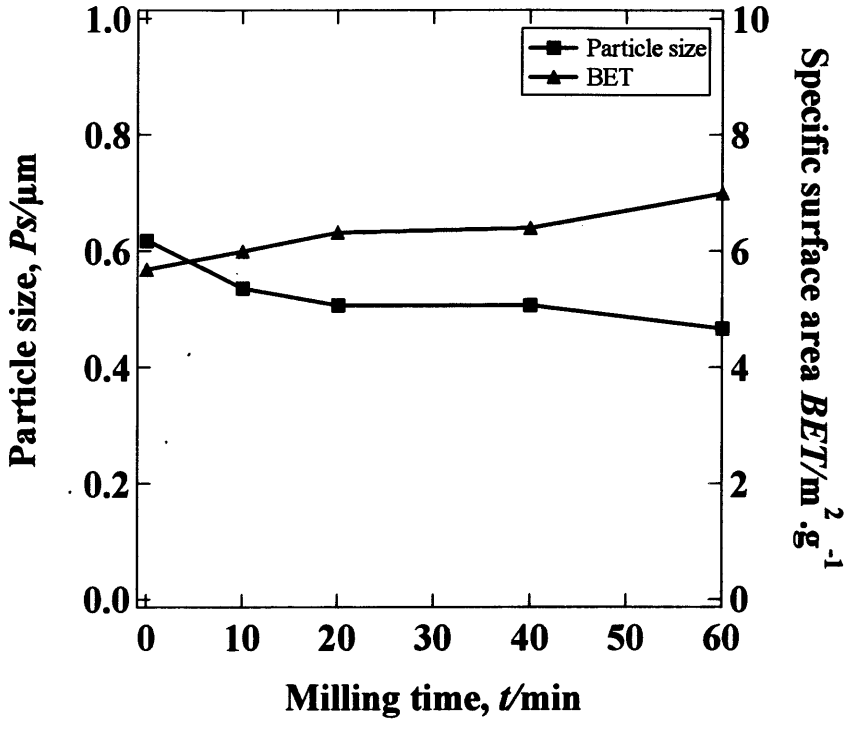

Figure 2.19 BET surface area and Mean particle size of mechano-chemical treated alumina by planetary ball mill at different milling time at 300 rpm

2.3.2.3 ICP characterization of activated powder

Figure 2.20 showing quantitative evolution of aluminum ion at different milling time which confirms leaching of concentration of aluminium ion increases significantly with mechano-chemical treatment. The trend of graph has similarity with according to rotation speed conditions as previous mentioned.

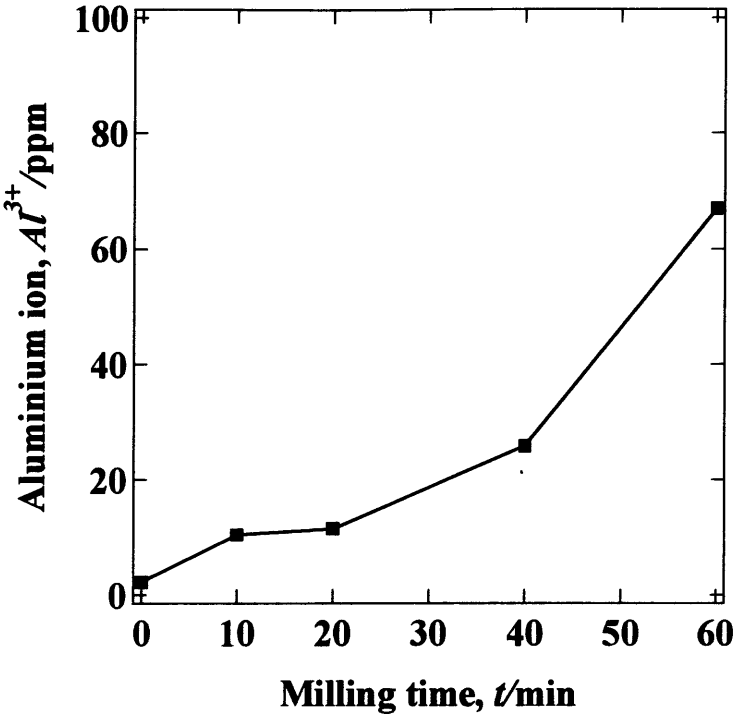

Figure 2.20 Elution behavior of the alumina by planetary ball mill at different milling time at 300 rpm

2.3.2.4 TG-DTA analysis

The thermogravimetric (TG) and differential thermal analysis (DTA) curves for milled alumina powder before and after solidified of mechano-chemical treatment at different milling time for 300 rpm are shown in figure 2.21 and figure 2.22, respectively. According to the TG analysis the total loss of weight for mechanochemically activated alumina before solidified raw, 300-10, 300-20, 300-40 and 300-60 respectively, are 0.30, 0.14, 0.29, 0.17 and 0.35%. And alumina after solidified raw, 300-10, 300-20, 300-40 and 300-60 respectively are 3.63, 3.72, 2.78, 3.92 and 4.01%. The trend of graph has similarity with according to rotation speed conditions as previous mentioned.

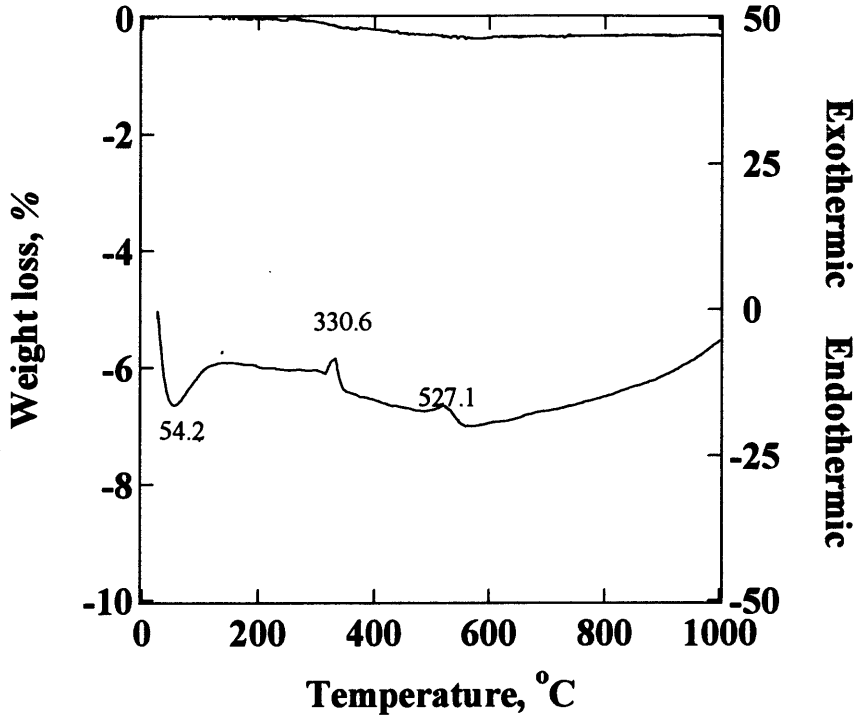
0
-2
-4
-6
-8
-10
Weight loss, %
50
25
0
-25
-50
Exothermic
Endothermic
330.6
527.1
54.2
0
200
400
600
800
1000
Temperature, °C

(a)

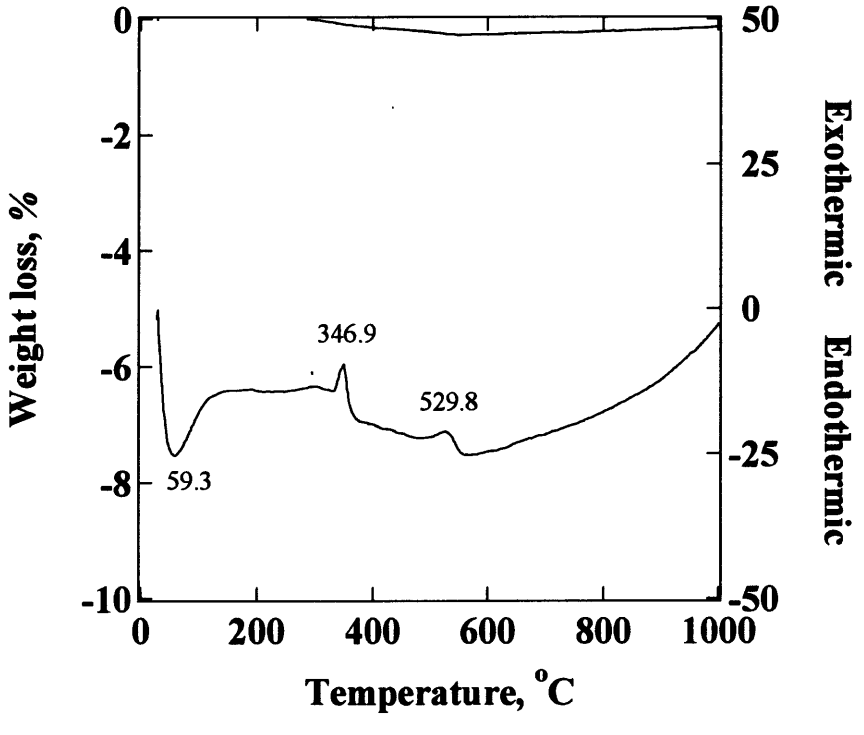
0
-2
-4
-6
-8
-10
Weight loss, %
50
25
0
-25
-50
Exothermic
Endothermic
346.9
529.8
59.3
0
200
400
600
800
1000
Temperature, °C

(g)

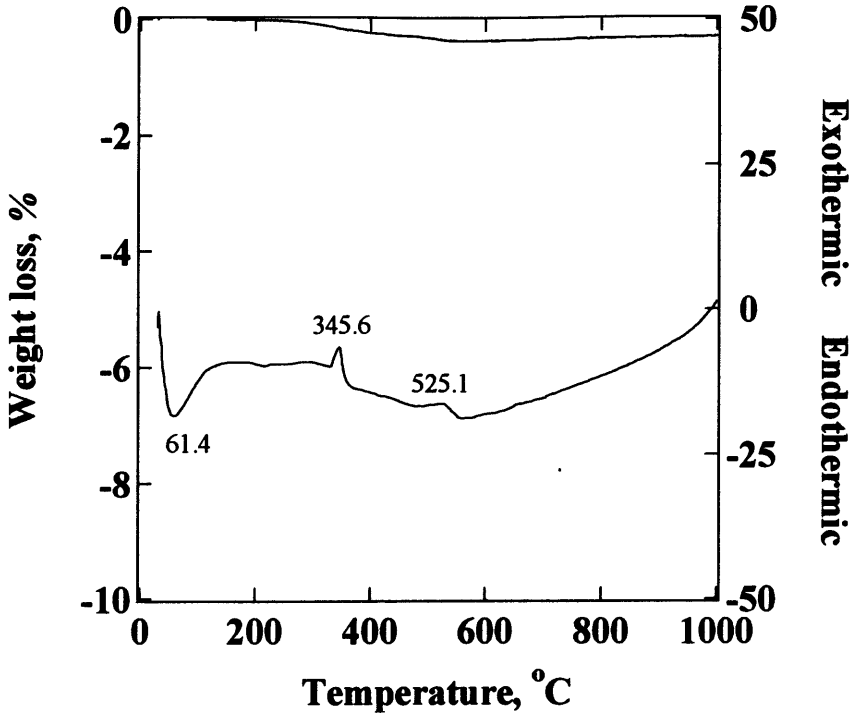
Weight loss, %
Exothermic Endothermic
Temperature, °C
345.6
525.1
61.4
0
-2
-4
-6
-8
-10
50
25
0
-25
-50
0
200
400
600
800
1000

(h)

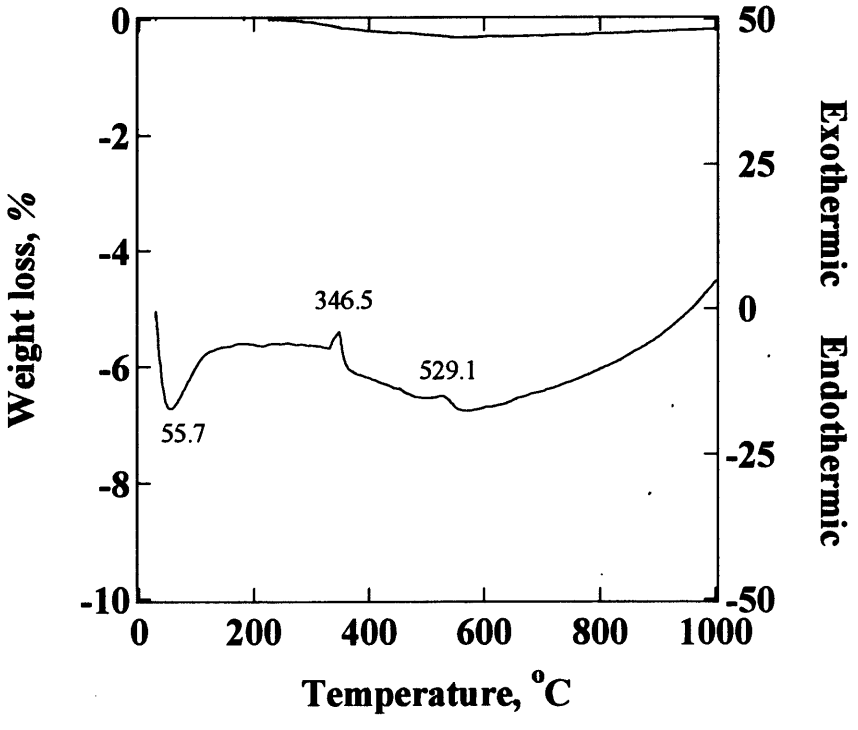
Weight loss, %
Exothermic Endothermic
Temperature, °C
346.5
529.1
55.7
0
-2
-4
-6
-8
-10
50
25
0
-25
-50
0
200
400
600
800
1000

(i)

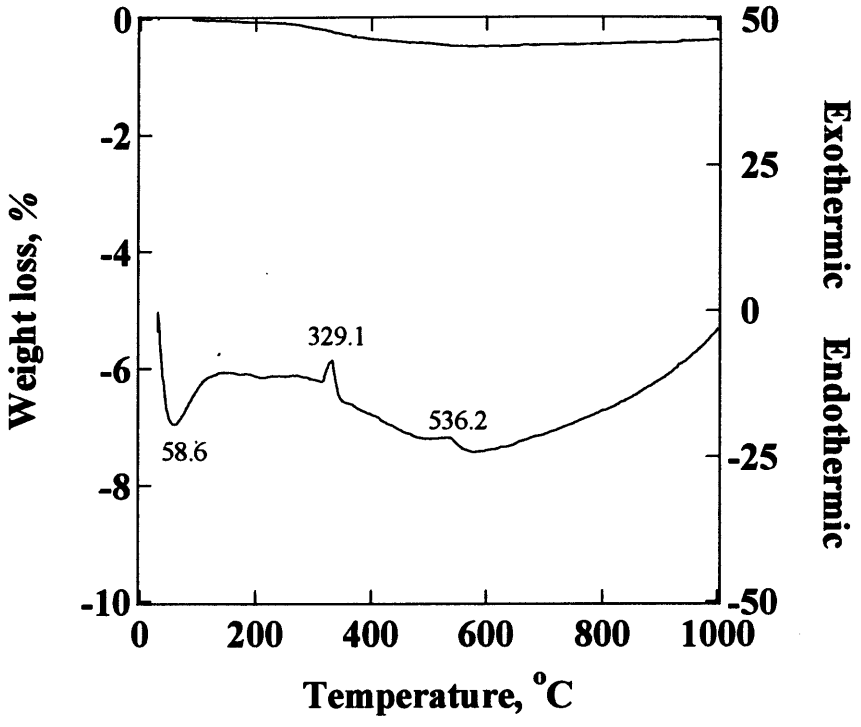

(f)

Figure 2.21 TG-DTA of activated alumina at different mechano-chemical treatment;

(a) raw, (g) 300-10, (h) 300-20, (i) 300-40, (f) 300-60

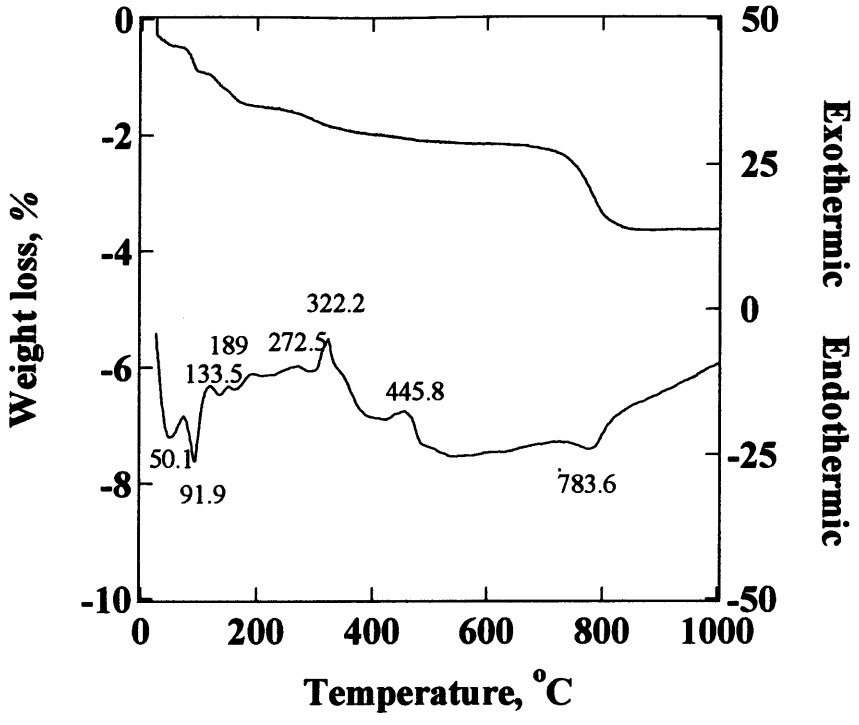
Weight loss, %
Exothermic Endothermic
Temperature, °C
0
-2
-4
-6
-8
-10
50
25
0
-25
-50
0
200
400
600
800
1000
322.2
189
272.5
133.5
445.8
50.1
91.9
783.6

(a)

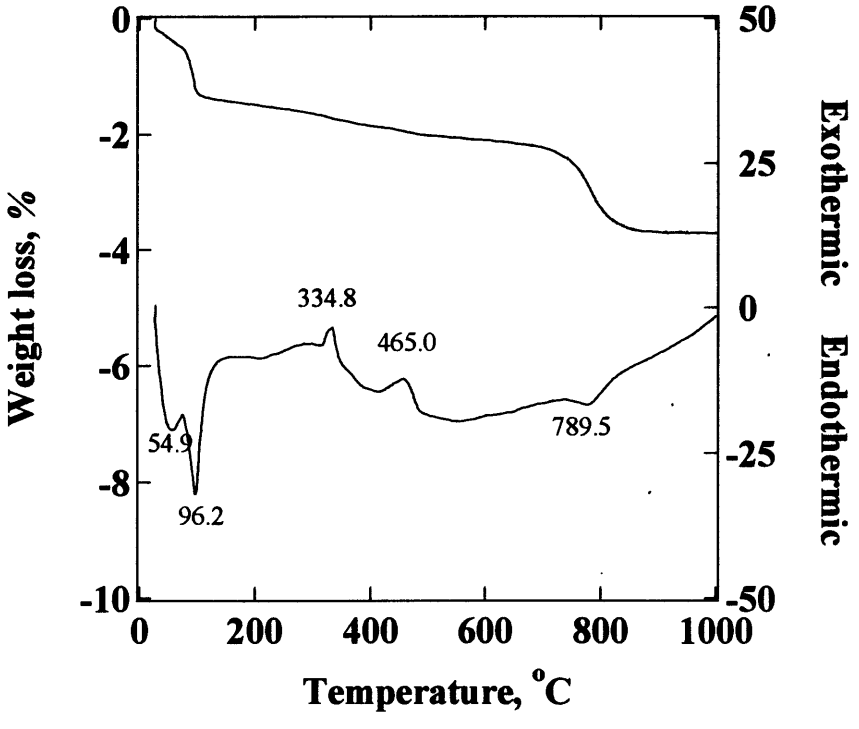
Weight loss, %
Exothermic Endothermic
Temperature, °C
0
-2
-4
-6
-8
-10
50
25
0
-25
-50
0
200
400
600
800
1000
334.8
465.0
789.5
54.9
96.2

(g)

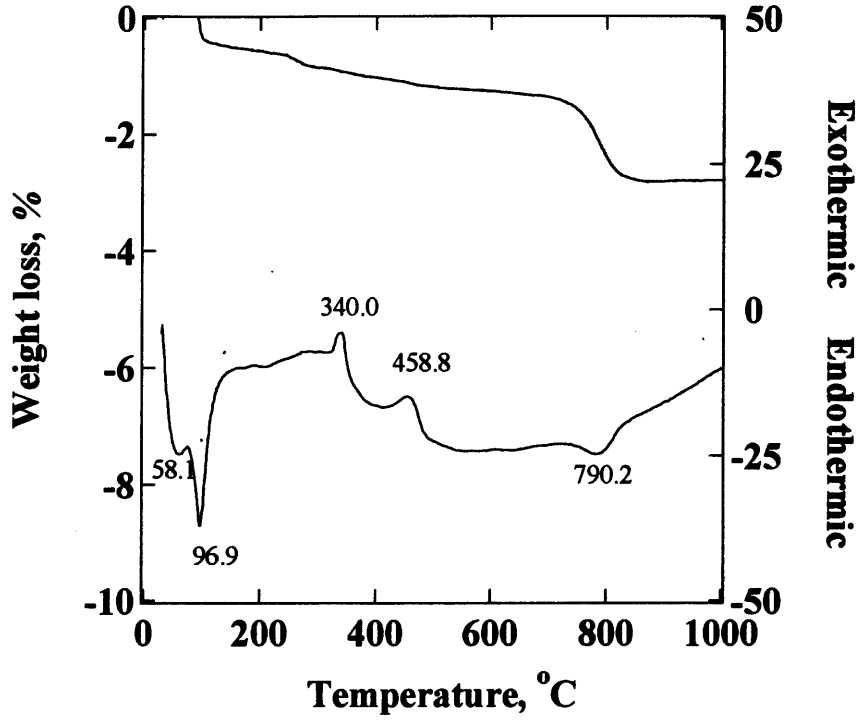
Weight loss, %
Exothermic Endothermic
Temperature, °C
0
-2
-4
-6
-8
-10
50
25
0
-25
-50
0
200
400
600
800
1000
340.0
458.8
58.1
96.9
790.2

(h)

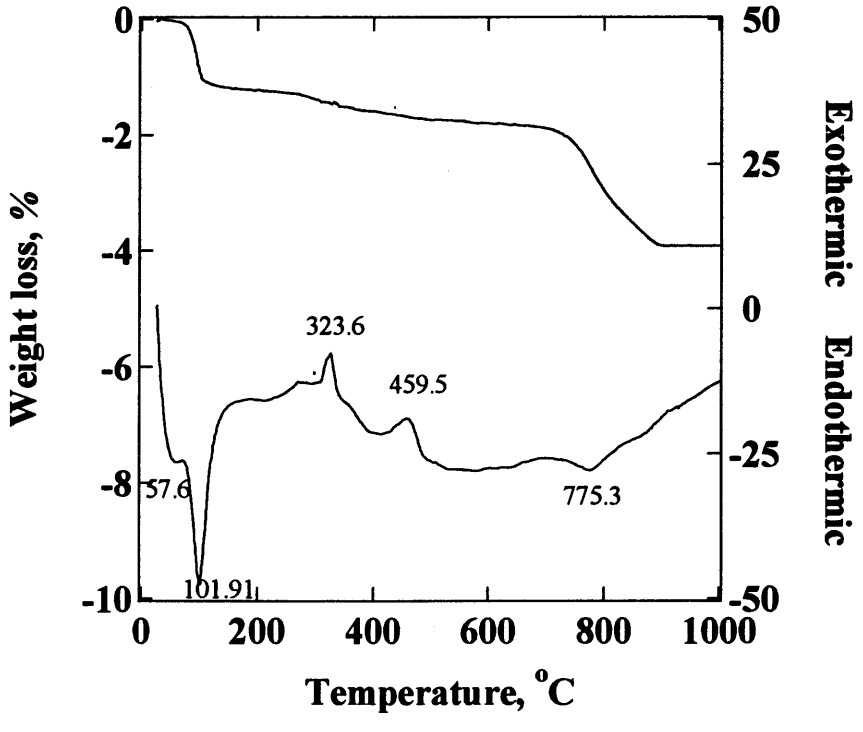
Weight loss, %
Exothermic Endothermic
Temperature, °C
0
-2
-4
-6
-8
-10
50
25
0
-25
-50
0
200
400
600
800
1000
323.6
459.5
57.6
101.91
775.3

(i)

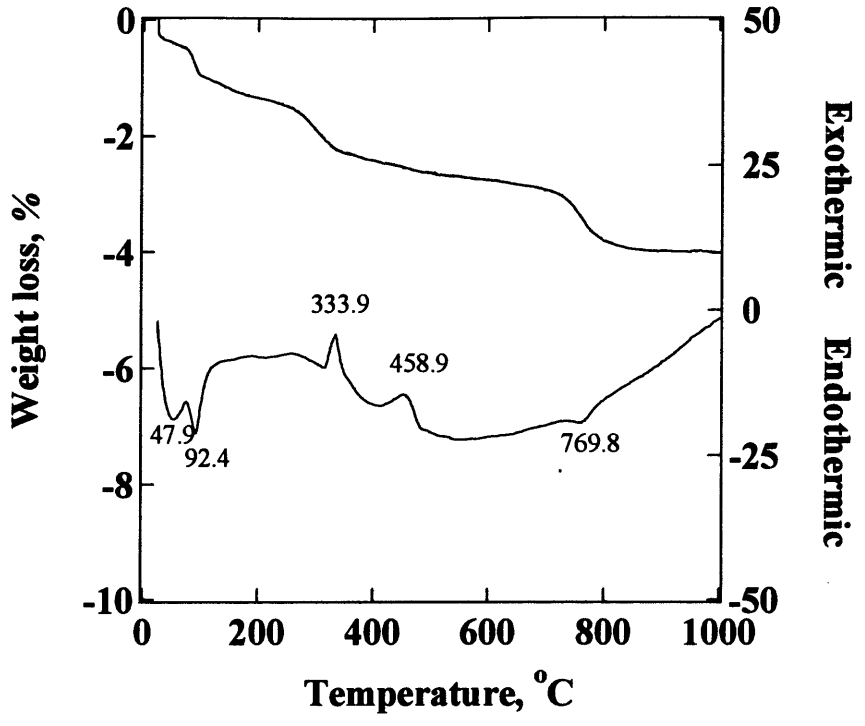

(f)

Figure 2.22 TG-DTA of solidified body at different mechano-chemical treatment;

(a) raw, (g) 300-10, (h) 300-20, (i) 300-40, (f) 300-60

2.3.2.5 Microstructure of activated powder

Figure 3.23 shows SEM images of the activated powders at different milling time. Since the mean particle size of activated particles slightly decreases with milling time, it was somehow different to verify the change of surface area, morphology and powder particle size distribution through planetary ball mill from these SEM images. The trend of graph has similarity with according to rotation speed conditions as previous mentioned.

(a)

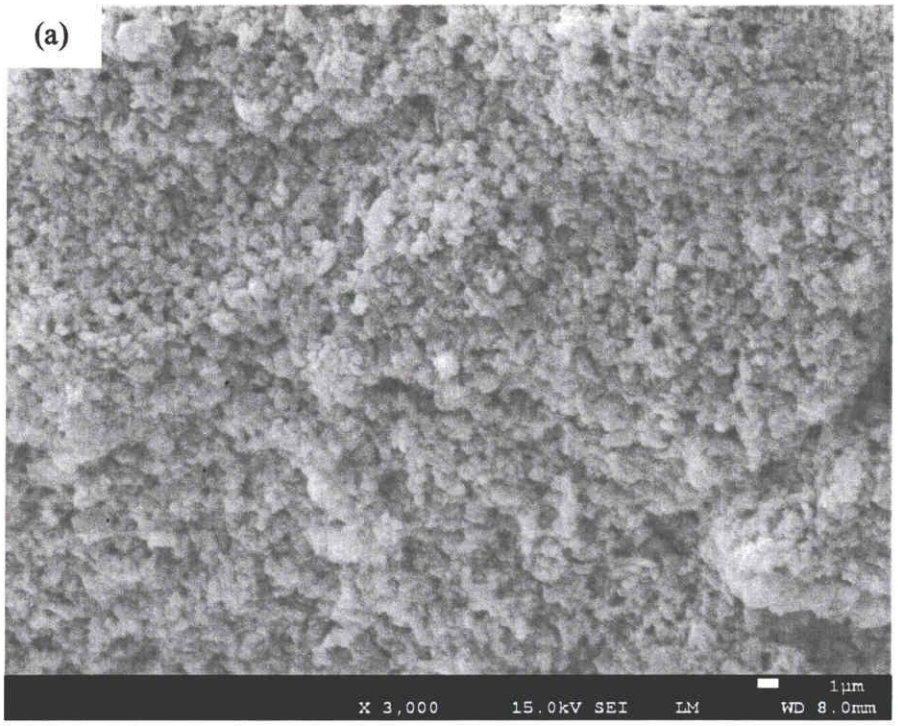

(g)

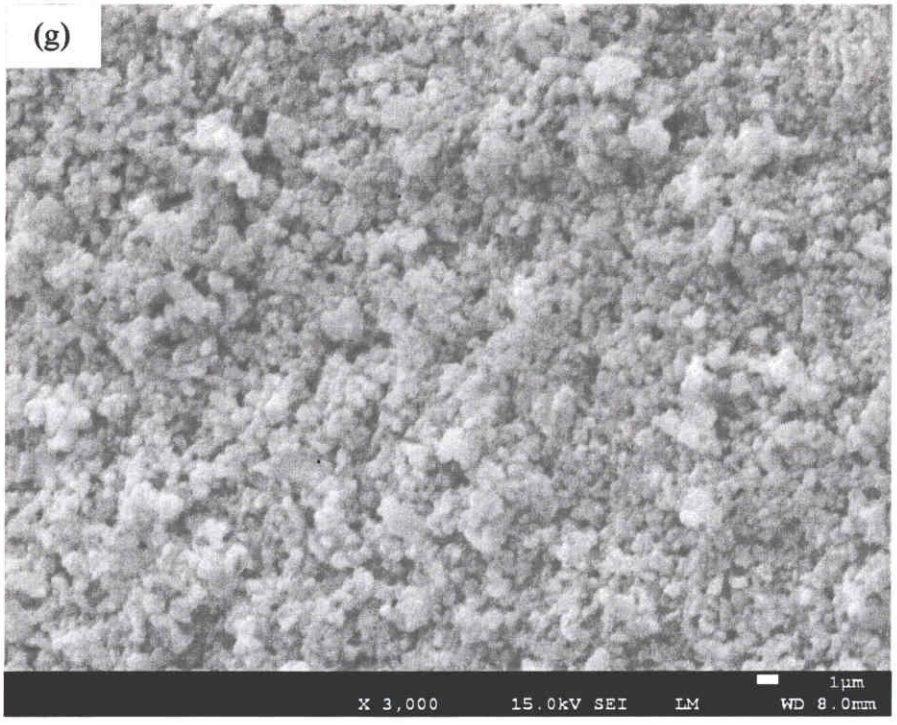

(h)

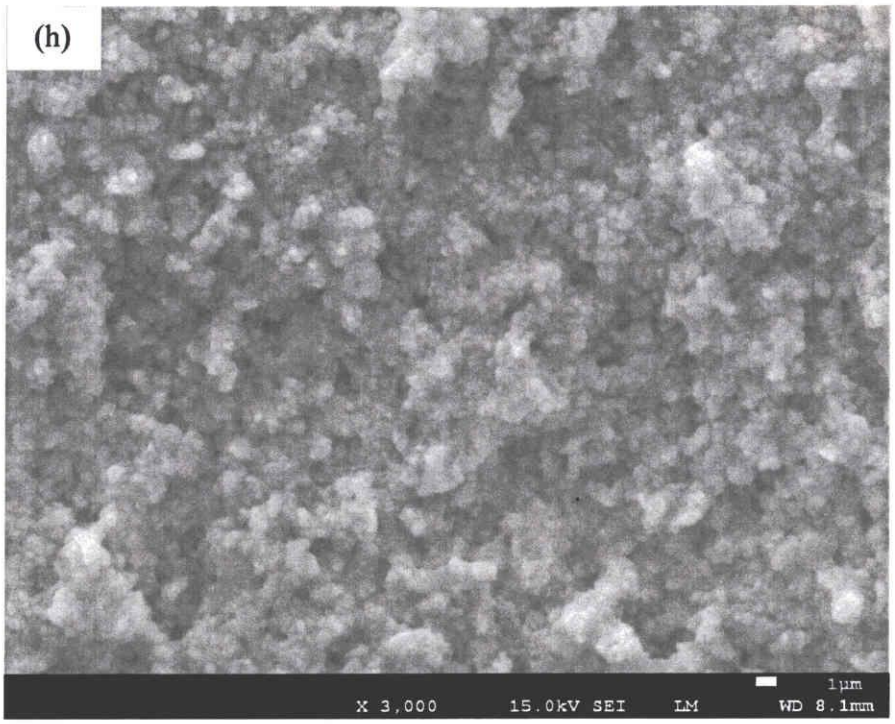

(i)

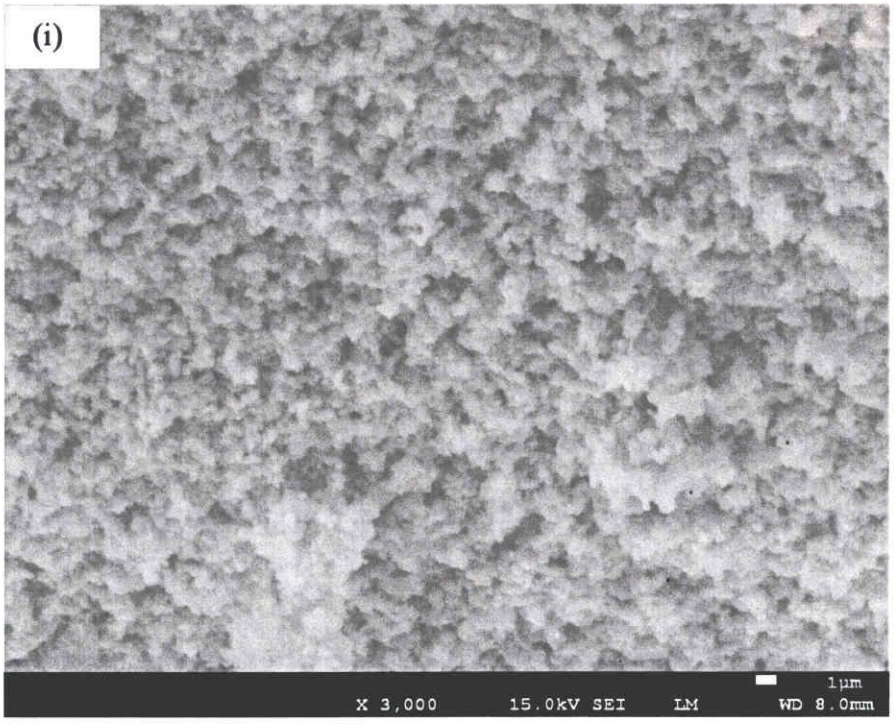

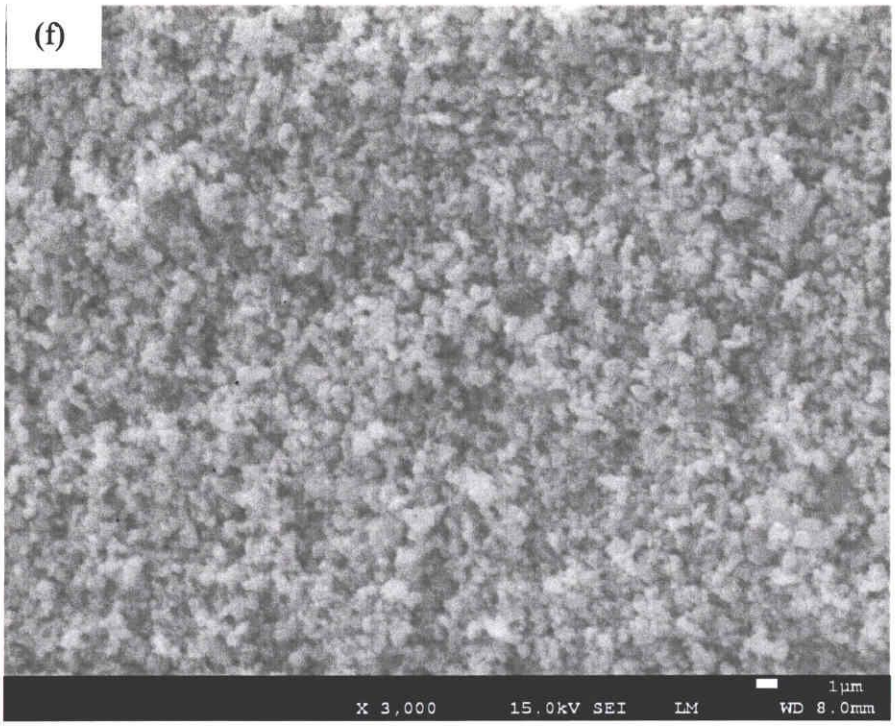

Figure 2.23 Microstructural evolution of activated alumina at different mechano-chemical treatment; (a) raw, (g) 300-10, (h) 300-20, (i) 300-40, (f) 300-60

The microstructural and morphological changes of samples during solidification at different milling time are shown in figure 2.24. The agglomeration of particles formed after alkaline reaction. This is because of new bonding were formed during solidification. SEM images did not show any noticeable increase from the value of solidified body measured from SEM images. The trend of graph has similarity with according to rotation speed conditions as previous mentioned.

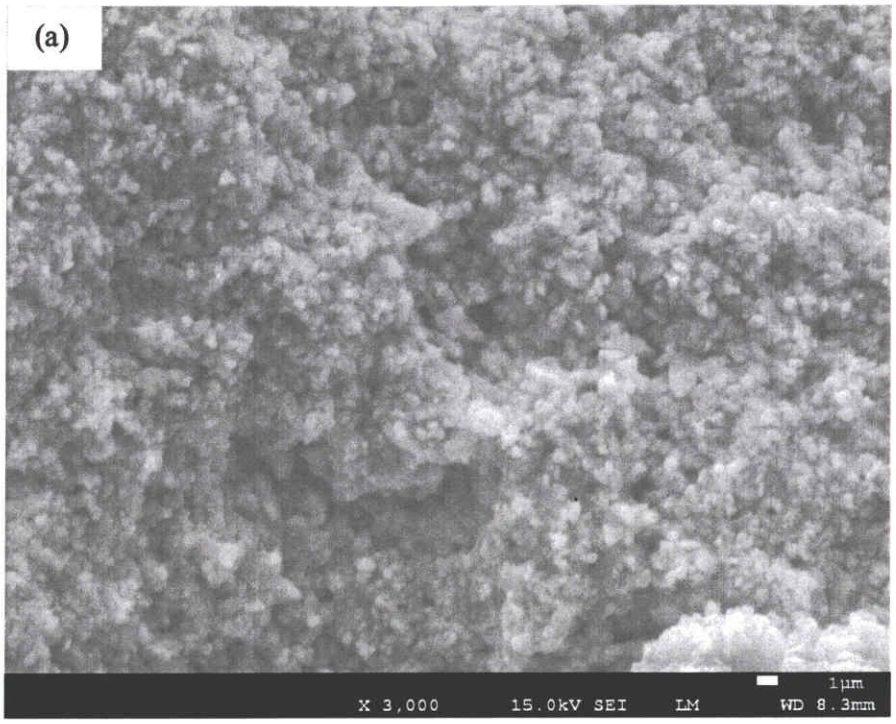
(a)
1μm
X 3,000 15.0kV SEI LM WD 8.3mm

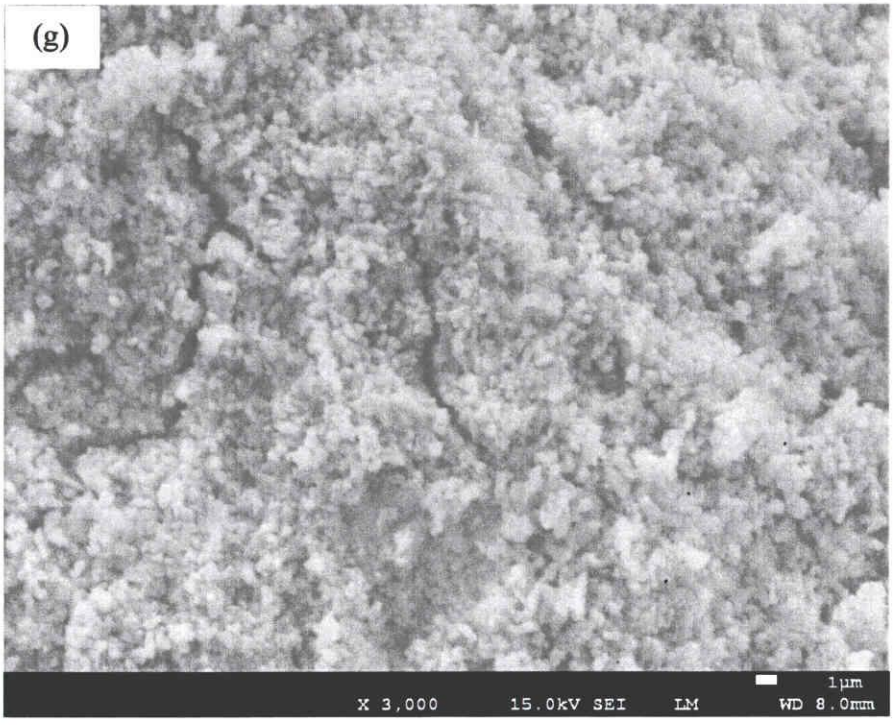
(g)
1μm
X 3,000 15.0kV SEI LM WD 8.0mm

(h)

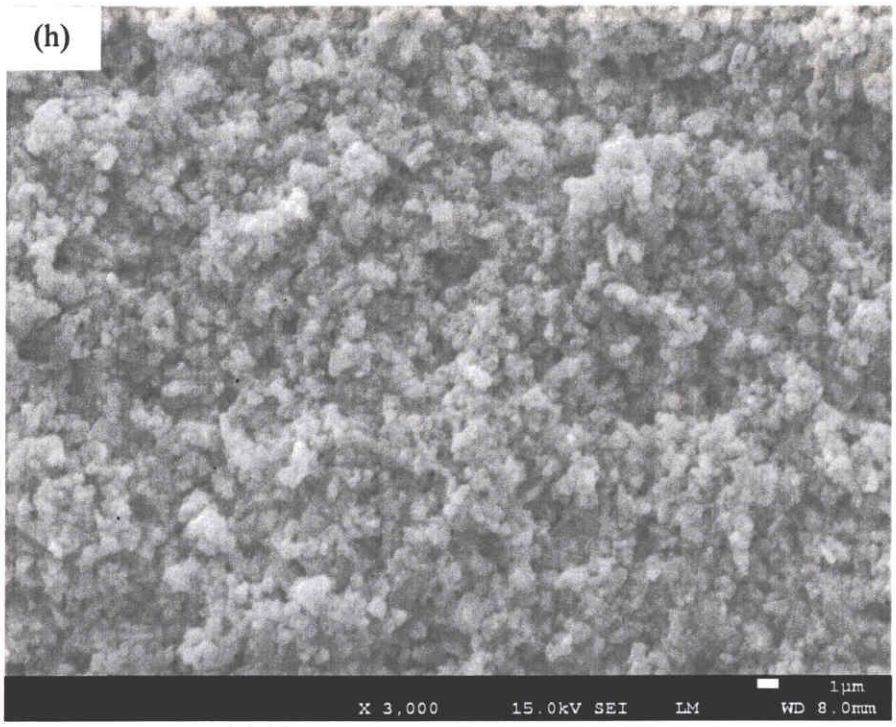

(i)

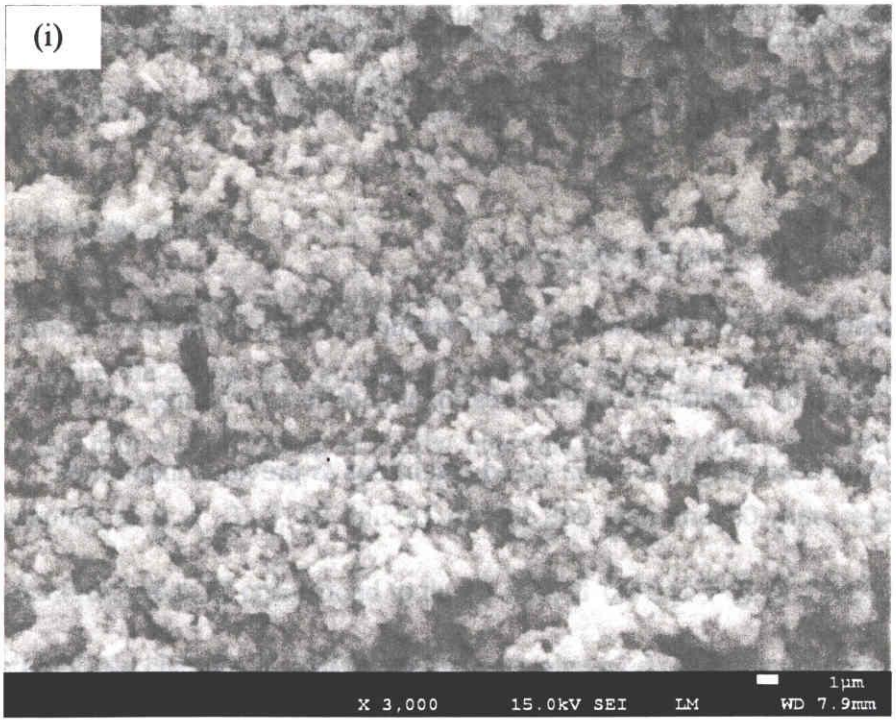

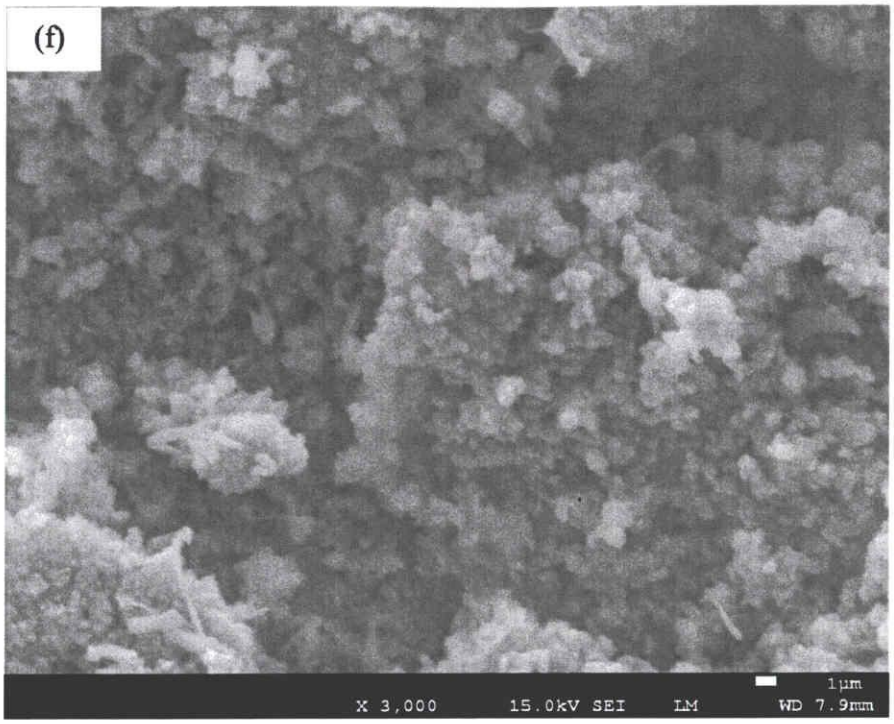

Figure 2.24 Microstructural evolution of solidified body at different mechano-chemical treatment; (a) raw, (g) 300-10, (h) 300-20, (i) 300-40, (f) 300-60

2.3.2.6 Solidification time and Bending strength

Fig. 2.25 represents, which illustrate the relationship between solidification time and bending strength of products by mechano-chemical treatment at different milling time. The trend of graph has similarity with according to rotation speed conditions as previous mentioned.

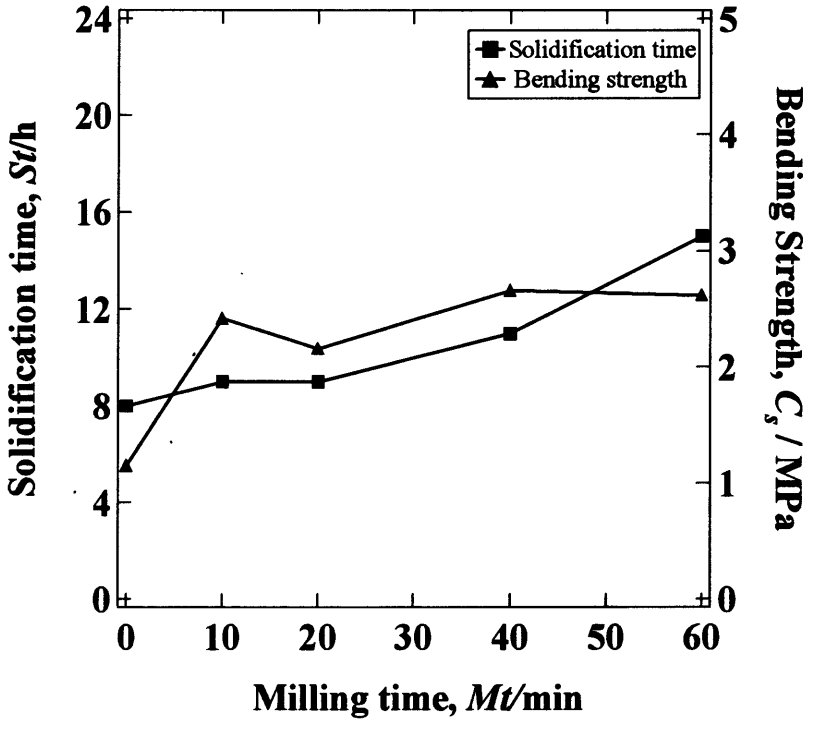

Figure 2.25 Relationship between solidification time and Bending strength by planetary ball mill at different milling time for 300 rpm

2.3.3 Effect of diameter of ball

2.3.3.1 XRD Characterization of activated powder

In order to determine the crystal size change of the treated alumina at different diameter of ball using planetary ball mill was picked up at regular intervals for X-ray diffraction analysis in figure 2.26 (a) corresponds to 0, 1, 3, 5, 10 and 15 mm at 300 rpm and 60 min, respectively. The diffraction peaks at different 2θ correspond to the (0 1 2), (1 0 4), (1 1 0), (1 1 3), (0 2 4), (1 1 6), planes, respectively. No changes in XRD patterns were observed. The raw powder presents sharp peaks indicating the high crystallinity of the sample. On the other hand, the effect of KOH addition on green body synthesis was investigated using activated samples at different mechano-chemical treatment of diameter of ball is shown in Figure 2.26 (b). The trend of graphs, XRD

patterns, FWHM, crystal size and lattice strain have similarity with according to rotation speed and milling time conditions as previous mentioned.

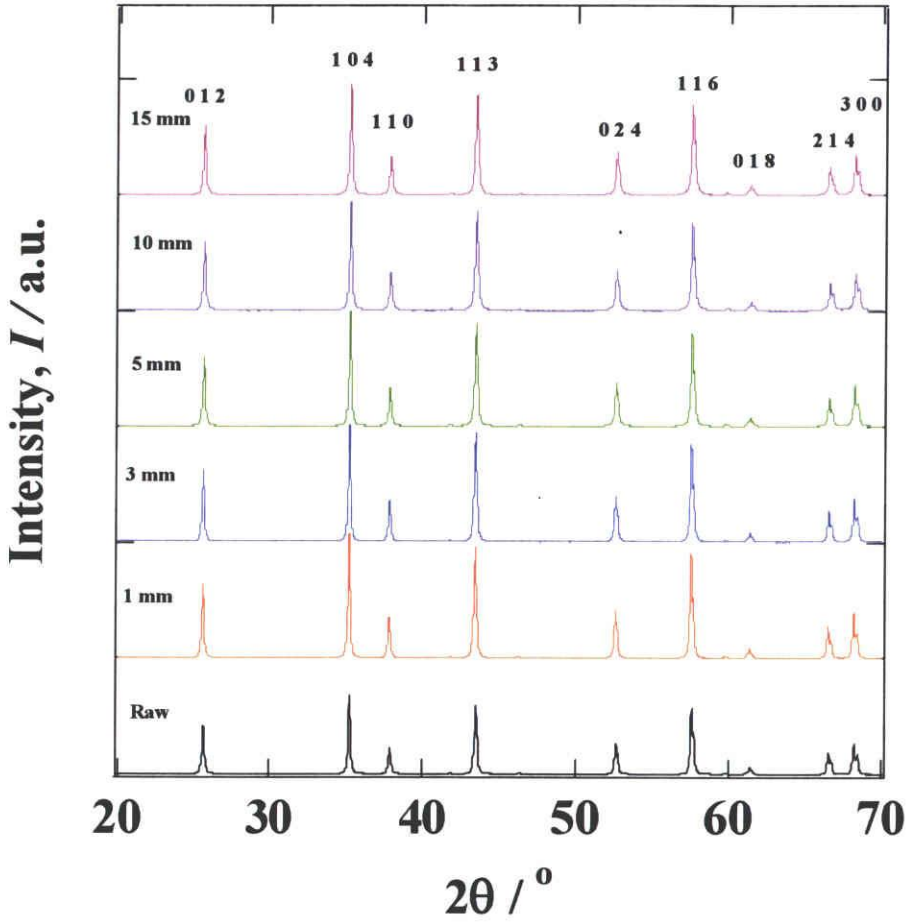

(a)

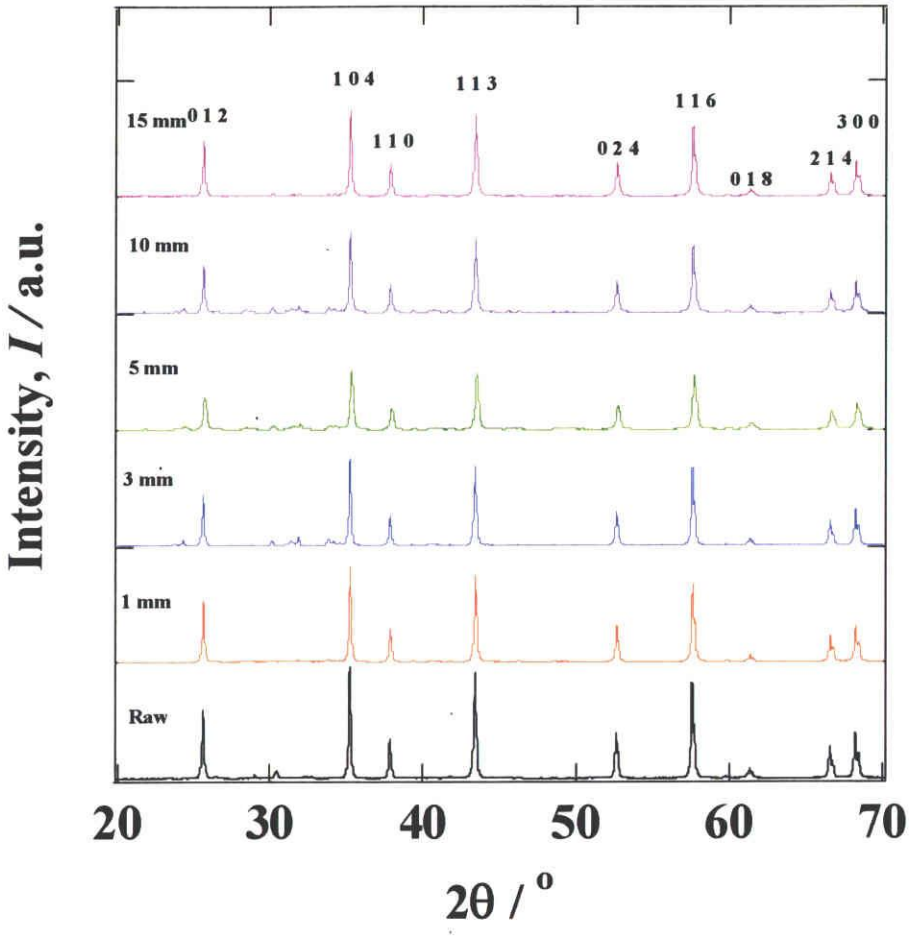

(b)

Figure 2.26 XRD patterns of mechano-chemical treated alumina by planetary ball mill at different diameter of ball; (a) activated powder, (b) ceramic green body

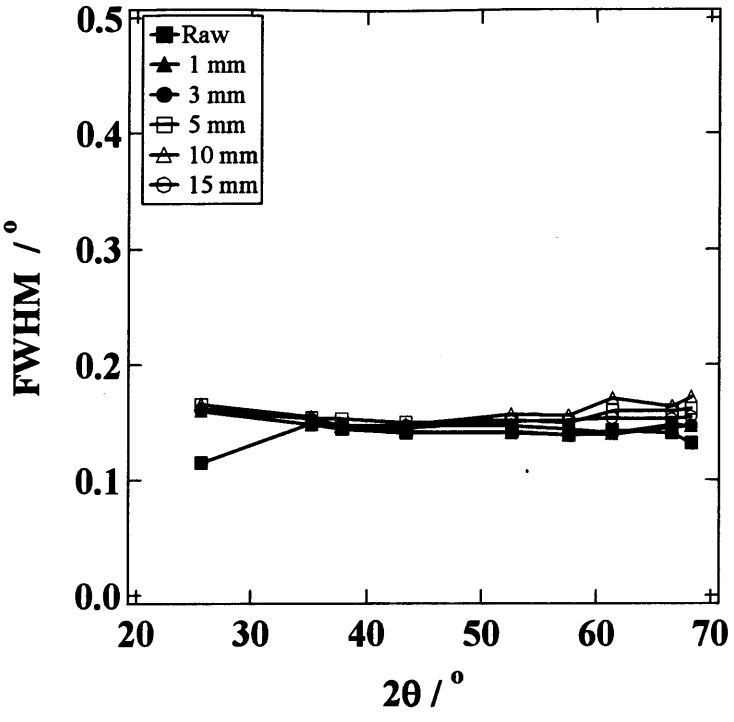

Figure 2.27 The changes of physical FWHM for activated alumina in different mechano-chemical treatment at different diameter of ball

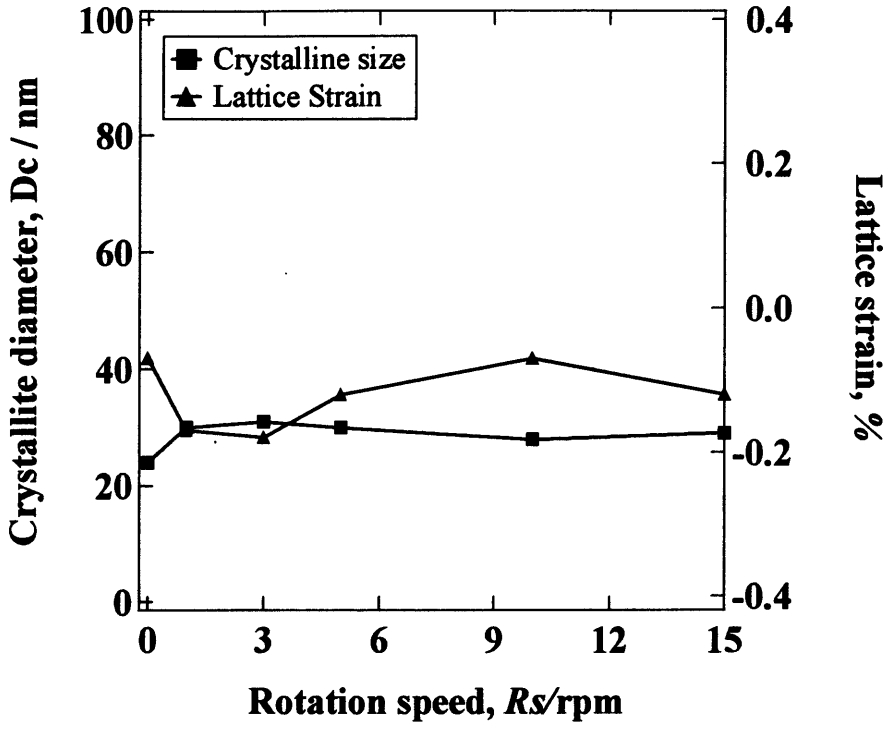

Figure 2.28 X-ray peaks broadening (β) as a function of Bragg angle (θ) for the milled sample and Evolution of crystalline size and lattice strain obtained from Williamson-Hall method at different diameter of ball

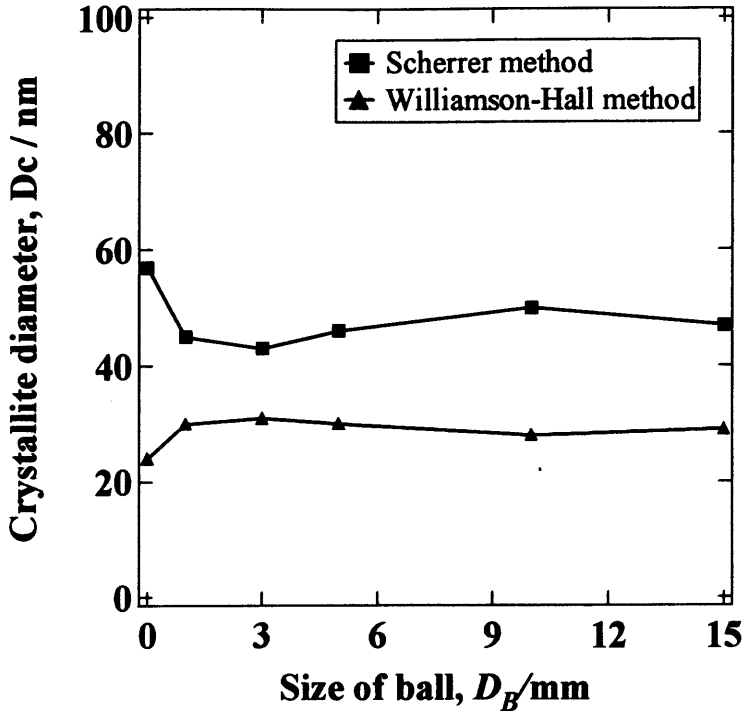

Figure 2.29 Comparison of the evolution of crystalline size between the Scherrer and Williamson-Hall methods at different diameter of ball

2.3.3.2 BET and Mean particle size characterization of activated powder

This figure show relationship BET and mean particle size at different mechano-chemical treatment of diameter of ball. By the BET surface area increases but average particle size (d_{50}) decreases with diameter of ball. On the other hand, BET surface area decrease but average particle size (d_{50}) increases as diameter goes up (15mm). The results give evidence to agglomeration of particles in intensive milling conditions, indicating that the agglomerates pores remain accessible for the nitrogen gas and probably mechano-chemical process prevails to the aggregation of particle. The effect of media surface appears to be more negative than rotation speed and milling time variables.

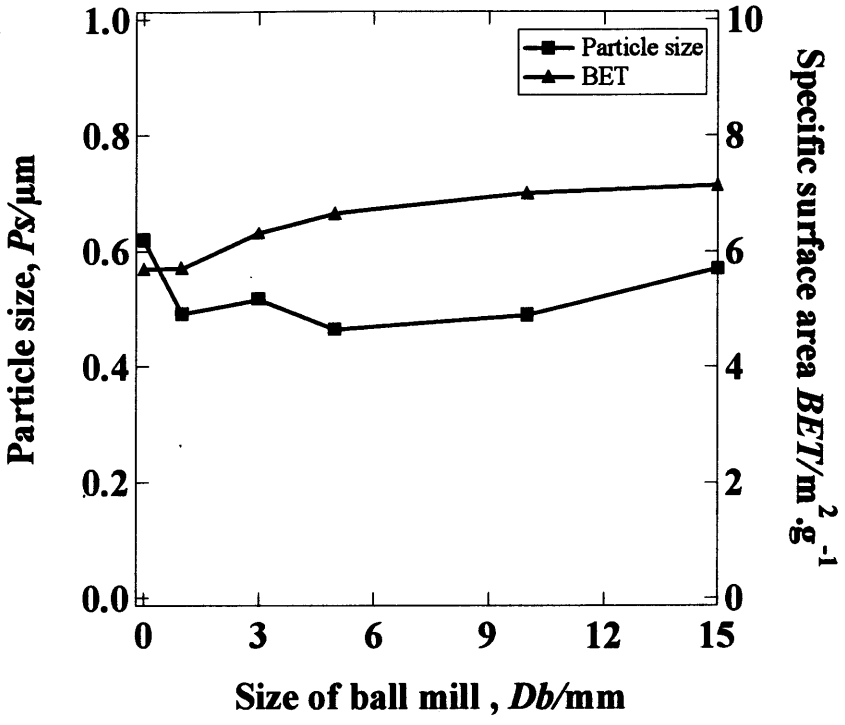

Figure 2.30 BET surface area and Mean particle size of mechano-chemical treated alumina by planetary ball mill at different diameter of ball

2.3.3.3 ICP characterization of activated powder

Figure 2.31 showing quantitative evolution of aluminum ion at different diameter of ball which confirms leaching of concentration of aluminium ion increases significantly with mechano-chemical treatment but decrease as diameter goes up (15mm). The results give evidence to agglomeration of particles in intensive milling conditions as mentioned in BET and mean particle size result that elution of aluminum ion depend on BET surface area in the same direction.

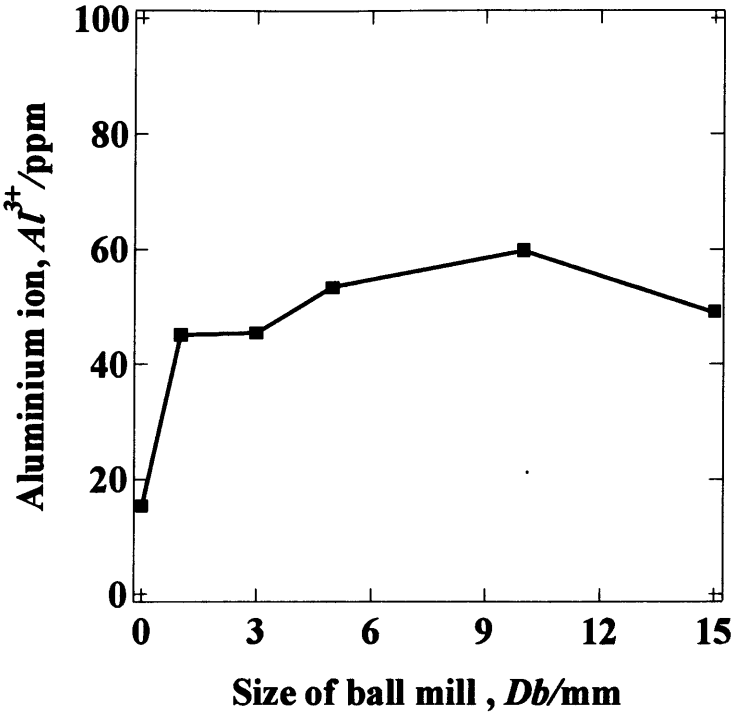

Figure 2.31 Elution behavior of the alumina by planetary ball mill at different diameter of ball

2.3.3.4 Solidification time and Bending strength

Fig. 2.32 represents, which illustrate the relationship between solidification time and bending strength of products by mechano-chemical treatment at different diameter of ball. By the solidification time and bending increased with diameter of ball but decrease as diameter from 5 mm goes up to 15 mm. It can be describe in term of the specific surface area of particle as mentioned in rotation speed variable.

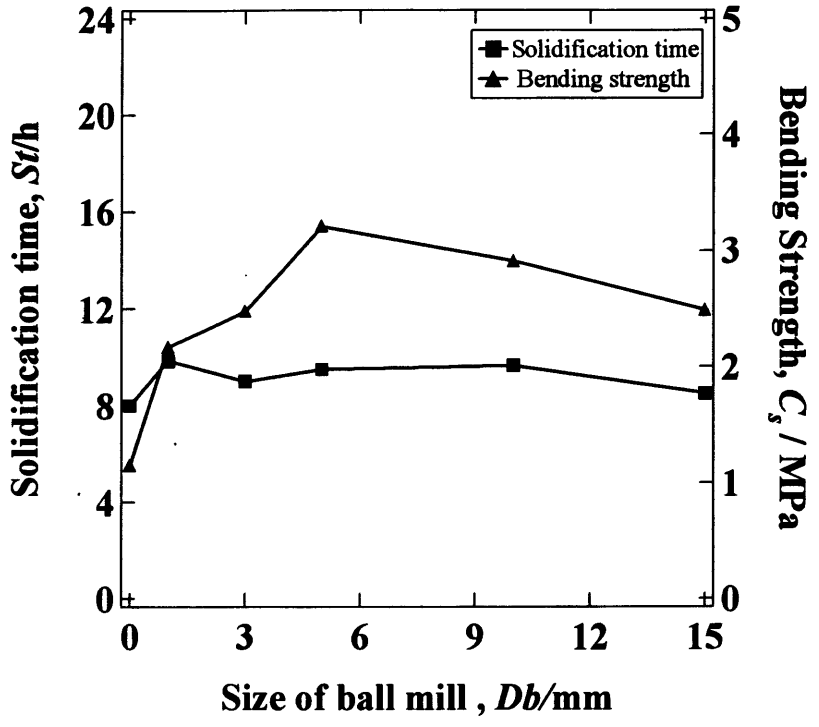

Figure 2.32 Relationship between solidification time and Bending strength by planetary ball mill at different diameter of ball

2.3.4 Effect of ball to powder weight ratio

The XRD results of the milling conditions as, rotation speed, milling time and diameter of ball, described in previous sections, indicated that no changes in XRD patterns were observed. The raw powder presents sharp peaks indicating the high crystallinity of the sample. The results after treated by mechanochemically indicate that the intensity peaks broaden slightly with increasing rotation speed, milling time and diameter of ball. The XRD results suggest that milling durations are required to activate particle or complete reaction in shearing mode. If this process were to be used for commercial production, such extended milling durations or increase rotation speeds would not be a commercially viable proposition. Therefore it is necessary to examine ways in which the milling parameters can altered to allow activate surface of powder with shorter milling

durations or decreasing rotation speed. When increasing the ball to powder weight ratio (BPR) lead to a decrease in the milling time required for the formation of alloying [17]. The starting powder mass was therefore reduced from 200 g to 10 g, so as to investigate whether increasing the BPR had a similar effect of rotation speed, milling time and diameter of ball. Figure 2.33 show results after treated by ball milling indicate that the intensity peaks broaden slightly with increasing BPR. However, when milling in shearing mode with a BPR of approximately 20:1, small peaks were detected after milling for 300 rpm and 60 min. These results suggest that, when milling in shearing mode, increasing the BPR significantly reduces the milling duration and rotation speed required for the formation of new material. Increasing the BPR has been widely reported to reduce the milling duration required to achieve a number of different milling results [18]. If the increase in BPR is achieved by increasing the number of balls, whist keeping the powder mass constant, then the number of ball collisions per unit time is increased and so milling process takes place faster. If as in the case of this study, the increase in BPR is achieved by reducing the powder mass, whist keeping the number of balls constant, then the same total amount of milling energy is now applied to a smaller amount of powder, which results in the changes occurring in the powder as a result of the milling process take place more rapidly. This can also be explained by assuming that the amount of powder involved in each ball collision remains constant as the BPR is varied. Of course, this assumption would not hold for very low BPR. Now, given the assumption that the amount of powder involved in each ball collision remains constant, when the total powder mass is reduced (and hence the BPR is increased), the amount of powder involved in each collision as a fraction of the total powder mass is increased. This would result in a shorter milling duration being required for the entire powder mass to have been involved in a ball collision, and so the milling process would take place more quickly as a result of an increase in the BPR. The XRD result is the preliminary characterization. Further

characterization should more investigation.

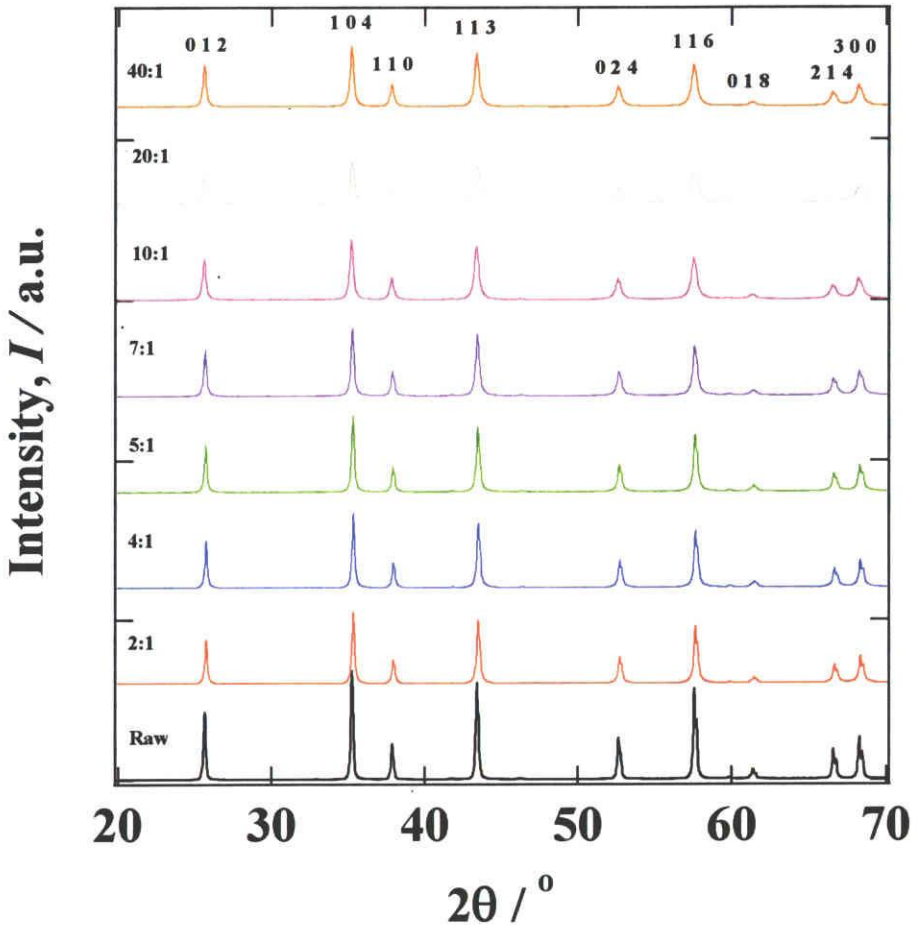

Figure 2.33 XRD patterns of mechano-chemical treated alumina by planetary ball mill at different ball to powder weight ratio

2.3.5 Application mechano-chemical treatment with different alumina

In this part, we investigated the surface activation of alumina (AA-04) on mechanochemically assisted chemical solidification to providing ceramic green body (non-firing ceramic) with improved mechanical strength. The physical and chemical properties are determined with XRD, FTIR, Raman, ICP, TEM and mechanical strength.

2.3.5.1 Analytical techniques

X-ray diffraction (Model RINT 1000, Rigaku, Cu Kα, 40kV) was used for the qualitative determination of the composition and crystalline phases present in samples over the scan range 20-70° for wide angle XRD. Fourier Transform Infrared Spectroscopy (FT-IR) was recorded in the 4000-400 cm^{-1} region using a (Jasco, FTIR-6200). Raman spectra were collected in the 750 cm^{-1} range using a Spectra Physics argon ion laser operating at 532 nm of power. Inductively coupled plasma (ICP) is an analytical technique used for the detection of trace metals using Plasma Spectrometer (SPS-7800). Surface activation of alumina were observed in the micrographs obtained using TEM (JEOL-2100F) operating at 299kV, after depositing the powder dispersed on carbon coated grids. The mechanical property was evaluated by three points testing (Compression strength) using universal testing machine (Shimadzu AGS-G). All tests were performed at room temperature. The test results were recorded using an average value of three measurements.

2.3.5.2 Results and Discussion

Figure 2.34 shows the X-ray diffraction patterns of the activated alumina, Fig 2.34(a) and ceramic green body, Fig 2.34(b). It can be seen that no significant change in the XRD patterns and the intensity peaks slightly decreased and broadened with milling time. This can be indicate that the formation of amorphous phase with shearing force during mechano-chemical treatment. On the other hand, as a result of alkaline activation we have confirmed that new bonding, Potassium Alanate ($KAlH_4$) in range $2\theta = 28\text{-}32°$ can be obtained from Al_2O_3 and KOH via alkali treatment.

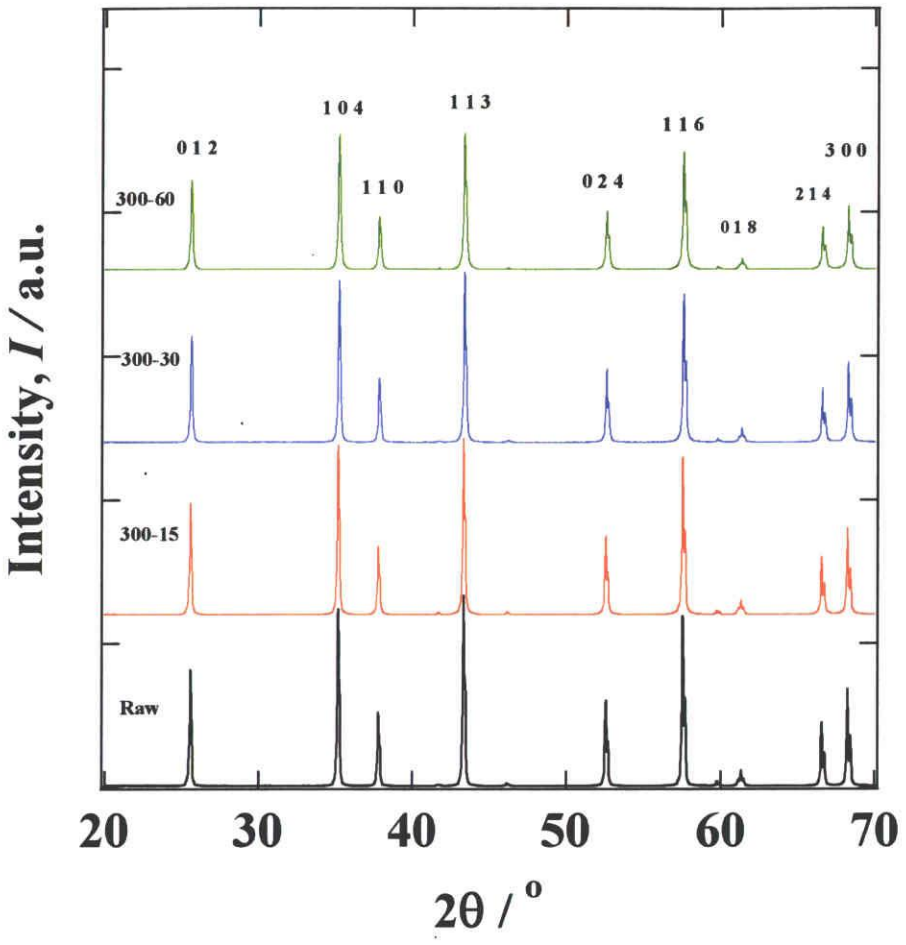
Intensity, I / a.u.
012
104
110
113
024
116
018
214
300
300-60
300-30
300-15
Raw
20
30
40
50
60
70
2θ / °

(a)

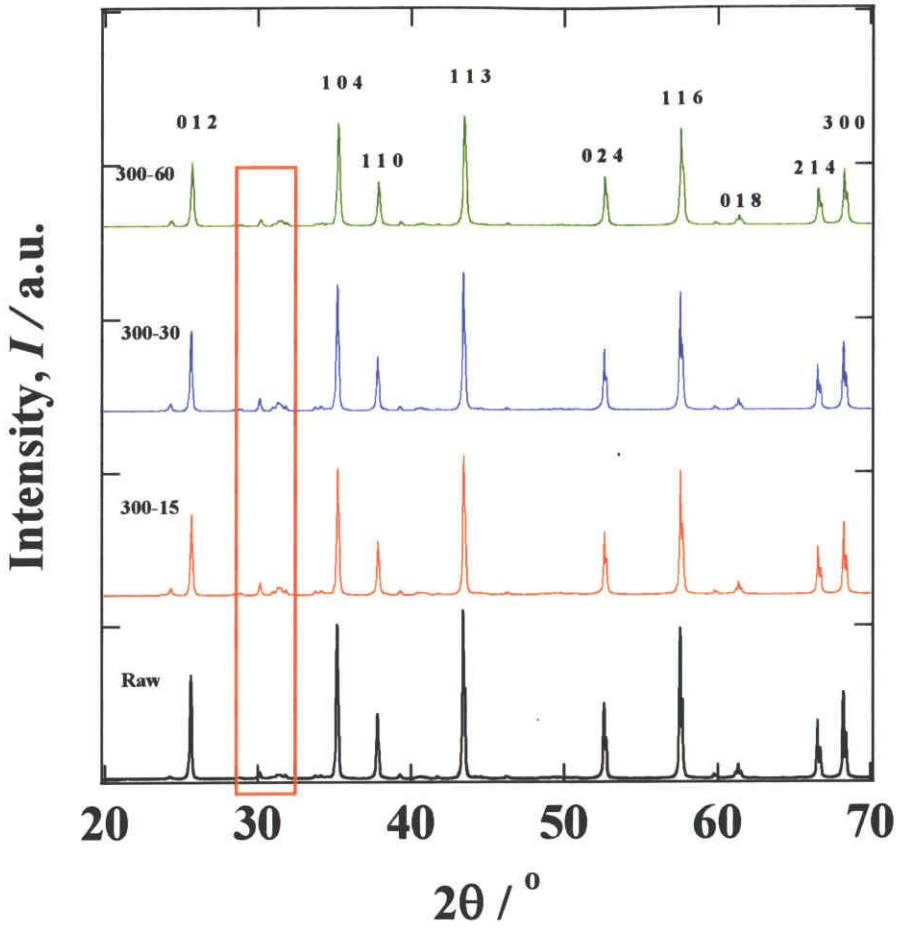

(b)

Figure 2.34 X-ray diffraction patterns of powder at different conditions;

(a) activated powder, (b) ceramic green body

Figure 2.35 shows the FTIR spectra from 4000-1000 cm^{-1} of the activated alumina, Fig 2.35(a) and ceramic green body, Fig 2.35(b). The adsorption bands were sharp and shift with prolong milling time. The adsorption bands from 3600-3200 cm^{-1} correspond to OH from water. As figure 2.35(b) several infrared active Al-H vibrations between 2000-1000 cm^{-1} [19]. The 1700-1450 cm^{-1} were combination bands of Al-H and also sharp in ceramic green body. It possible formation of

hydrogen bonds between AlH_x^- and K^+ could be assigned to the formation of $KAlH_4$ or an intermediate compound.

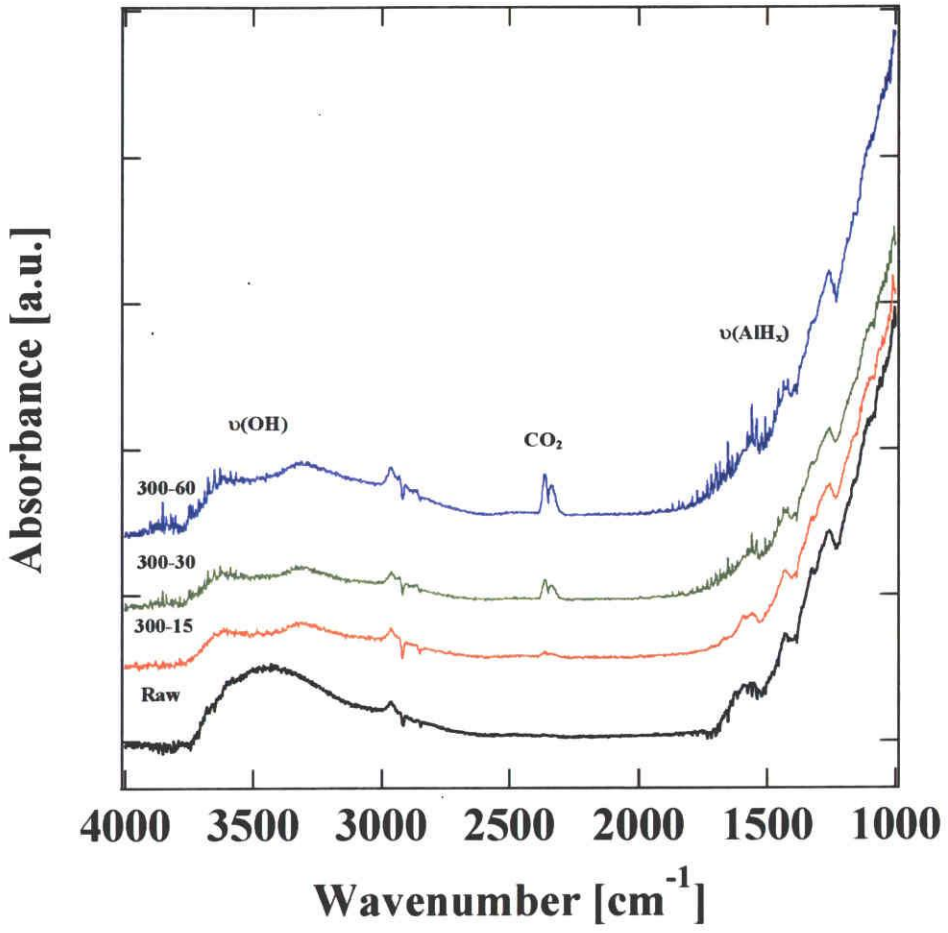

(a)

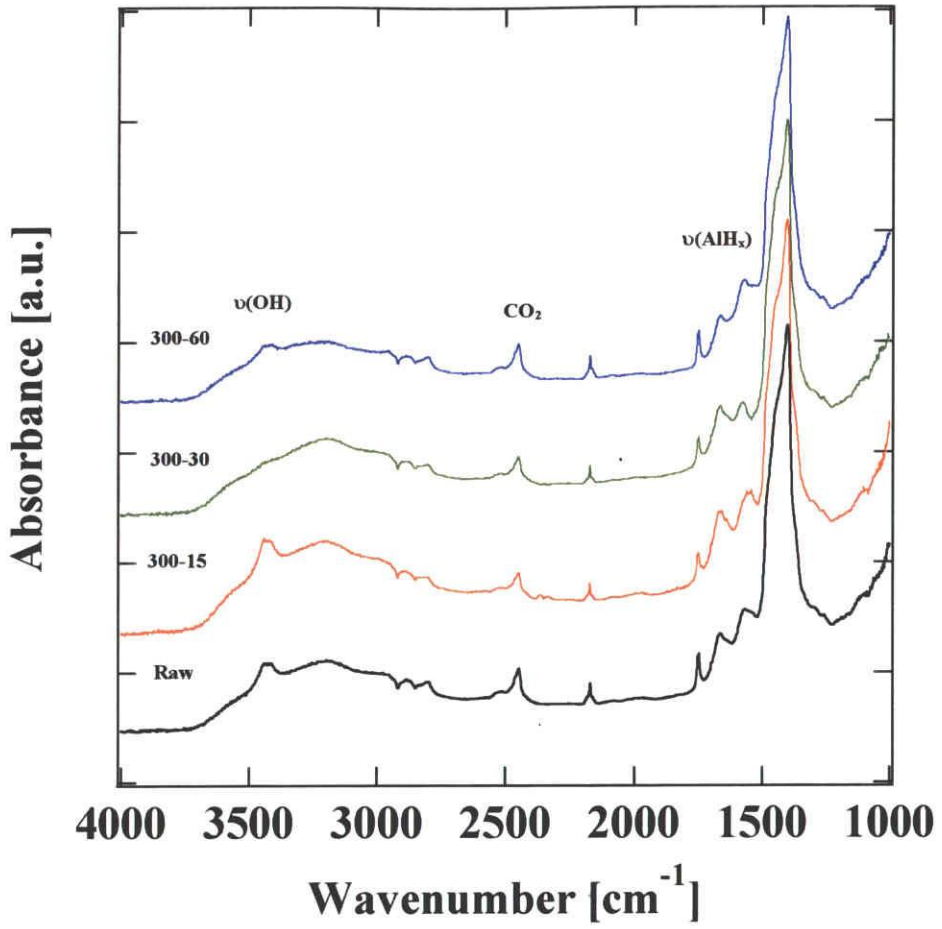

(b)

Figure 2.35 FTIR spectra of powder at different conditions;

(a) activated powder, (b) ceramic green body

Figure 2.36 show Raman spectra of powder at activated alumina, Fig 2.36(a) and ceramic green body, Fig 2.36(b). By figure 2.36(a) show all bands of corundum compound in mehanochemically activated powder [20]. On the other hand, Raman spectra in ceramic green body in figure 2.36(b) show broad band because effect of OH from H_2O [21]. The new band at 1080 cm^{-1} related to aluminate band [21-22].

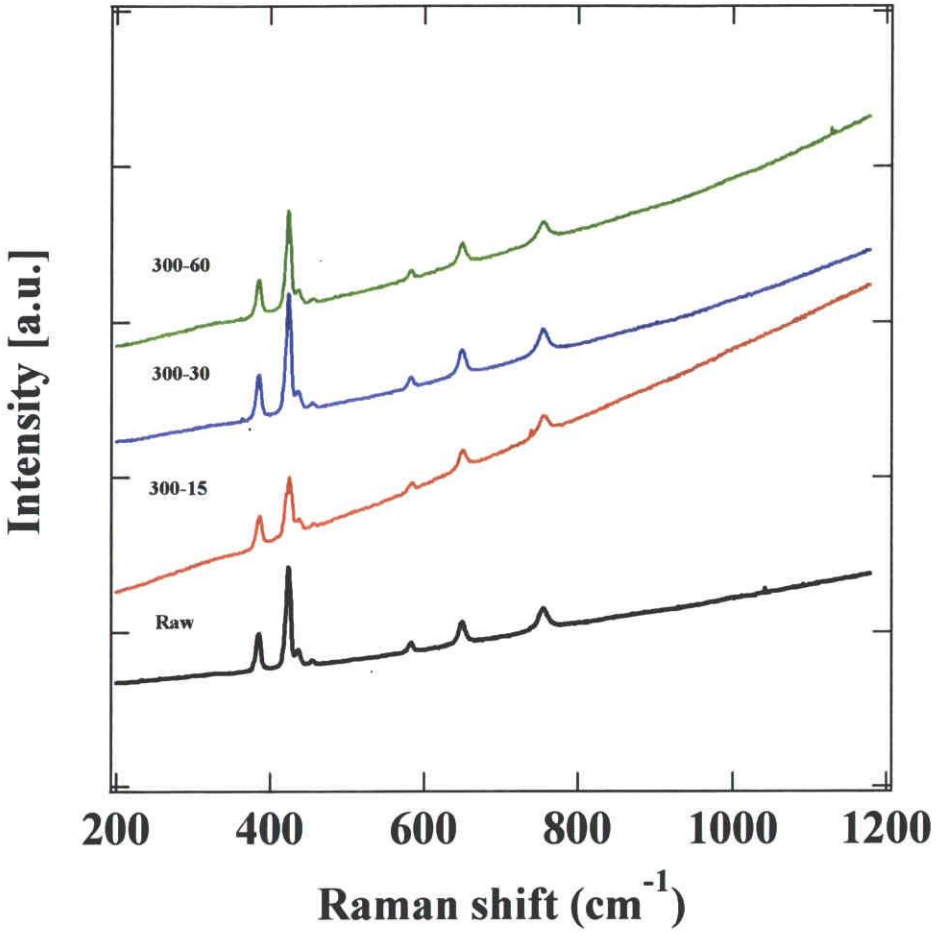
Intensity [a.u.]
300-60
300-30
300-15
Raw
200
400
600
800
1000
1200
Raman shift (cm-1)

(a)

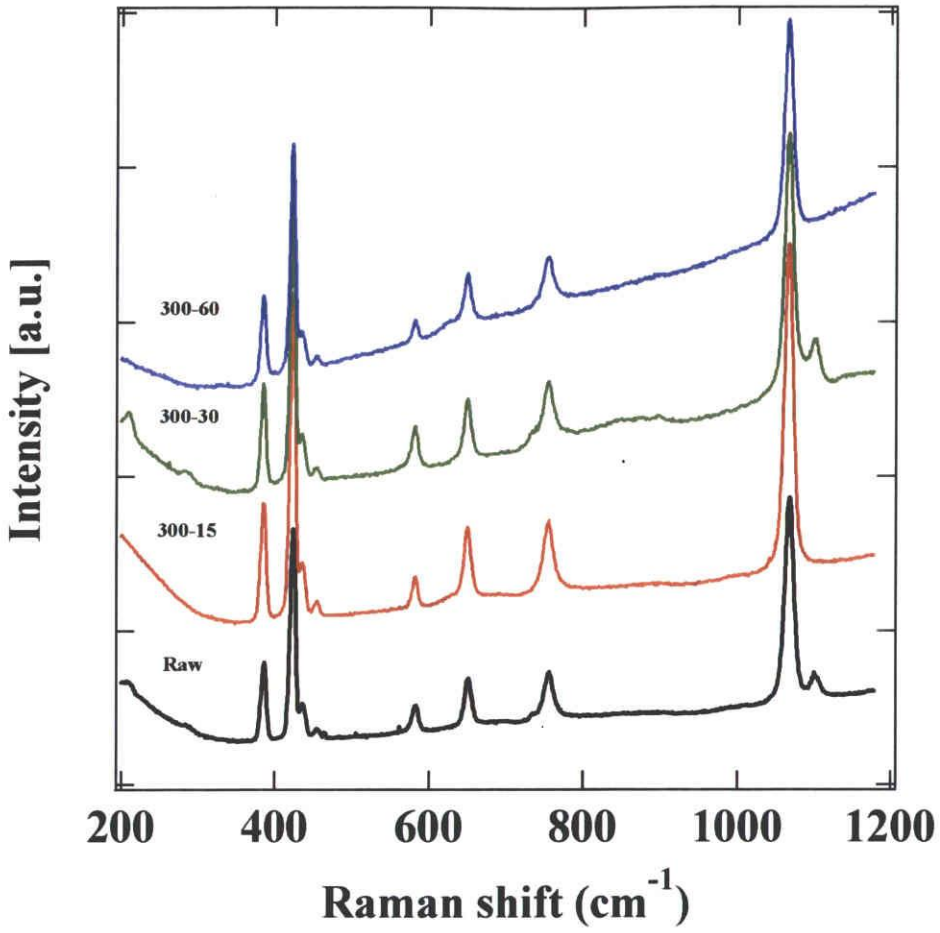

(b)

Figure 2.36 Raman spectra of powder at different conditions;

(a) activated powder, (b) ceramic green body

Figure 2.37 shows the elution behavior of activated and unactivated alumina powders at different mechano-chemical treatment. The Al^{3+} increased with increasing milling time. Such phenomenon is due to non-stable on surface of alumina with shearing force during mechano-chemical treatment. The dissolving alumina surface with mechano-chemical treatment will therefore be enhanced in enriched in Al, which is consistent with a surface reaction-controlled mechanism [20].

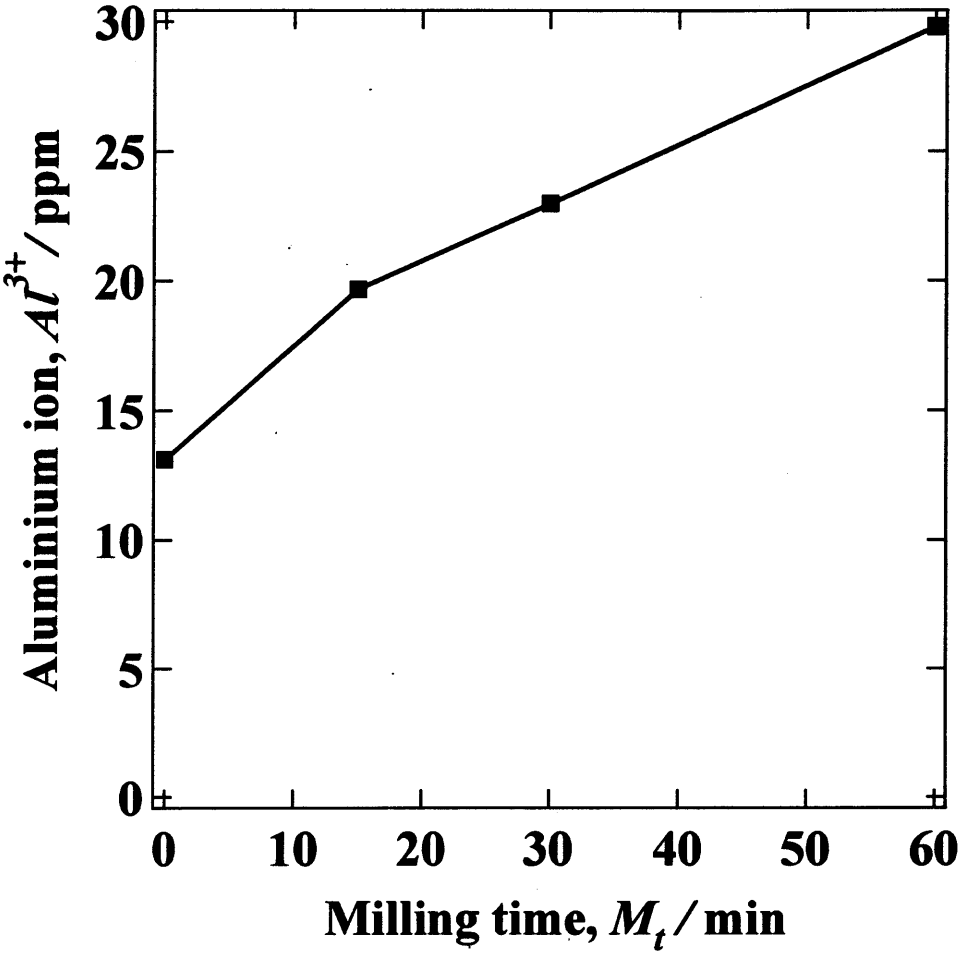

Figure 2.37 Elution behavior of mechanochemically activated alumina

TEM measurements can be applied for estimating the composition and microstructure of samples. A high resolution obtained in this type of microscopy allows single grains of the samples to be observed. The particle morphology of the raw, activated and ceramic green body samples were shown by TEM images in Fig 2.38(a), (b) and (c) respectively. As shown in Fig 2.38 (a) the alumina powder consists of regularly shaped plate-like particles. The presence of amorphous layer in the activated powder surface was confirmed in Fig 2.38 (b). The duration of milling would have determined the extent to which amorphization and temperature rise had been interaction between ball and powder. On the other hand, it can be seen in Fig 2.38 (c) that certain

lattice planes are continuous across the particle boundaries, which indicates the presence of bonding or solid bridge. The single oxide powder of Al_2O_3 consists of solid bridge or bonding with a reasonably narrow size distribution.

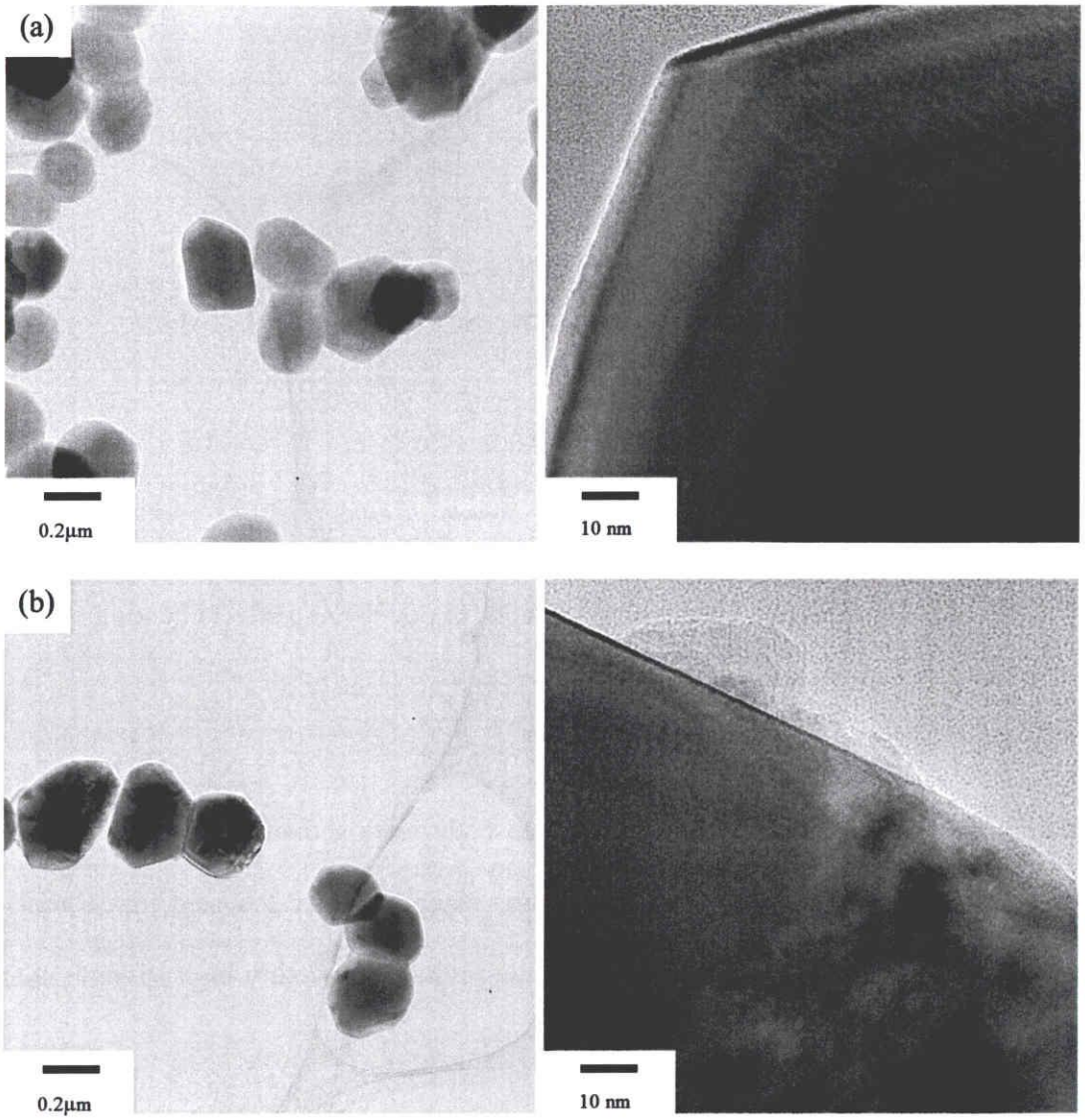
(a)
0.2μm
10 nm
(b)
0.2μm
10 nm

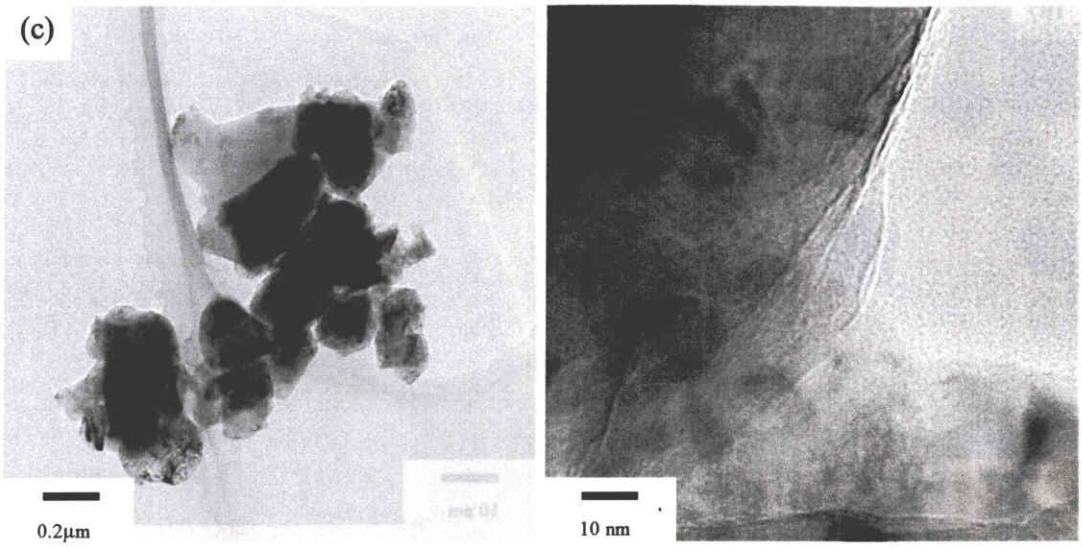

Figure 6 Transmission electron micrographs of powder at different conditions;

(a) raw, (b) 300-60, (c) ceramic green body

Results of compression strength of ceramic green body were shown in Fig 2.39. The strength increased with milling time. Maximal strength was reached, when activated for 30 min. Then, this strength decreased slightly in prolonged milling time. These early high strength characters are noteworthy in view of practical applications.

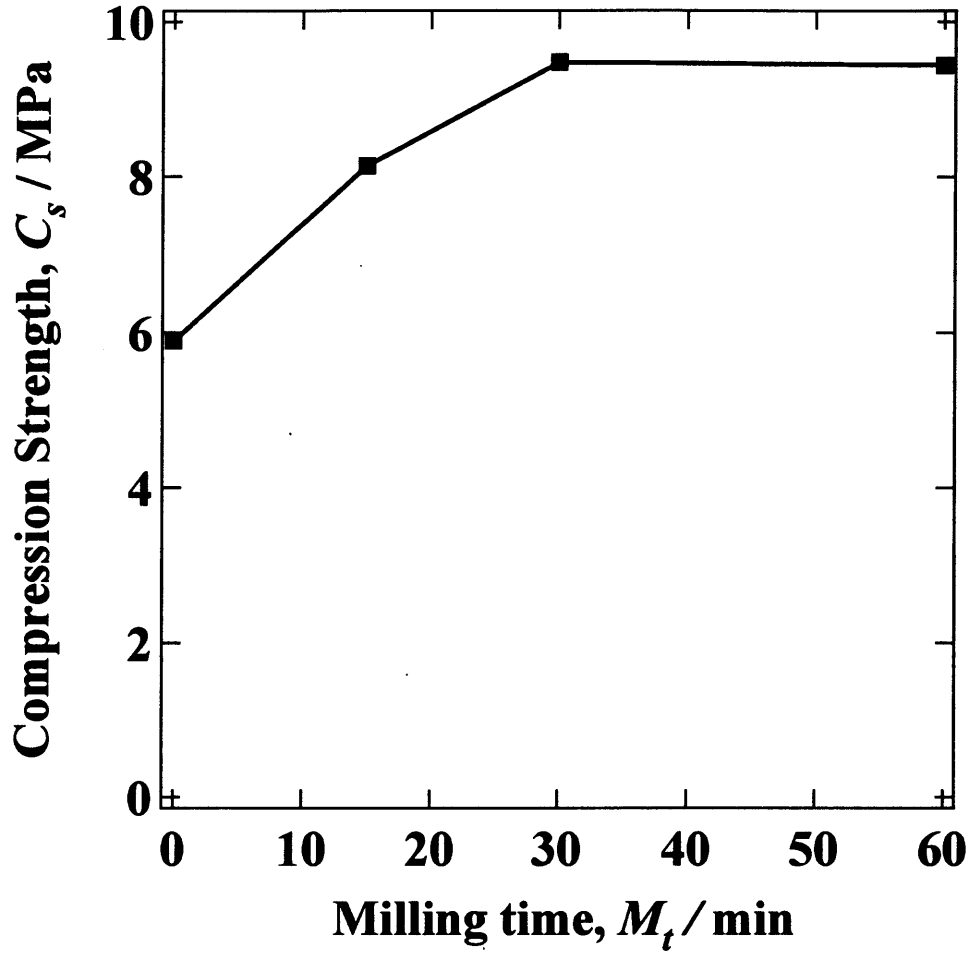

Figure 2.39 Compression strength of ceramic green body

2.4 Conclusion

The results presented in this thesis show that the techniques developed and used in this study are well suited for the investigation of the influence of mechano-chemical parameters on the interface surface of particles and properties of activated powder as well as on the milling energy values. Further detailed conclusions from the investigation of the influence of mechano-chemical variables on the activation of alumina are:

- As the rotation speed, milling time and diameter of ball increase, the line broadening increases and integral intensity decreases. The lattice and unit cell volume of alumina expanded during mechano-chemical activation.
- From the Williamson-Hall plots, it was understood that strain and size contributions exist simultaneously in the activated powders.
- The use of higher speed, prolonged milling and larger diameter of ball lead to higher specific surface area, X-ray amorphous material, physical broadening microstrain, smaller crystallites size and mean particle size distribution.
- Agglomerates during mechano-chemical treatment are formed rapidly in planetary ball mill for higher media surface (diameter of ball).
- Increasing the BPR also reduces the milling duration or rotation speed required for the activate surface of powder or the formation of new material.

Reference

[1] C. Miclea, C. Tanasoiu, I. Spanulescu, C.F. Miclea, A. Gheorghiu, L. Amarande, M. Cioangher, C. T. Miclea, Microstructure and properties of barium titanate ceramics prepared by mechanochemical synthesis. Rom. J. Info. Sci. Tec., 10 (2007) 335-345.

[2] H. Yang, Y. Hu, X. Zhang, G. Qio, Mechanochemical synthesis of cobalt oxide nanoparticles. Mat. Let. 58 (2004) 387-389.

[3] K. Wieczorex-Ciurowa, K. Gamrat, Some aspects of mechanochemical reaction. Mat. Sci-Pol. 25 (2007) 219-232.

[4] P. Pourghahramani, Effects of grinding variables on structural changes and energy conversion during mechanical activation using Line Profile Analysis (LPA). Doctoral thesis, Lulea University of Technology, 2006.

[5] W.S. Jung, H.S. Park, Y.J. Kang, D.H. Yoon, Lower the sintering temperature of Gd-doped ceria by mechanochemical activation. Ceram. Int. 36 (2010) 371-374.

[6] H-I. Hsiang, F-S. Yen, Effects of mechanical treatment on phase transformation and sintering of nano-sized γ-Fe_2O_3 powder. Ceram. Int., 29 (2003) 1-6.

[7] T. Tsuzuki and P. G. McCormick, Synthesis of Cr_2O_3 nanoparticles by mechanochemical processing. Acta. mater., 48 (2000) 2795-2801.

[8] K. H. Yoon, H. S. Park, J. Y. Cho, E. S. Kim, Microwave dielectric properties of $(Pb_{0.4}Ca_{0.6})(Fe_{0.5}Ta_{0.5})O_3$ ceramics prepared by mechanochemical processing. J. Eur. Cer. Soc., 23 (2003) 2579-2582.

[9] A. Moure, L. Pardo. C. Alemany, P. Millan, A. Castro, Piezoelectric ceramics based on Bi_3TiNbO_9 from mechanochemically activated precursors. J. Eur. Cer. Soc., 21 (2001) 1399-1402.

[10] A. Eiad-ua, T. Shirai, H. Watanabe, M. Fuji, K. Orito and M. Takahashi, Fabrication of non-firing ceramics assisted by particle surface activation using a planetary ball mill. Ceram. Trans., 219 (2010) 129-135.

[11] A. Eiad-ua, T. Shirai, T. Kato, K. Orito, H. Watanabe, M. Fuji and M. Takahashi, Novel fabrication route for porous ceramics using waste materials by non-firing process. J. Cer. Soc. Jap., 118 (2010) 745-748.

[12] M.E. Rabanal, A. Varez, B. Levenfeld, J.M. Torralba, Magnetic properties of Mg-ferrite after milling process. J. Mat. Pro. Tech., 143-144 (2003) 470-474.

[13] W.K.W. Lee, J.S.J. van Deventer, Chemical interactions between siliceous aggregates and low-Ca alkali-activated cements. Cem. Concr. Res., 37 (2007) 844-855.

[14] H. Mio, J. Kano, F. Saito, K. Kaneko, Effect of rotational direction and rotation-to-revolution speed ratio in planetary ball milling. Mater. Sci. Eng. A., 332 (2002) 75-80.

[15] F. Delogu, R. Orru, G. Cao, A novel macrokinetic approach for mechanochemical reactions. Chem. Eng. Sci., 58 (2003) 815-821.

[16] F. Delogu, G. Cocco, Compositional effects on mechanochemical synthesis of Fe-Ti and Cu-Ti amorphous alloys by mechanical alloying. J. Alloy. Comp., 352 (2003) 92-98.

[17] G. B. Schaffer, J. S. Forrester, Influence of collision energy and strain accumulation on the kinetics of mechanical alloying. J. Mat. Sci., 32 (1997) 3157-3162.

[18] C. Suryanarayana, Mechanical alloying and milling. Pro. Mat. Sci., 46 (2001) 1-184.

[19] J. R. Ares, K-F. Aguey-Zinsou, F. Leardini, I. J. Ferrer, J-F. Fernandez, Z-X Guo, and C. Sanchez, Hydrogen Absorption/Desorption Mechanism in Potassium Alanate (KAlH4) and Enhancement by TiCl3 Doping. J. Phys. Chem. C., 113 (2009) 6845-6851.

[20] T. Assih, A. Ayral, M. Abenoza, J. Phalippou, Raman study of alumina gels. J. Mater. Sci., 23 (1998) 3326-3331.

[21] J. R. Schoonover, S. L. Zhang and C. T. Johnston, Raman spectroscopy and multivariate curve resolution of concentrated Al_2O_3–Na_2O–H_2O Solutions. J. Raman. Spectrosc., 34 (2003) 404-412.

[22] S. F. Agnew, J. R. Schoonover, Microstructrual Properties of High Level Waste Concentrates and Gels with raman and Infrared Spectrocopies. DOE Environmental Management Science Program (EMSP). 1996.

[23] W.K.W. Lee, J.S.J. van Deventer, Chemical interactions between siliceous aggregates and low-Ca alkali-activated cements. Cem. Concr. Res., 37 (2007) 844-855.